EMIDS WORKSHOP

"The breakthrough of Molecular Imaging in the field of the future in vivo diagnostic procedures"

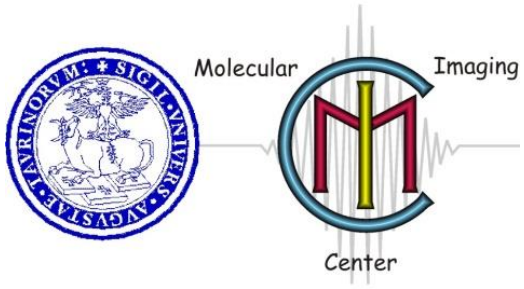

Chemical Exchange Saturation Transfer agents

Giuseppe Ferrauto

Torino, 11/09/2014

Chemical Exchange Saturation transfer

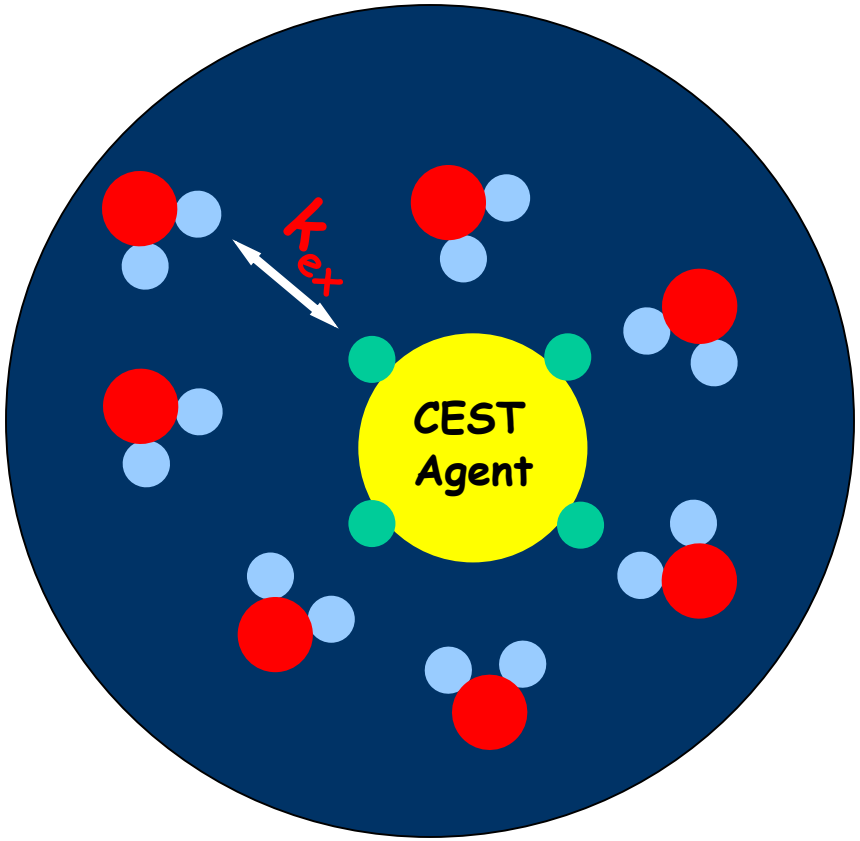

$\Delta\omega$ (rad·Hz) = ω_{WAT} - ω_{CEST}

If $\Delta\omega > k_{ex}$ then….

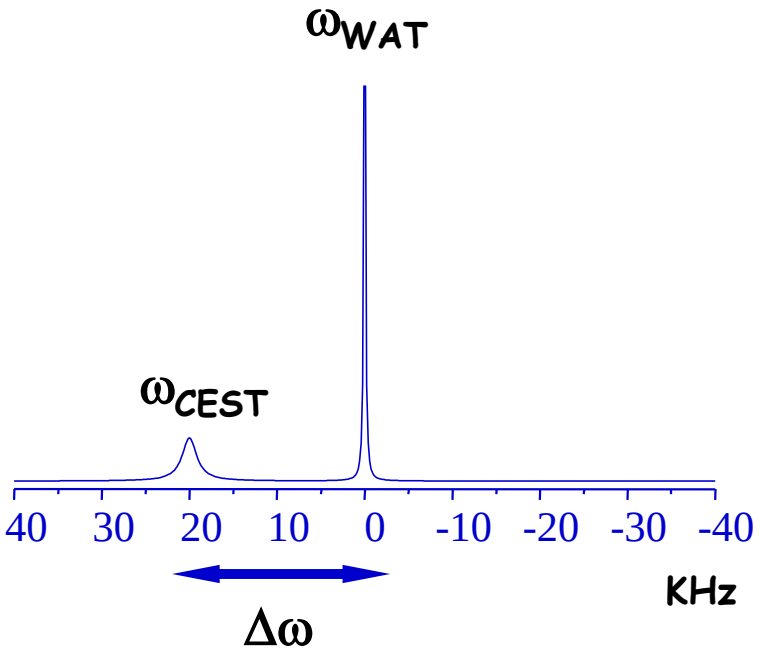

water molecule

CEST agent mobile protons

Chemical Exchange Saturation transfer

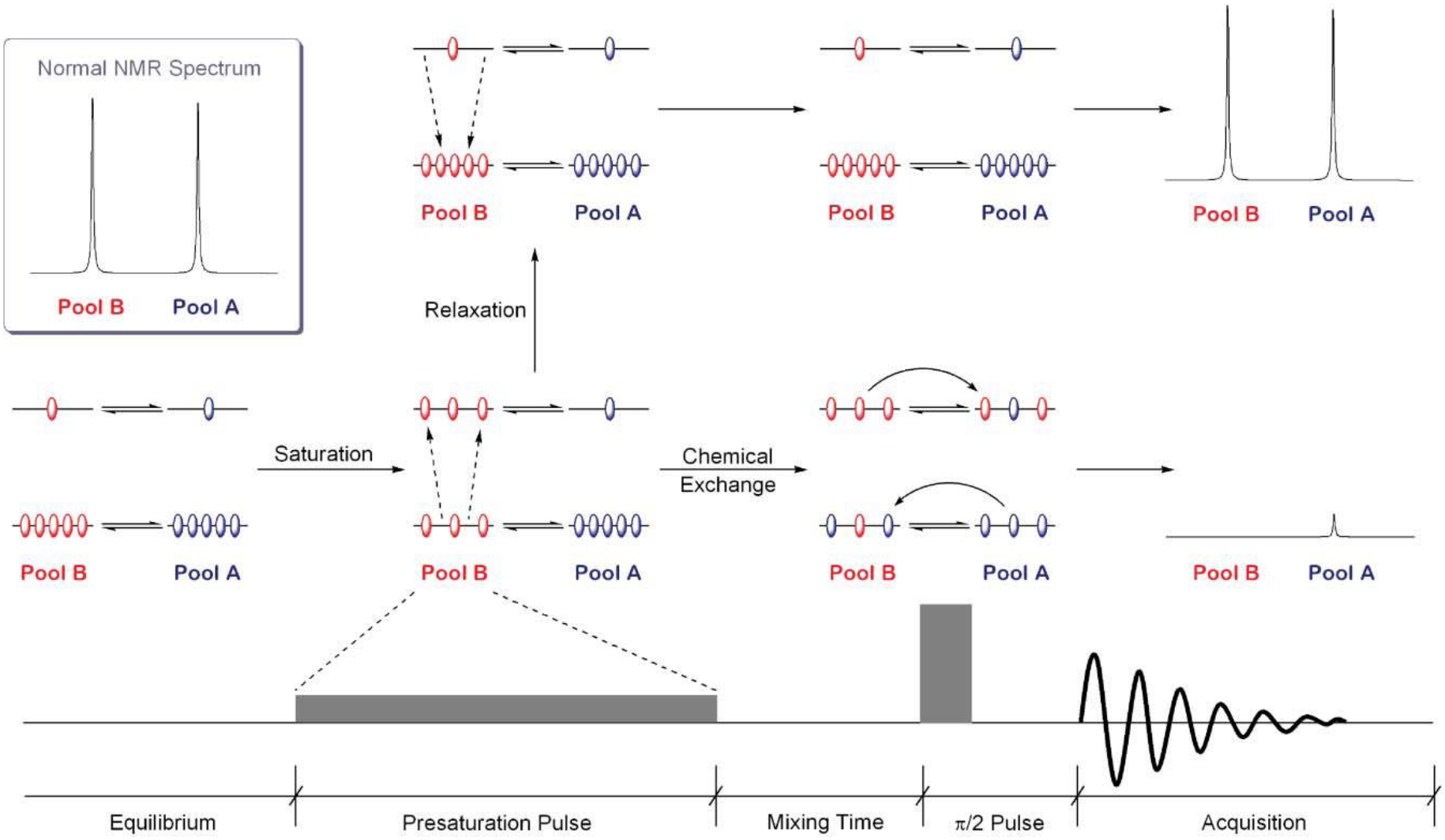

Sherry D. et al.*Chem. Soc. Rev., 2006, 35, 500–511*

The MR-CEST experiment

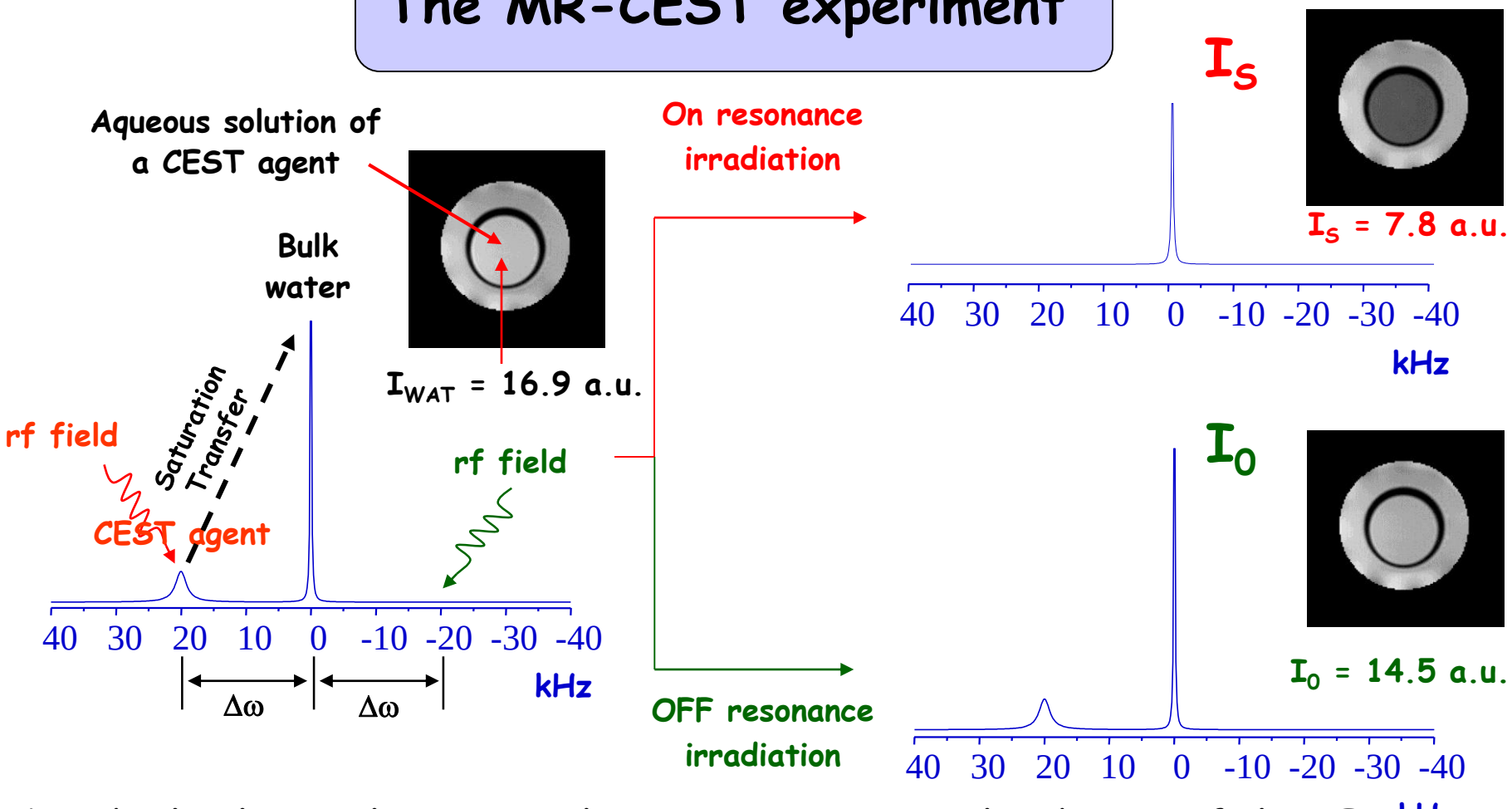

Drawback: the irradiation may decrease I_{WAT} even in the absence of the CEST agent

ON-OFF difference image

ST % = (1 - I_S/I_0)*100

46.2 %

ST-weighted image

The decr… I_{WAT} is the source o… contrast

The net S… ect is calculated as … /I_0) · 100

- presence of in… mobile protons (in biologi… *ca.* 100 KHz broad)

The MR-CEST experiment

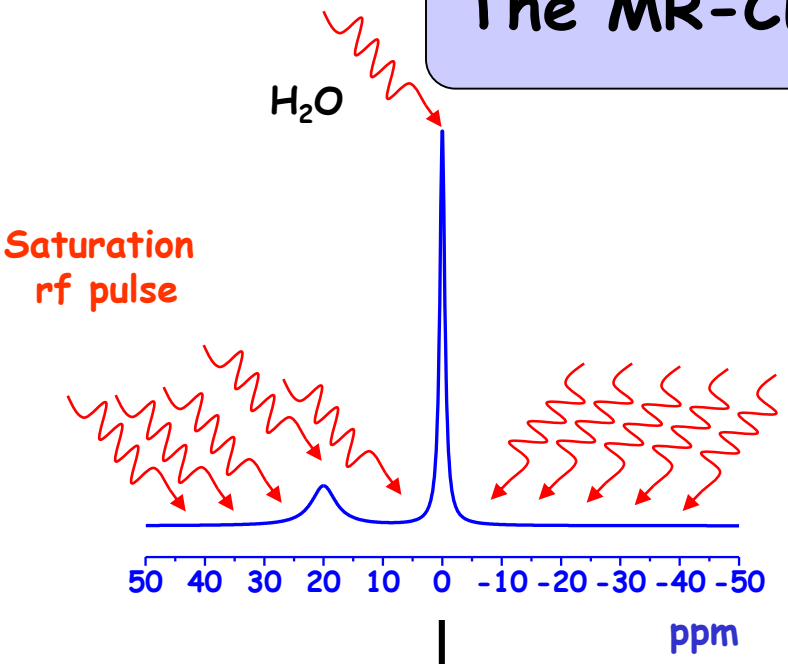

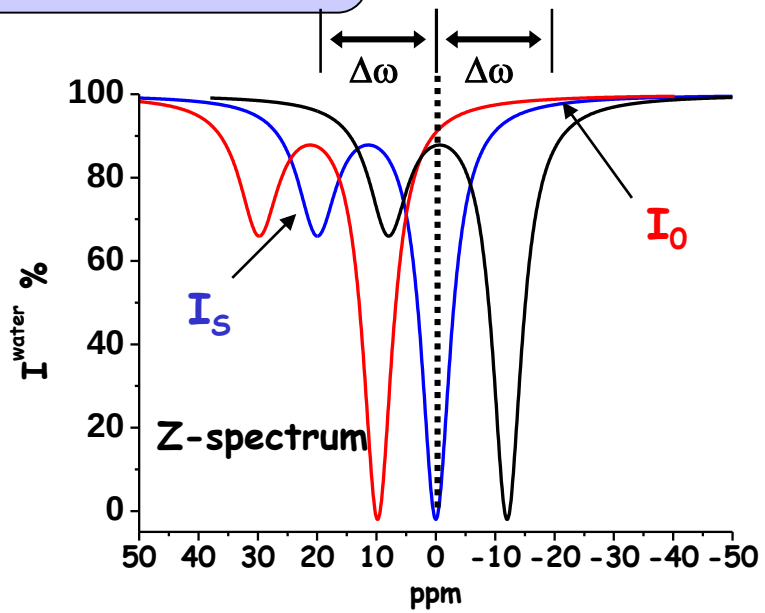

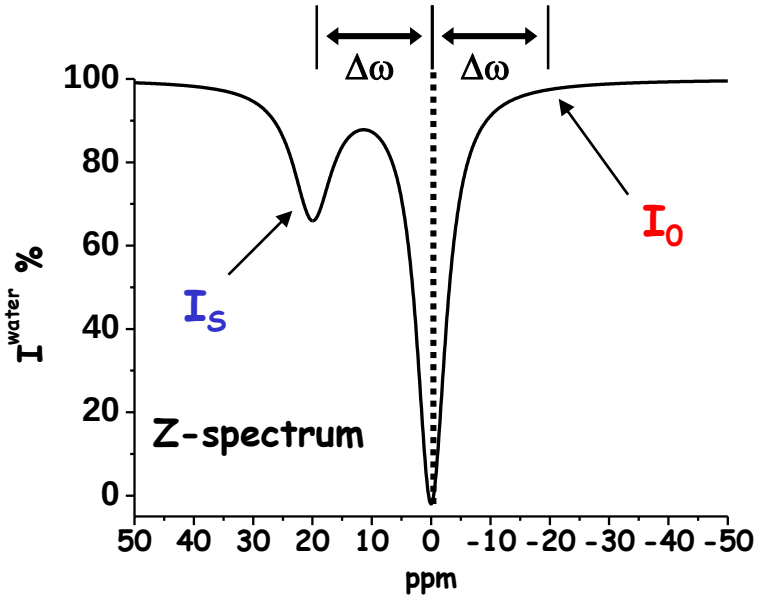

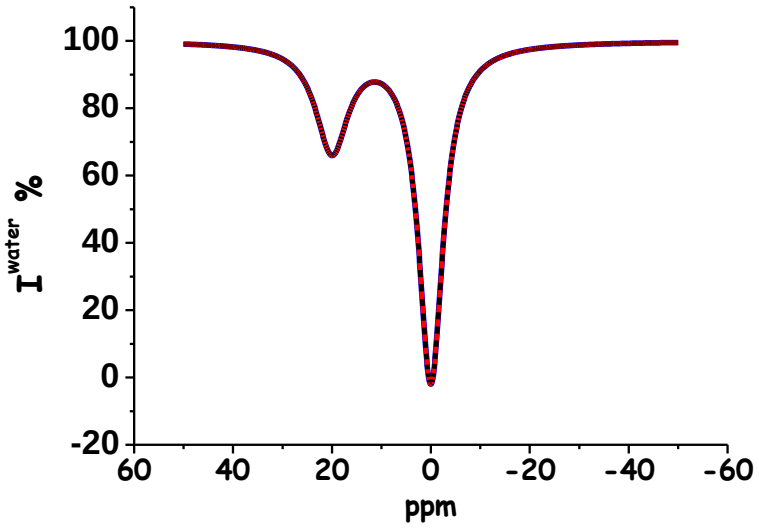

Main parameters affecting the CEST sensitivity

$$ST = 1 - \frac{I_S}{I_0} = \frac{k_{ex} f_{CEST}}{R_1^w + k_{ex} f_{CEST}} \left(1 - e^{-t_{sat}\left(R_1^w + k_{ex} f_{CEST}\right)}\right)$$

Where:

$$f_{CEST} = \frac{n[CA]}{2[BulkW]}$$

Exchange rate of the mobile protons belonging to the contrast agent(CA)

Sensitivity of CEST agents: playing with k_{ex}

In principle, the CEST efficiency is proportional to k_{ex}, but the exchange rate cannot be increased at will, because:

i) the condition $\Delta\omega > k_{ex}$ has to be satisfied

ii)

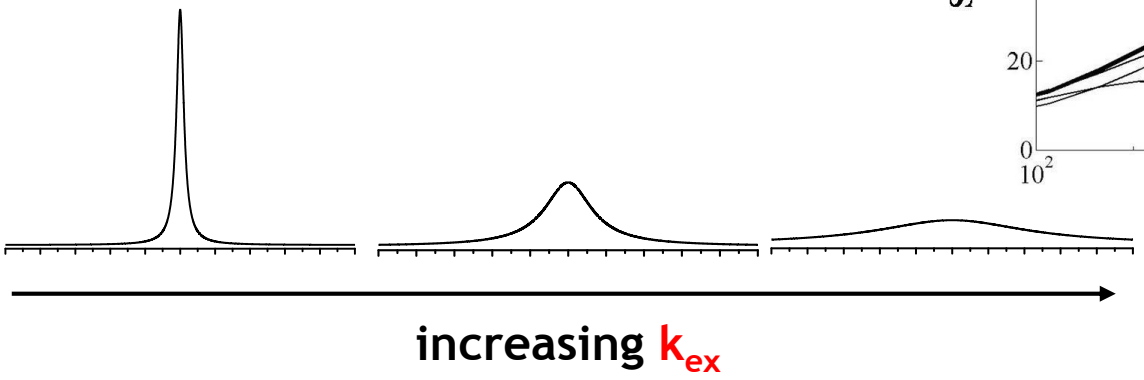

increasing k_{ex}

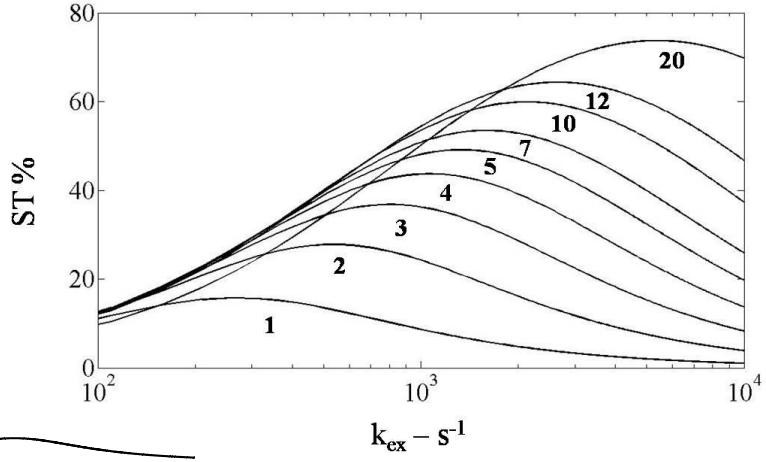

Max. CEST $\frac{k_{ex}}{B_2} = 2\pi$

Fast exchange requires high-intensity saturation fields for achieving full saturation

- overcoming SAR* limitations ➡ unsafe saturation
- direct saturation of bulk water ➡ less efficient CEST contrast

*SAR = Specific Absorption Rate. It is defined as the RF power absorbed per unit of mass of an object, and is measured in watts per kilogram (W/kg).*SAR* of 1 Wkg^{-1} applied for an hour would result in a temperature rise of about 1 °C.

Main parameters affecting the CEST sensitivity

$$ST = 1 - \frac{I_S}{I_0} = \frac{k_{ex} f_{CEST}}{R_1^w + k_{ex} f_{CEST}} \left(1 - e^{-t_{sat}\left(R_1^w + k_{ex} f_{CEST}\right)}\right)$$

Where:

$$f_{CEST} = \frac{n[CA]}{2[BulkW]}$$

Exchange rate of the mobile protons belonging to the contrast agent(CA)

Relaxation rate of the bulk water protons

$$ST = 1 - \frac{I_S}{I_0} = \frac{k_{ex} f_{CEST}}{R_1^w + k_{ex} f_{CEST}} \left(1 - e^{-t_{sat}\left(R_1^w + k_{ex} f_{CEST}\right)}\right)$$

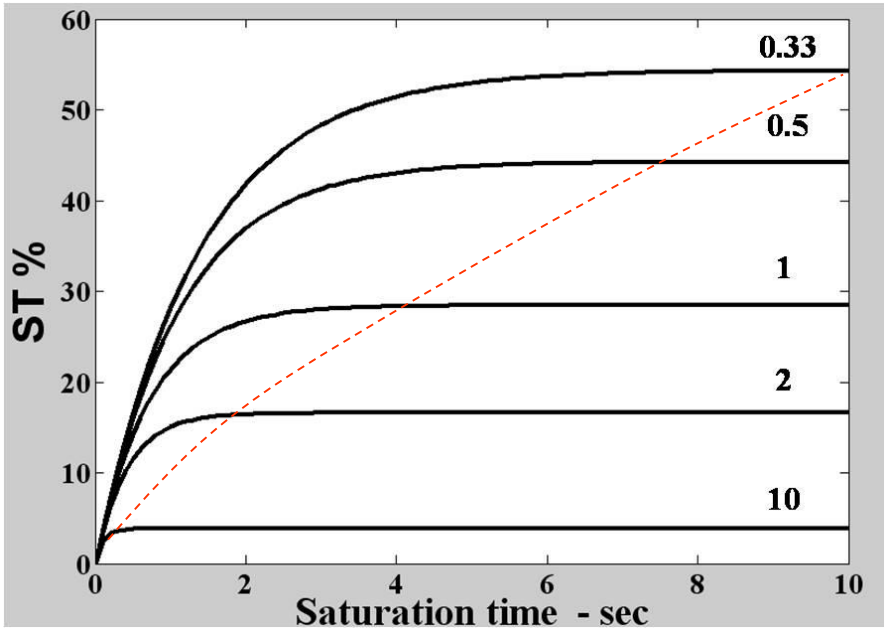

Increase of R_1 bulk water pool

Simulation parameters* f_{CEST}= 5×10^{-4}, R_2^{bw}= 2×R_1^{bw}, R_1^{CEST} = 2 s^{-1}, R_2^{CEST} = 50 s^{-1}, k^{CEST} = 1600 s^{-1}, B_2 = 6 μT
Woessner et al, MRM 2005

The steady-state condition is reached when $e^{-t^{sat}\left(R_1^{bw} + k_{ex}^{CEST} f_{CEST}\right)} = 0$

↓

In addition to R_1^{bw}, also an increase of the exchange rate accelerates the achievement of the steady state condition

$$ST = 1 - \frac{I_S}{I_0} = \frac{k_{ex} f_{CEST}}{R_1^w + k_{ex} f_{CEST}} \left(1 - e^{-t_{sat}\left(R_1^w + k_{ex} f_{CEST}\right)}\right)$$

Where:

$$f_{CEST} = \frac{n[CA]}{2[BulkW]}$$

Exchange rate of the mobile protons belonging to the contrast agent(CA)

Relaxation rate of the bulk water protons

Concentration of the contrast agent

Number of magnetically equivalent mobile protons

Sensitivity of CEST agents: increasing the number of saturated protons

The CEST efficiency is proportional to the number of mobile protons

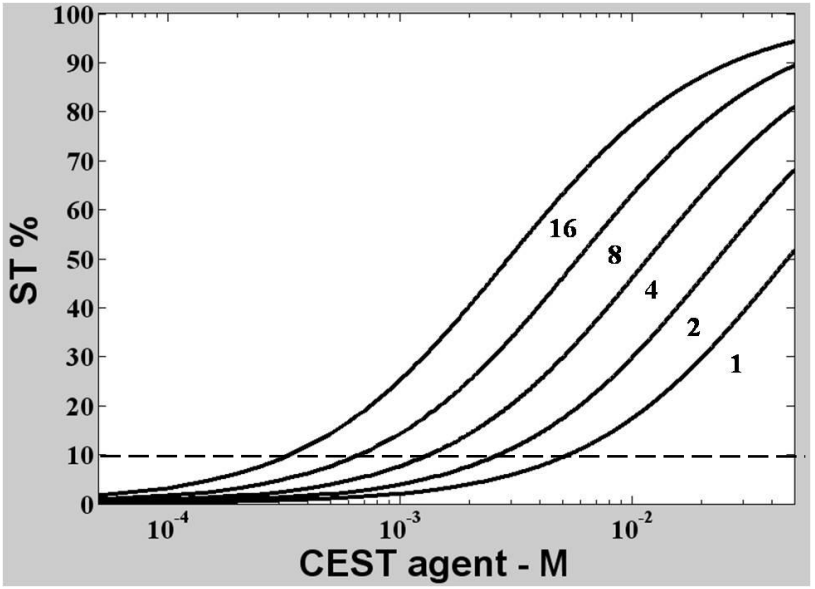

A CEST contrast of 10% requires few millimolar of mobile protons

The sensitivity can be improved by increasing the number of mobile protons (with equal or similar $\Delta\omega$ values) per CEST molecule

Mobile protons	Sensitivity	Chemical system
< 10	mM	Low MW molecules
10^3	μM	Macromolecules
10^6	nM	Nanoparticles

$$ST = 1 - \frac{I_S}{I_0} = \frac{k_{ex} f_{CEST}}{R_1^w + k_{ex} f_{CEST}} \left(1 - e^{-t_{sat}\left(R_1^w + k_{ex} f_{CEST}\right)}\right)$$

Where:

$$f_{CEST} = \frac{n[CA]}{2[BulkW]}$$

Exchange rate of the mobile protons belonging to the contrast agent(CA)

Relaxation rate of the bulk water protons

Concentration of the contrast agent

Number of magnetically equivalent mobile protons

Experimental parameter: irradiation time

Optimizing the saturation scheme

The overall saturation time can be covered by:

- **a single cw rectangular pulse**

- **a train of shaped pulses**

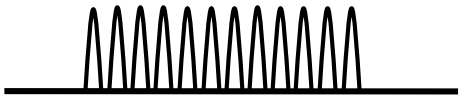

Single cw saturation pulses (2-10 s long) have been observed to be more efficient in case of probes with relatively slow exchange: DIACEST (B_2 1-3 μT), PARACEST (typically amide protons or slowly exchanging Ln-bound water protons, B_2 12-24 μT), and LipoCEST (B_2 6-12 μT)

BUT

Pulsed shaped pulses are definitely better in terms of deposited energy and clinical translation

CEST agents: the sensitivity issue

CEST contrast is quite sensitive because few millimolar of saturated mobile protons are sufficient to affect the MRI signal (> 100 molar)

However, the development of highly sensitive agents is an hot issue, especially for molecular imaging purposes.

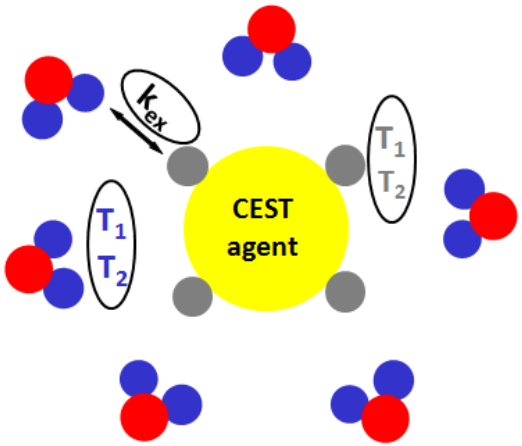

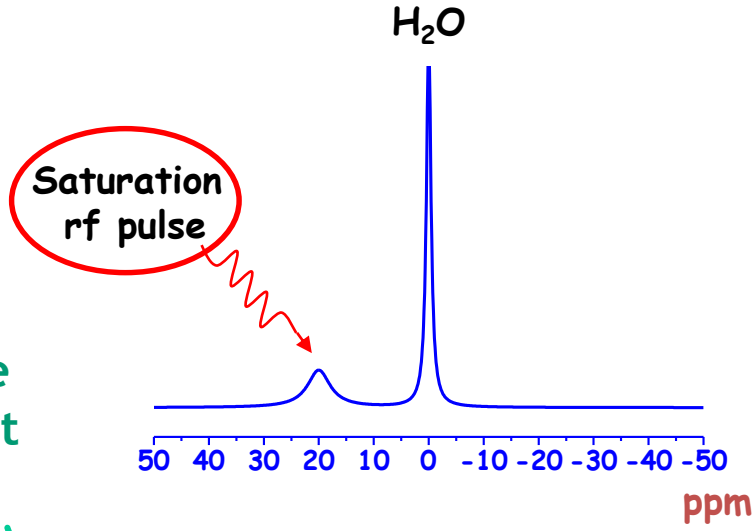

Variables affecting the CEST contrast

- Exchange rate of the CEST protons
- Total concentration of saturated spins
- T_1 and T_2 of both the exchanging sites
- Duration of saturation time
- Saturation scheme (cw, pulsed)
- Saturation pulse power
- Magnetic field strength (affects $\Delta\omega$, T_1 and T_2)

CEST agents: the sensitivity issue

- **Low sensitivity**, lower than classical T_1 and T_2 MRI probes

Main issues to improve CEST agents sensitivity

The ST efficiency ∝ k_{ex}

(But Δω has to be > than k_{ex})

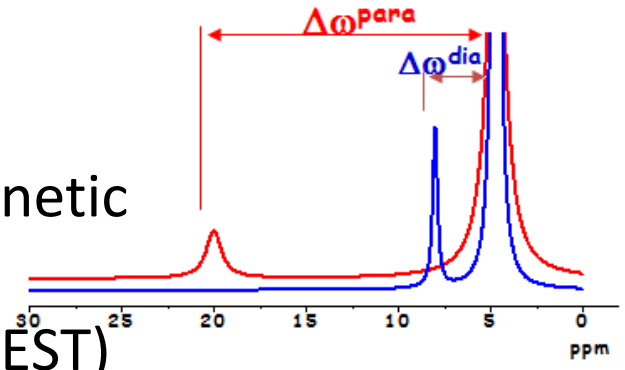

✓Use of paramagnetic probes (PARACEST)

The ST efficiency ∝ number of mobile protons

✓Use of nano-syster

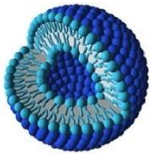

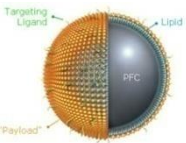

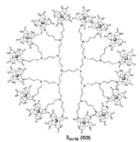

CEST *vs* conventional CAs: advantages

CEST agents do not require a pre-contrast image (the contrast is detected by comparing two post-contrast experiments)

Responsiveness (ST effects may be made independent of the agent concentration)

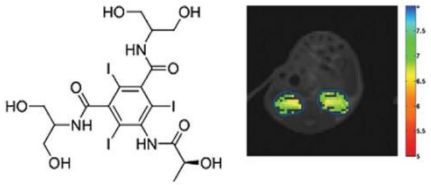

Longo DL, Aime S. et al. 2011, 65:202–211

CEST agents

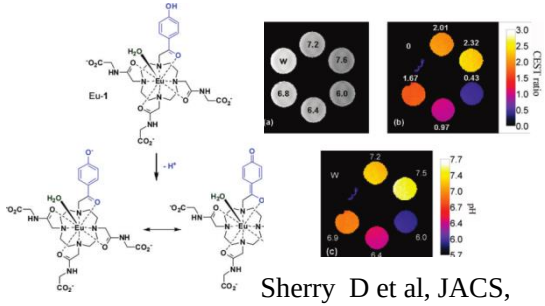

Sherry D et al, JACS, 2010, 132 (40)

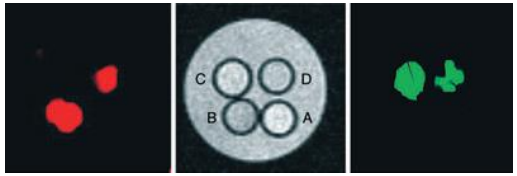

Aime S et al. , Angew. Chem. Int. Ed., 2005, 44, 1813

Multiplex visualization

More CEST agents can be visualised in the same image (provided that their saturation frequencies are not overlapped)

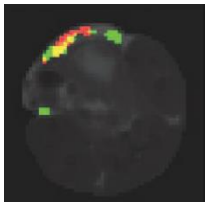

Ferrauto G. et al. MRM, 2011; 69: 1703–1711.

CEST agents vs conventional MRI contrast agents

3D-Gd-MR Angiography

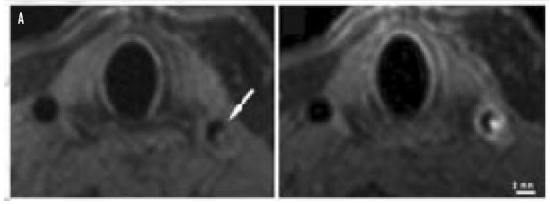

Gd-based fibrin-targeting agent
(visualisation of non-occlusive thrombi)

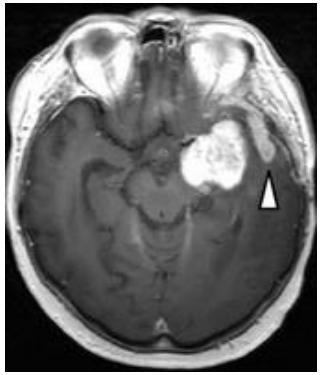

Gd-enhanced MR images
(Glioma)

Do we actually need a new class of MRI agent ?

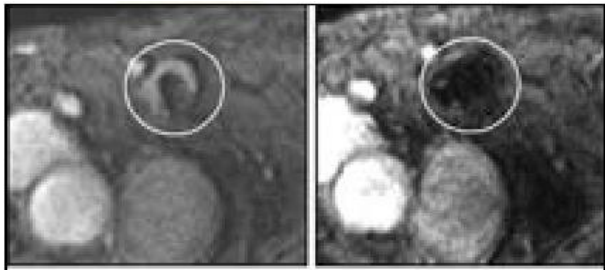

MRI cell tracking experiment
(Limph node targeting by tumor specific SPIO-labeled dendritic cells)

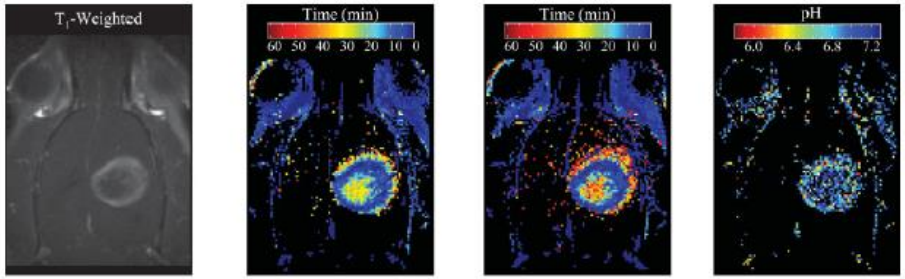

in vivo pH mapping of tumors

Multiple visualization of MRI agents

In vivo **multiple visualization of MRI probes would considerably improve the potential of MRI in many molecular imaging experiments (e.g. multi-detection of epitopes, simultaneous tracking of different cell populations, dynamic measurements,...)**

Example: vivo **Fluorescence image of a lymph node**

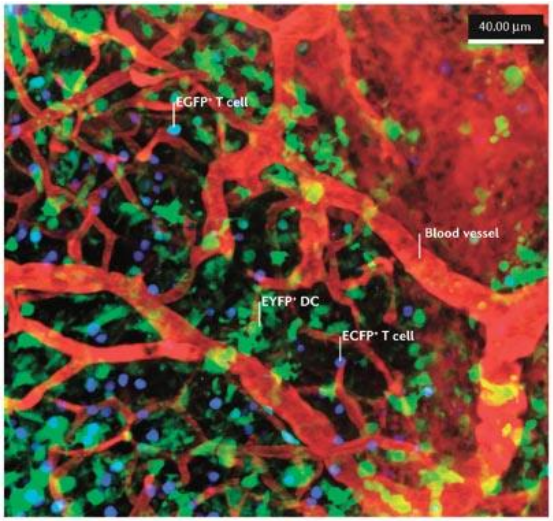

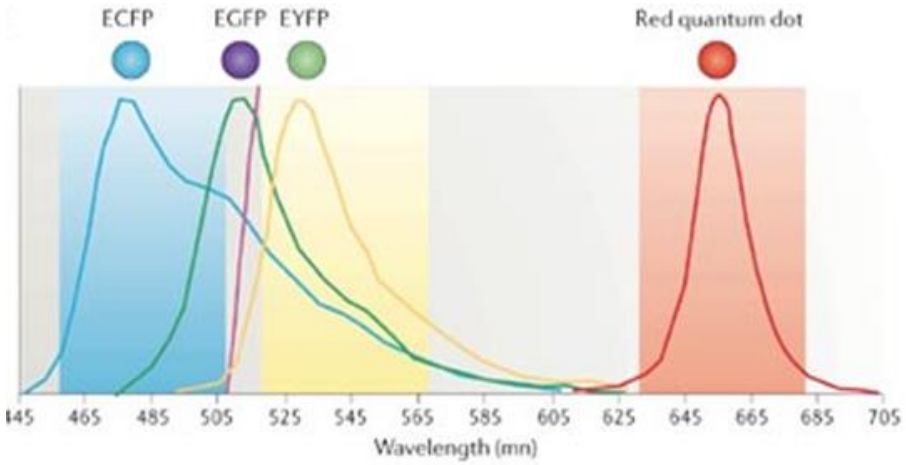

R .N. Germain *et al, Nature Rev. Imm., 2006, 6, 497*

Can we get similar results using MRI agents?

NMR provides a parameter that can characterise any molecule:

the resonance frequency of its spins

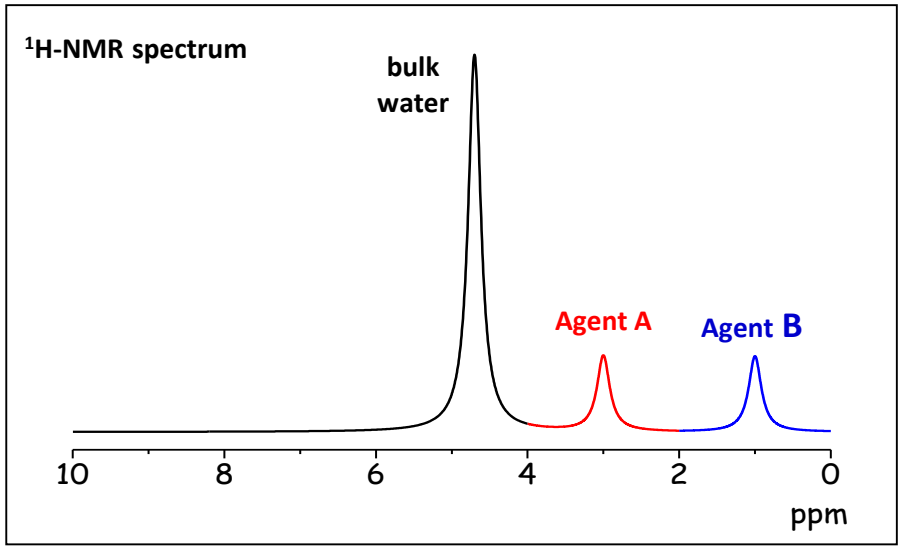

Multiple detection can be achieved by generating a "frequency encoded" contrast

For imaging purposes, this information must be transferred to the intensity of bulk water protons

CEST agents vs conventional MRI agents

MULTIPLE DETECTION

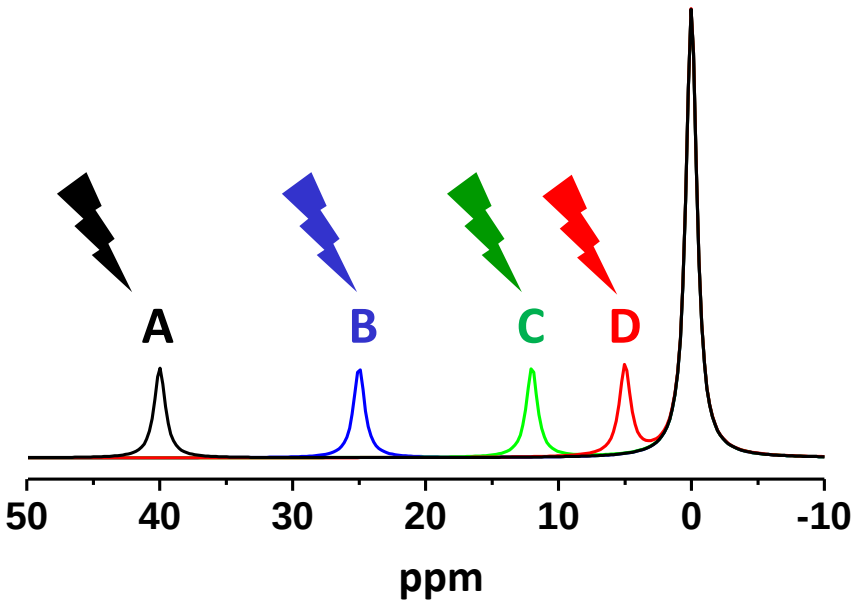

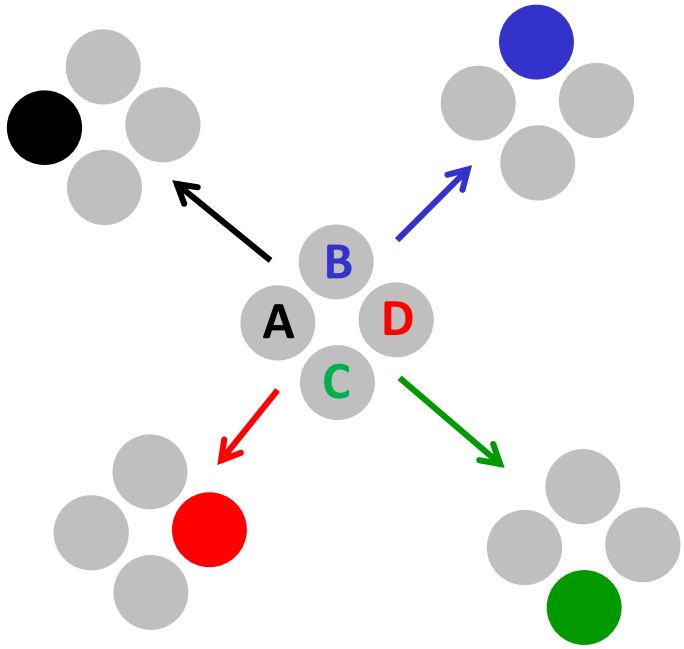

Multicolor MRI

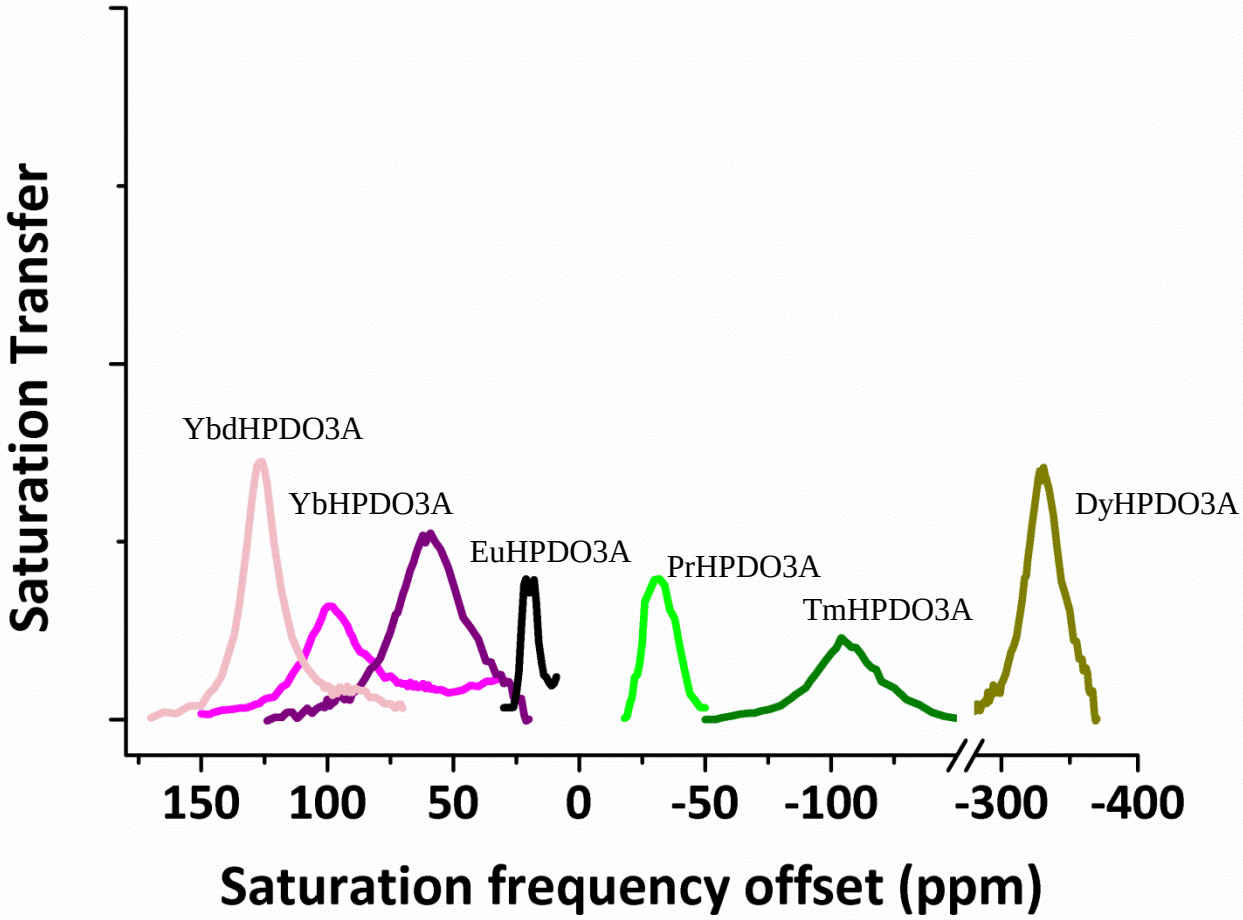

Multicolor MRI

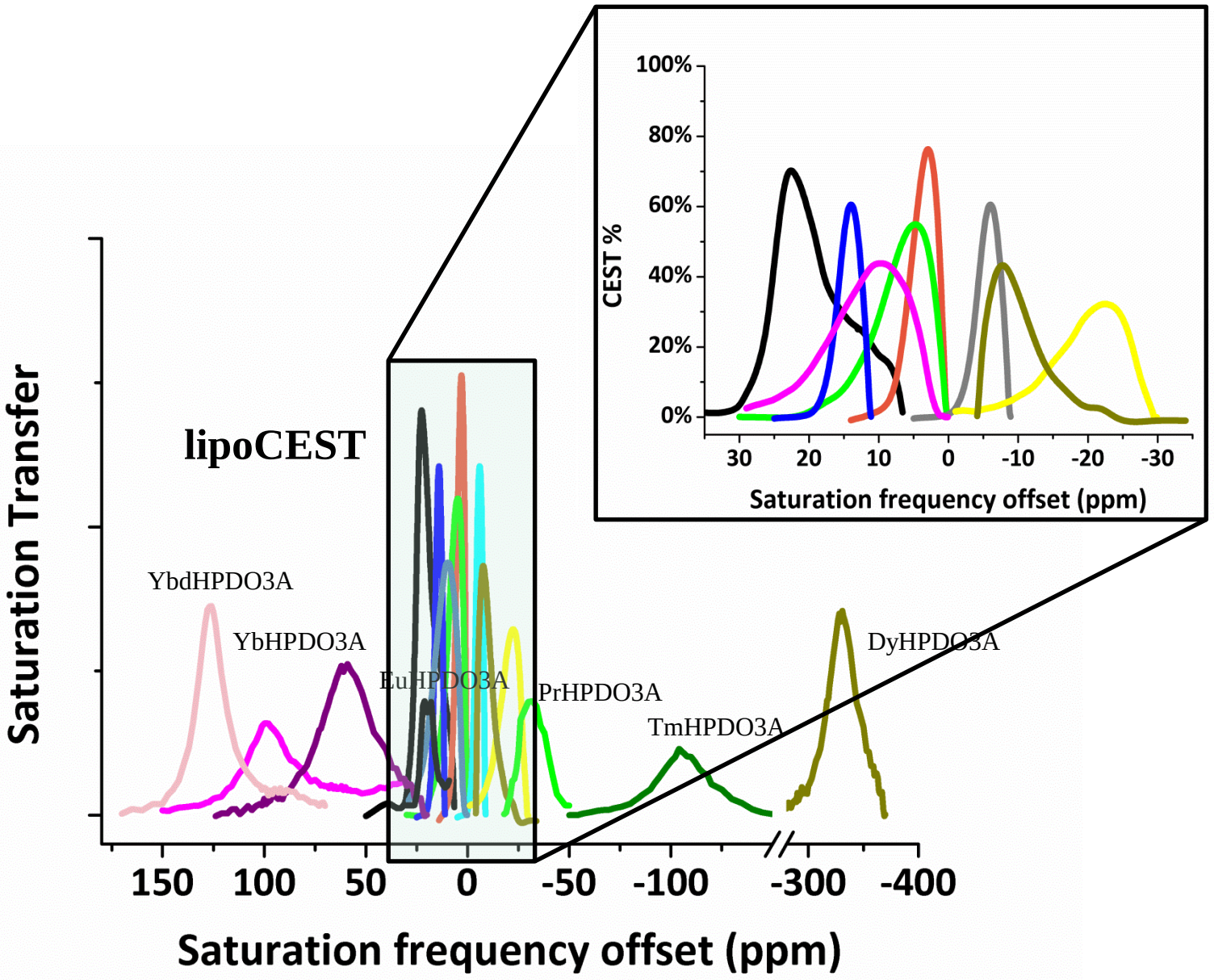

Multicolor MRI

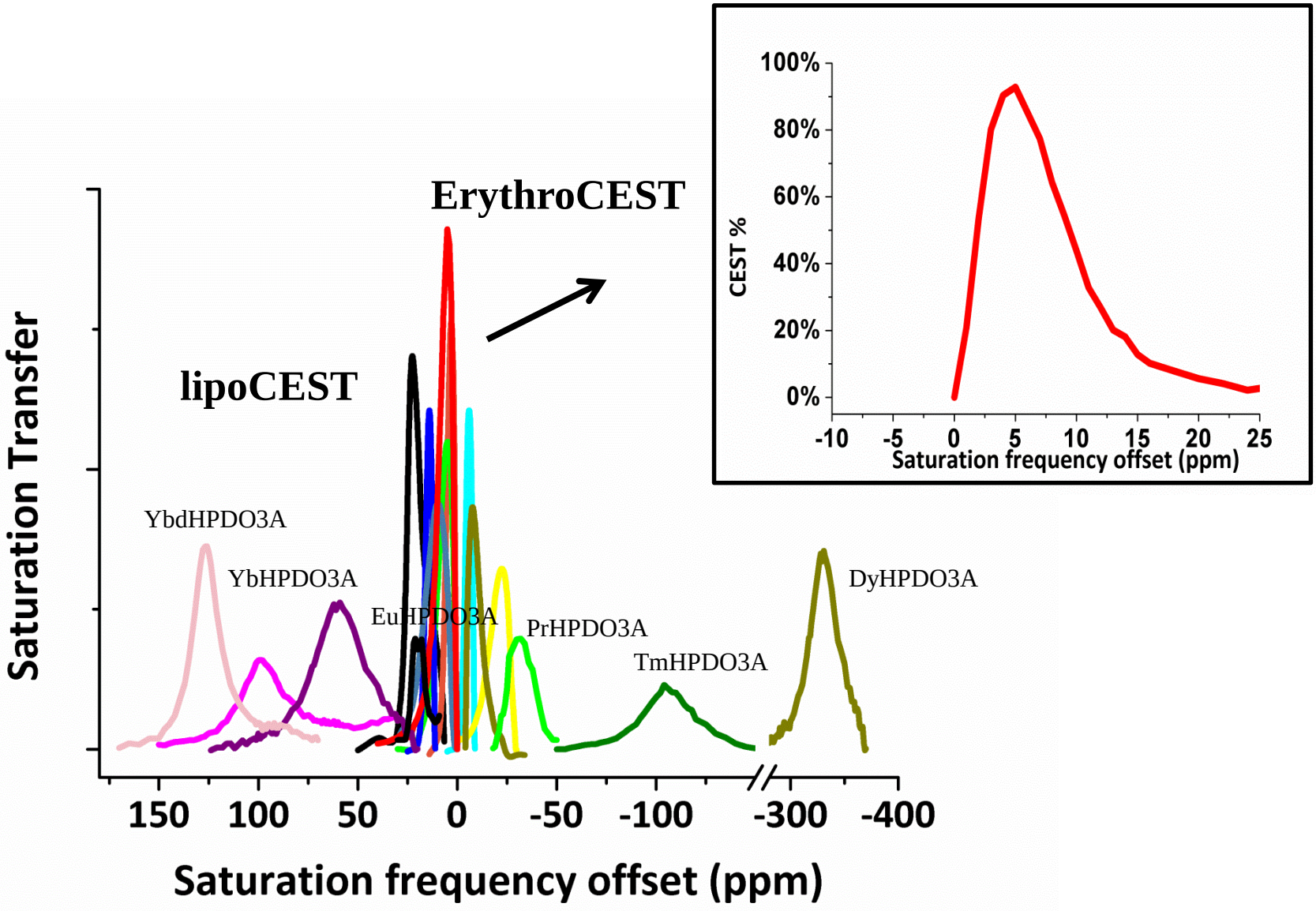

Concentration dependence of the MRI contrast

$$ST = 1 - \frac{I_S}{I_0} = \frac{k_{ex} f_{CEST}}{R_1^w + k_{ex} f_{CEST}} \left(1 - e^{-t_{sat}\left(R_1^w + k_{ex} f_{CEST}\right)}\right)$$

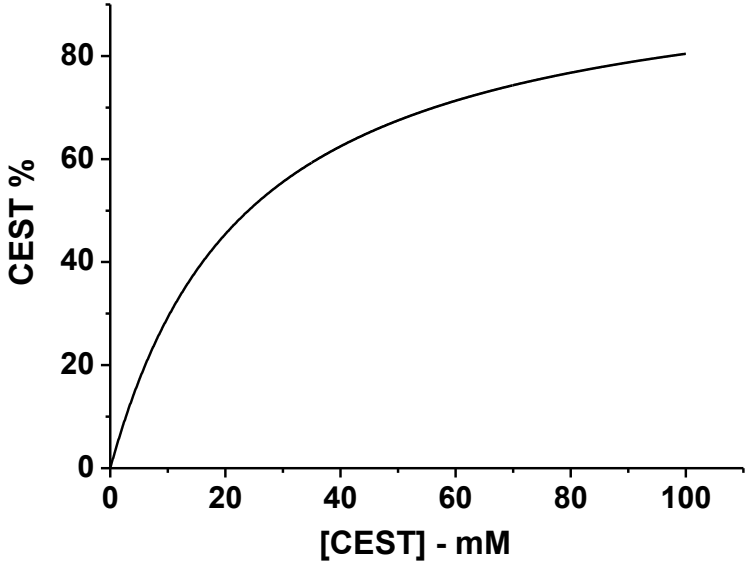

Where:

$$f_{CEST} = \frac{n[CA]}{2[BulkW]}$$

Responsive contrast requires the MRI observable to depend only on the parameter of interest

A ratiometric analysis of the intensity of the water signal after the irradiation of two different mobile pools allows to get rid of the concentration of the MRI probes

CEST agents are very suitable Responsive probes

Ratiometric analysis

$$ST = 1 - \frac{I_S}{I_0} \quad (1); \qquad \frac{I_S}{I_0} = \frac{1}{1 + k_{bw} T_{1w}} \quad (2); \qquad k_{bw} = \frac{k_{ex} n [CA]}{2[BulkW]} \quad (3);$$

by substitution of eq.3 into eq.2 $\longrightarrow$ $$\frac{I_S}{I_0} = \frac{1}{1 + \frac{k_{ex} n [CA]}{2[BulkW]} T_{1w}} \quad (4);$$

$\longrightarrow$ $$\frac{I_0}{I_S} = 1 + \frac{k_{ex} n [CA] T_{1w}}{2[BulkW]} \quad (5); \longrightarrow \frac{I_0}{I_S} - 1 = \frac{k_{ex} n [CA] T_{1w}}{2[BulkW]}$$

If two exchanging pools (A and B) are present in a known ratio (*R*) then...

$$\frac{\left(\frac{I_0}{I_S} - 1\right)^{poolA}}{\left(\frac{I_0}{I_S} - 1\right)^{poolB}} = \frac{\frac{k_{ex}^A n^A [CA]^A T_{1w}}{2[BulkW]}}{\frac{k_{ex}^B n^B [CA]^B T_{1w}}{2[BulkW]}} = \frac{k_{ex}^A n^A [CA]^A}{k_{ex}^B n^B [CA]^B} = \frac{k_{ex}^A}{k_{ex}^B} R$$

Classification of CEST agents

Diamagnetic CEST agents

Paramagnetic CEST agents

Diamagnetic - *vs.* Paramagnetic -CEST agents

$\Delta\omega > k_{ex}$

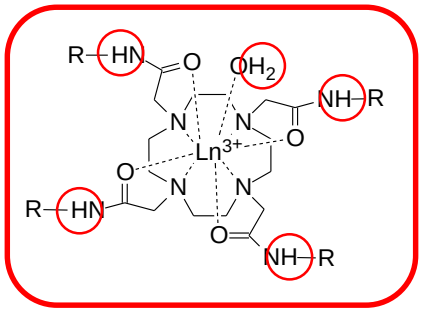

PARACEST

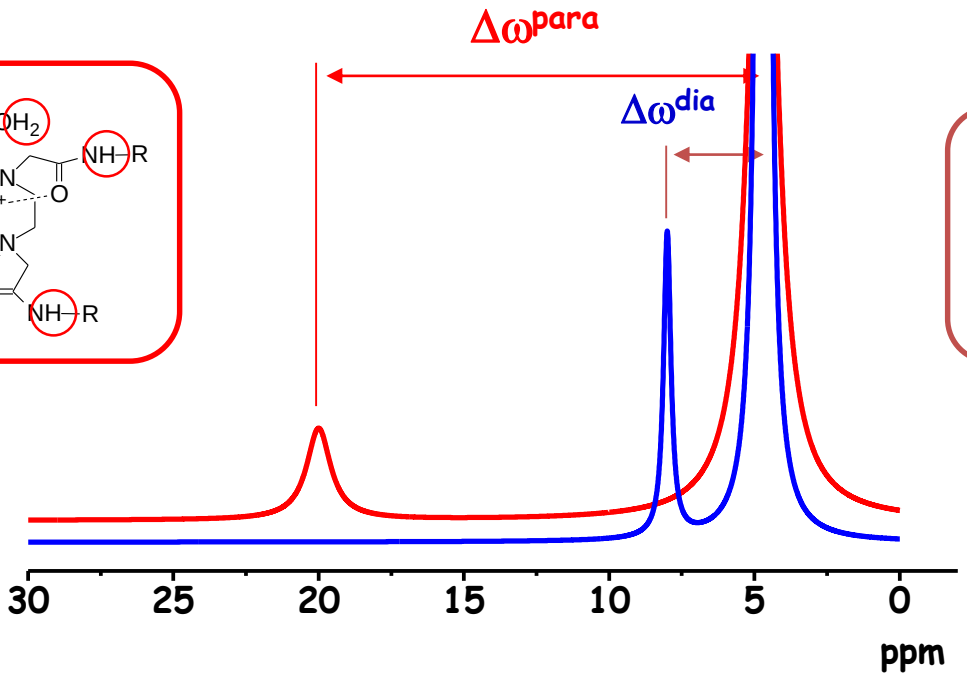

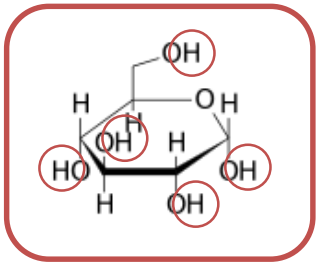

DIACEST

The extension of the $\Delta\omega$ range facilitates multiple visualization and allow to exploit larger exchange rate before coalescence takes place, but the associated line broadening may introduce SAR issues and the T_1 and T_2 shortening may be detrimental for the CEST eficacy

Field homogeneity and highly shifted agents

The detrimental effect of B_0 inhomogeneity progressively vanishes moving away from the resonance of the bulk water

mouse bearing a
B16 melanoma xenograft

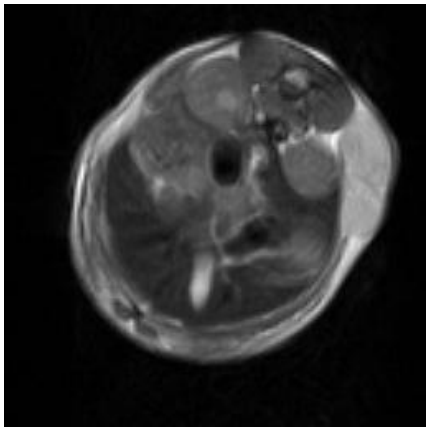

Morphological T_{2w}- image

(B_2 6 μT)

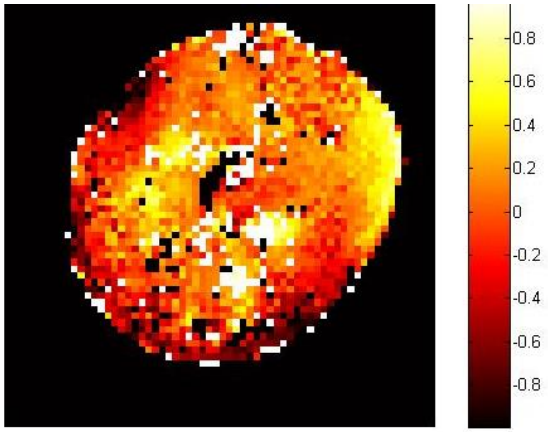

Water shift map

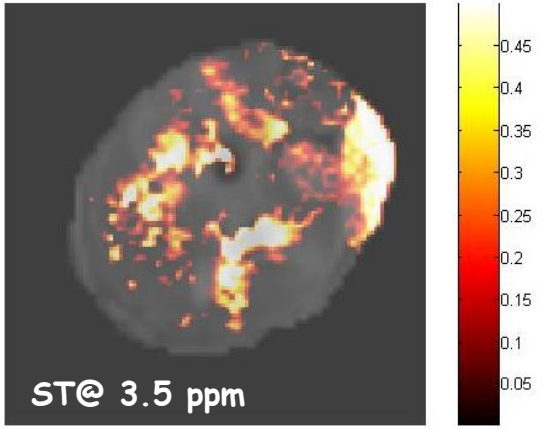

Uncorrected CEST maps

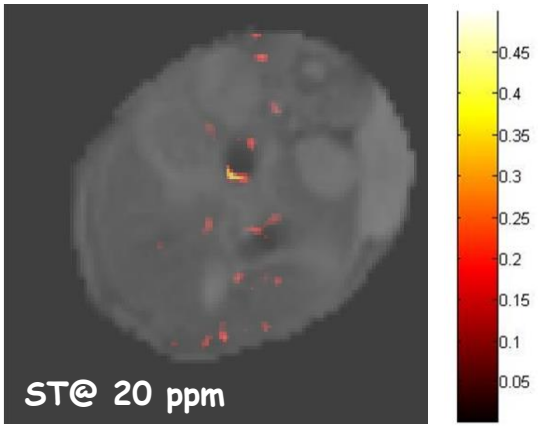

Highly shifted CEST agents can be accurately detected by a simple two scans experiments

Classification of CEST agents

K. M. Ward,[1] A. H. Aletras, and R. S. Balaban[2]

Journal of Magnetic Resonance **143,** 79–87 (2000)

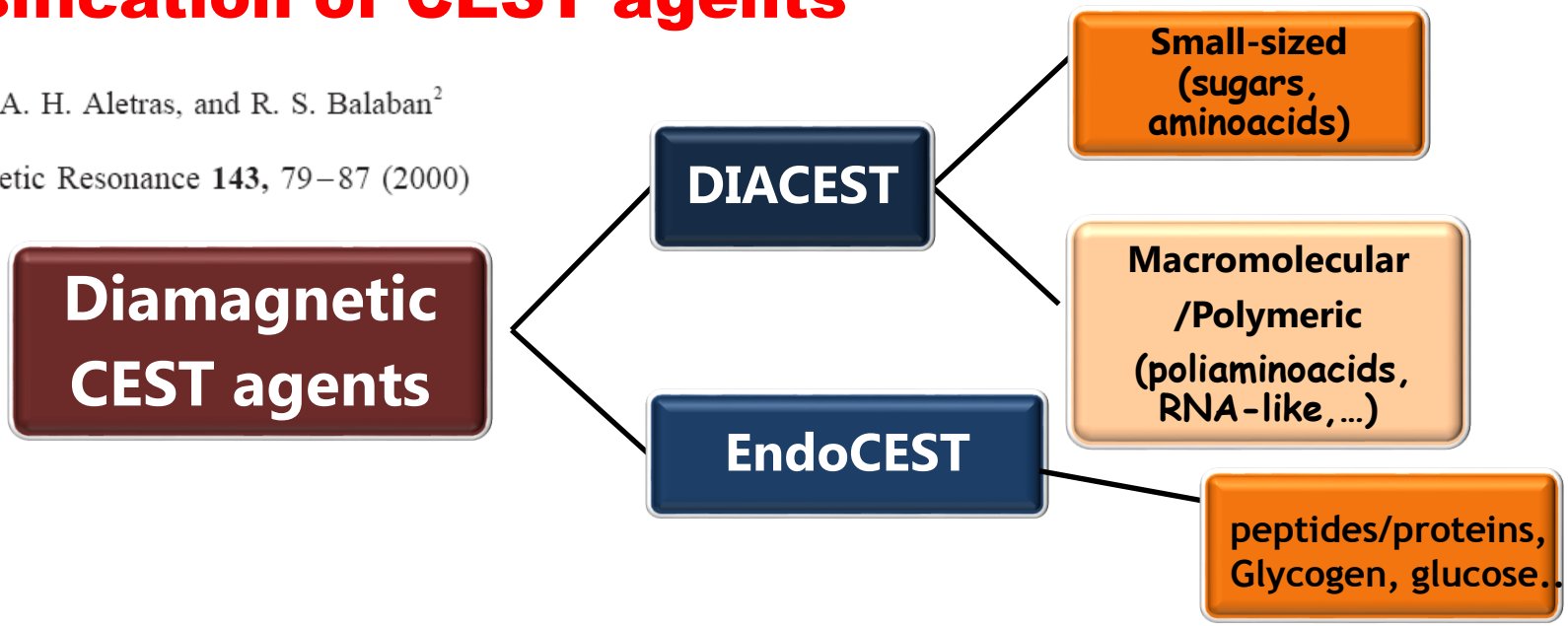

Paramagnetic CEST agents

Endogenous CEST agents : APT imaging

Magnetic Resonance in Medicine 56:585–592 (2006)

Amide Proton Transfer Imaging of Human Brain Tumors at 3T

Craig K. Jones,[1,2] Michael J. Schlosser,[3] Peter C.M. van Zijl,[1,2] Martin G. Pomper,[2] Xavier Golay,[1,2,4] and Jinyuan Zhou[1,2*]

Human patient with a meningioma (3 T)

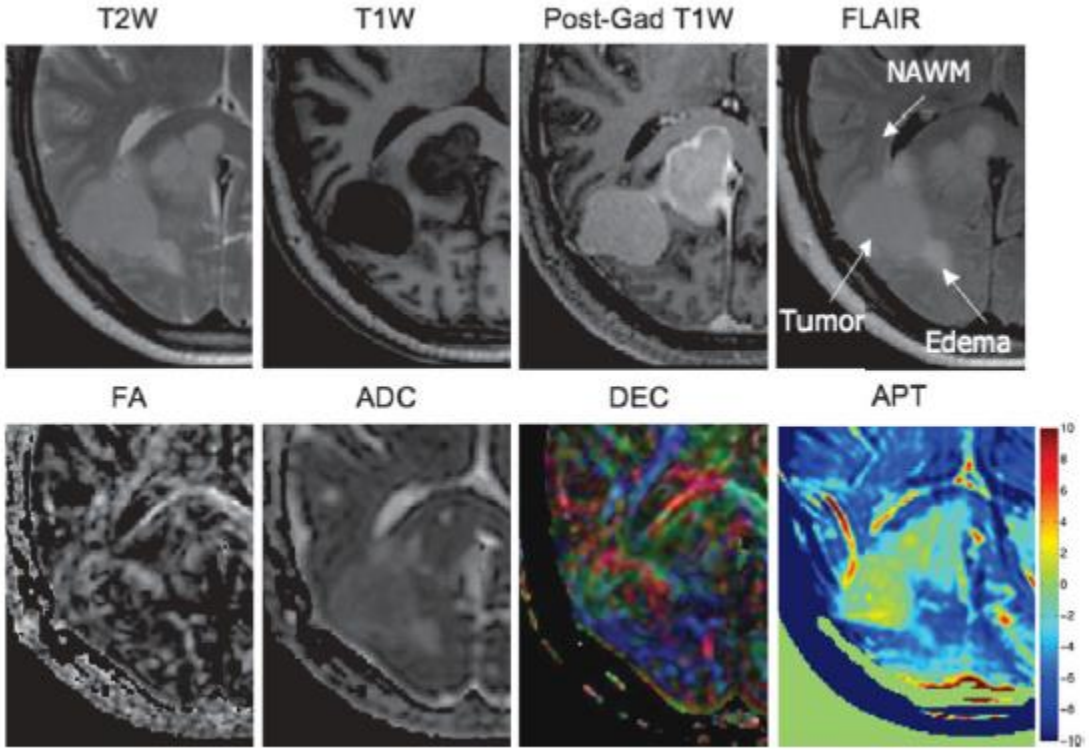

APT imaging may help to discriminate between tumor and edema

Classification of CEST agents

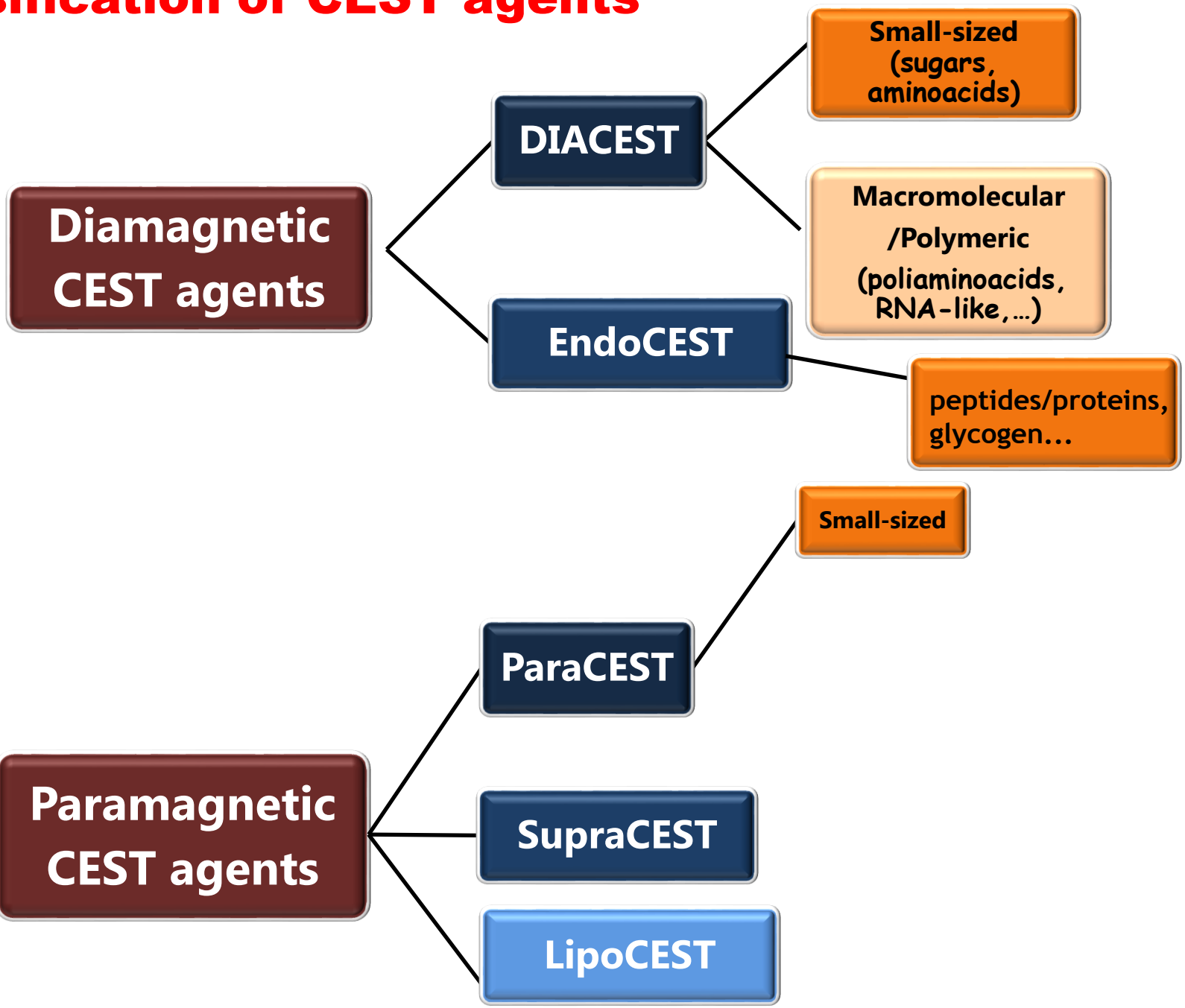

A Novel Europium(III)-Based MRI Contrast Agent

Shanrong Zhang,[†] Patrick Winter,[‡] Kuangcong Wu,[†] and A. Dean Sherry*[,†,‡]

J. Am. Chem. Soc. **2001,** *123,* 1517−1518

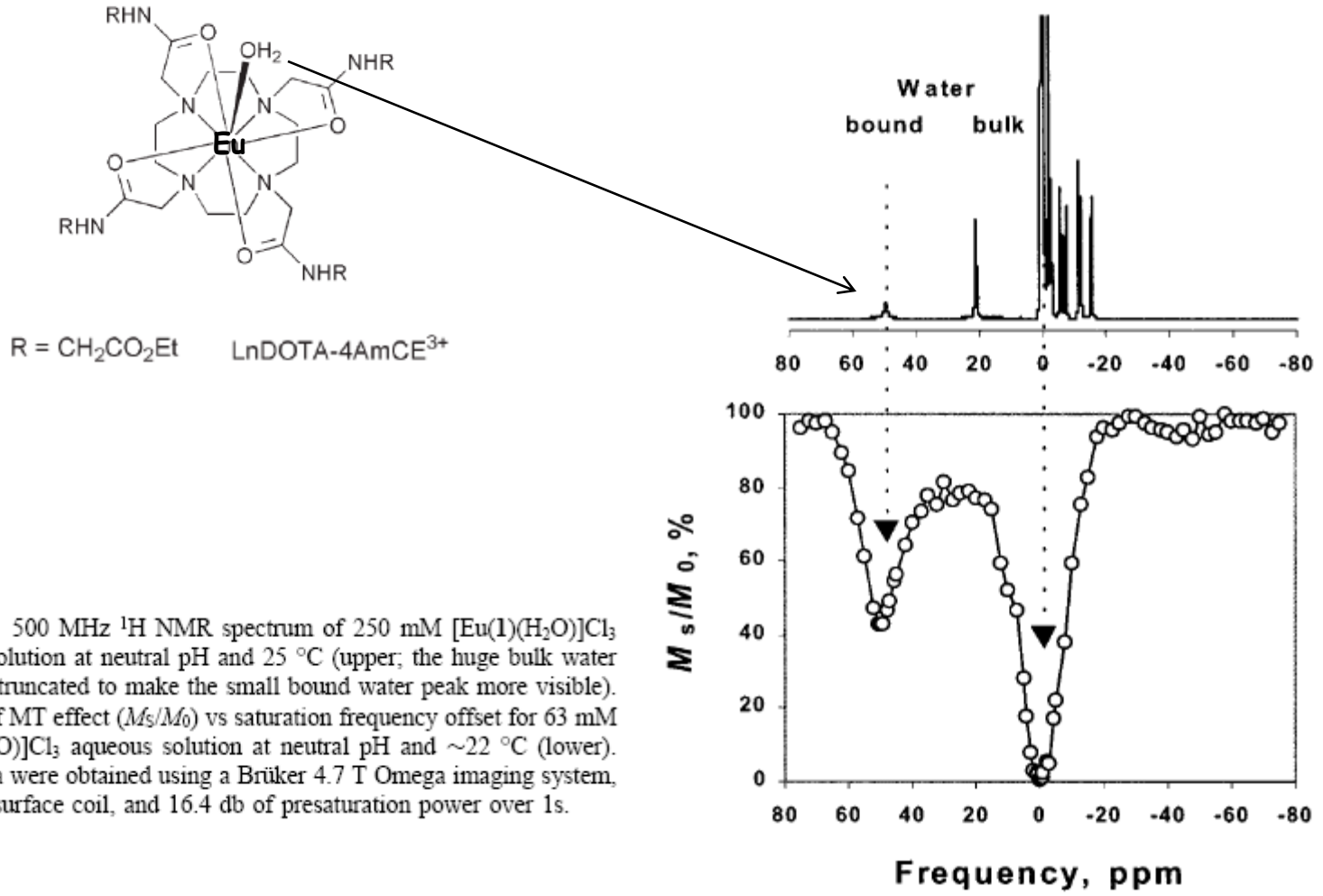

Figure 1. 500 MHz ^{1}H NMR spectrum of 250 mM [Eu(1)(H_2O)]Cl_3 aqueous solution at neutral pH and 25 °C (upper; the huge bulk water peak was truncated to make the small bound water peak more visible). A curve of MT effect (M_S/M_0) vs saturation frequency offset for 63 mM [Eu(1)(H_2O)]Cl_3 aqueous solution at neutral pH and ~22 °C (lower). These data were obtained using a Brüker 4.7 T Omega imaging system, a 2.5 cm surface coil, and 16.4 db of presaturation power over 1s.

Controlling the variation of axial water exchange rates in macrocyclic lanthanide(III) complexes†

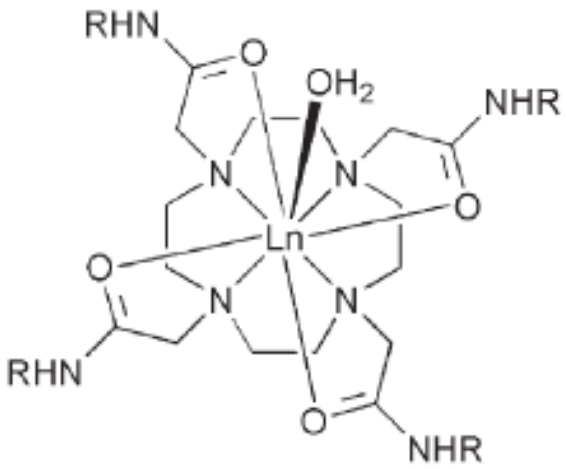

R =	H	**DOTAM**	
R =	CH_2CO_2Et	**1**	
R =	$CH_2COOtBu$	**2**	
R =	CH_2Ph	**3**	
R =	CH_2CO_2nBu	**4**	
R =	$CH_2CO_2CH_2Ph$	**5**	
R =	CH(Me)Ph	**6**	

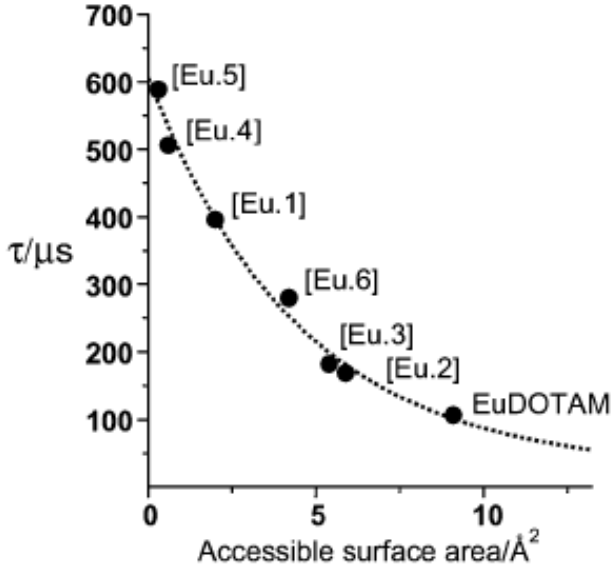

Chem. Commun.,2002, 1120-1121

Novel pH-Reporter MRI Contrast Agents**

Angew. Chem. Int. Ed. **2002**, *41*, No. 22

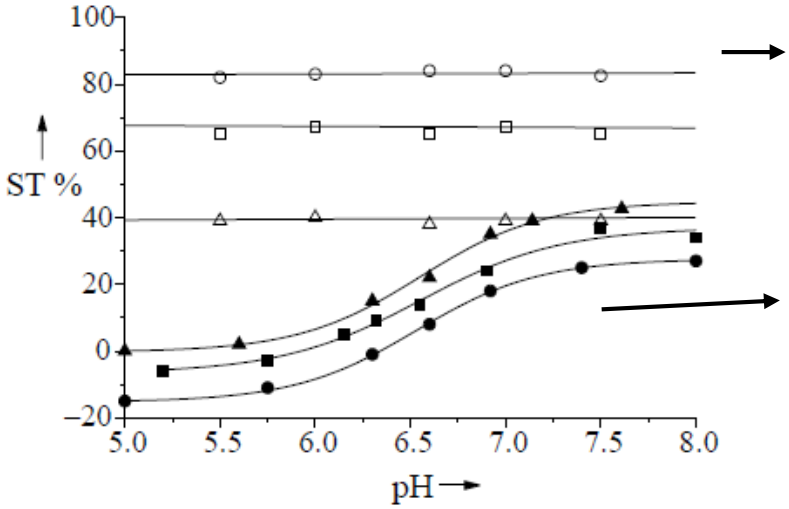

Irradiation of metal bound water protons

Irradiation of amide protons

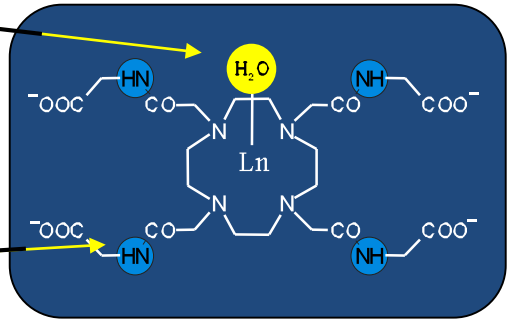

- 4 equivalent amide protons of the ligand
- 2 equivalent metal-coordinated water protons

$$\frac{\left(\frac{I_0-I_S}{I_0}\right)_{NH}}{\left(\frac{I_0-I_S}{I_0}\right)_{H_2O}} = \frac{n^{NH}\,k_{NH}\,R_{1,irr}^{H_2O}}{n^{H_2O}\,k_{H_2O}\,R_{1,irr}^{NH}}$$

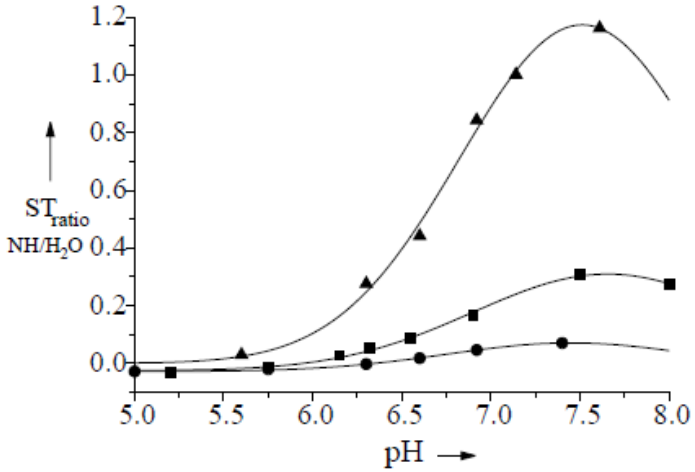

Ln-HPDO3A complexes as PARACEST agents

Gd(III)HPDO3A

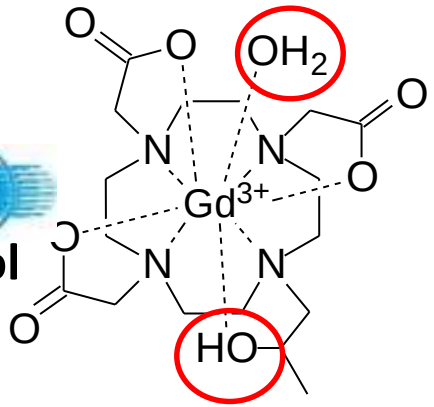

ProHance

Gadoteridol

Ln≠Gd

Yb(III)HPDO3A

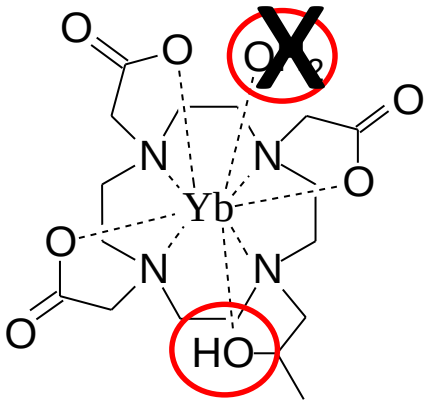

Fast Exchange

$k_{ex} > \Delta\omega$

'Clinically safe' (but approval required)

58	59	60	61	62	63	64	65	66	67	68	69	70	71
Ce	Pr	Nd	Pm	Sm	Eu	Gd	Tb	Dy	Ho	Er	Tm	Yb	Lu
140,1	140,9	144,2	(144,9)	150,4	152,0	157,3	158,9	162,5	164,9	167,3	168,9	173,0	175,0

Yb-HPDO3A for measurement of pH and temperature

SAP

TSAP

SAP/TSAP: 70:30

^{1}H-NMR - Yb-HPDO3A – D_2O - 14 T – 15 °C

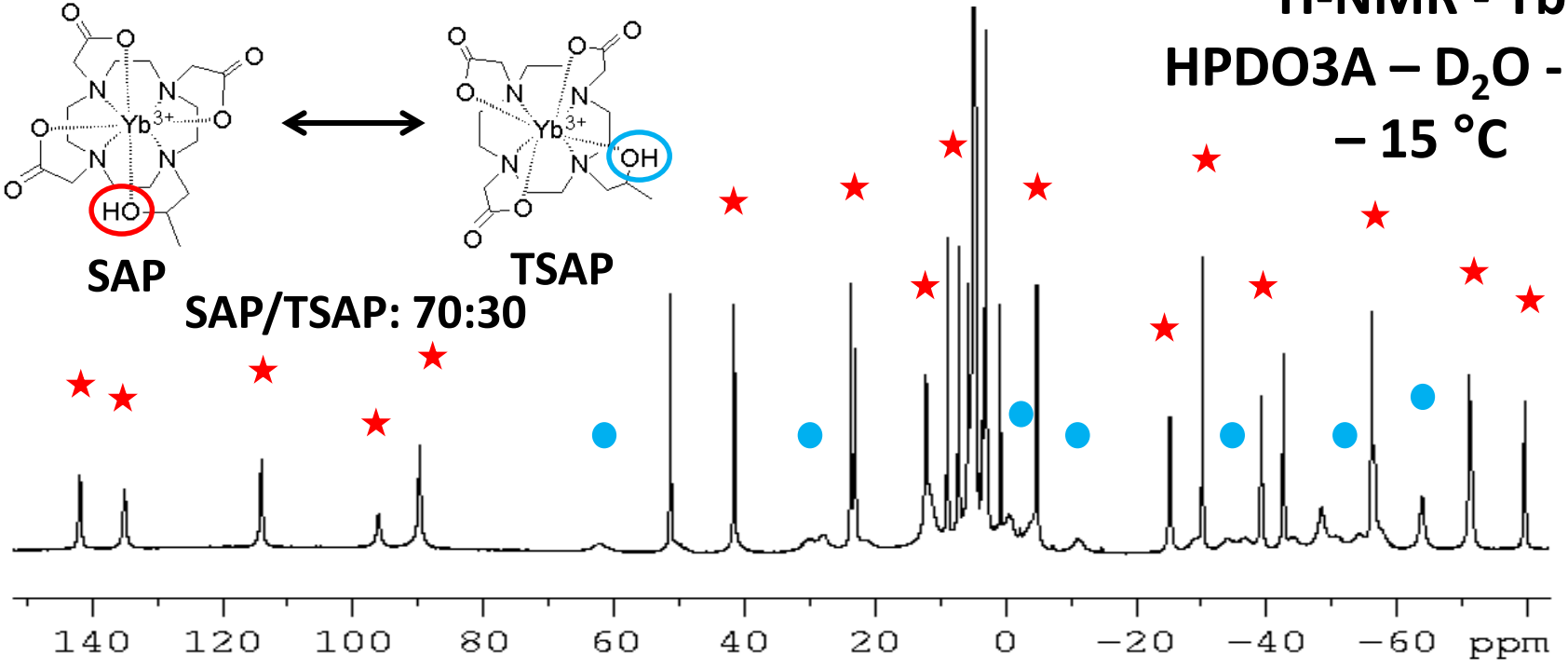

Yb-HPDO3A for measurement of pH and temperature

SAP TSAP

SAP/TSAP: 70:30

^{1}H-NMR - Yb-HPDO3A – D_2O - 14 T – 15 °C

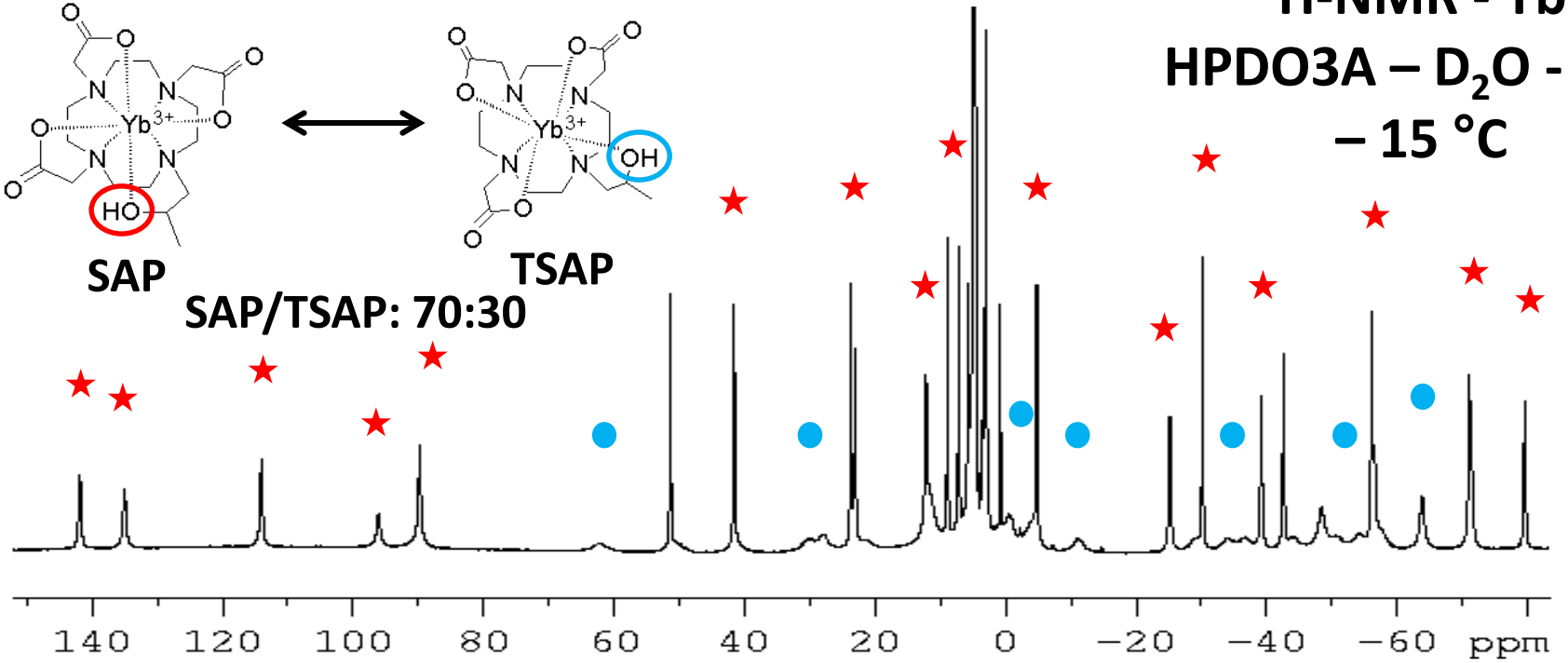

pH=5.05 20°C

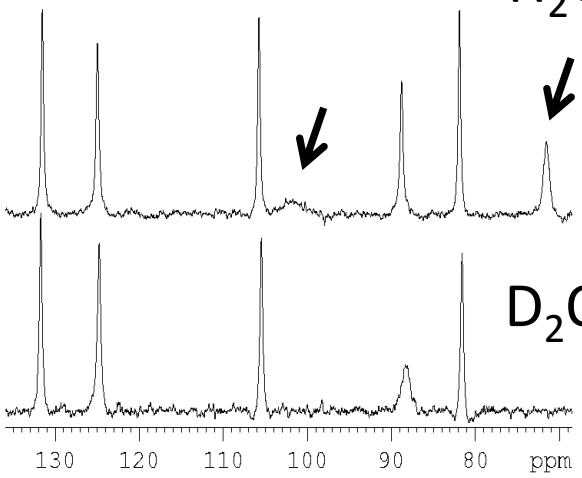

Z-spectrum 20°C pH 7.4 irr. power 24 µT

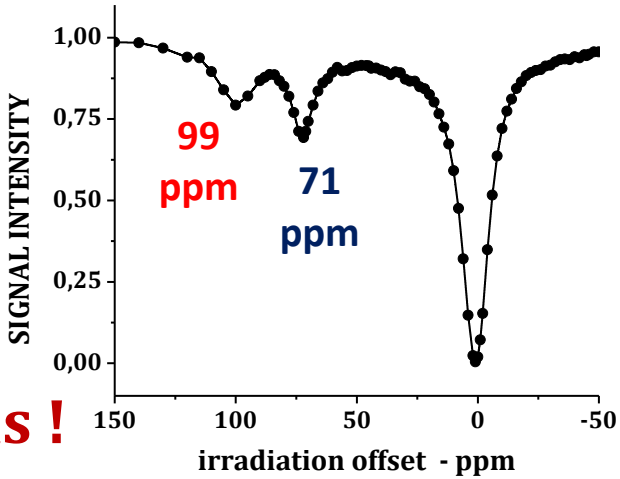

Two isomers in solution

Two OH signals !

Yb-HPDO3A for measurement of pH and temperature

20°C pH 7.4 irr. power 24 μT

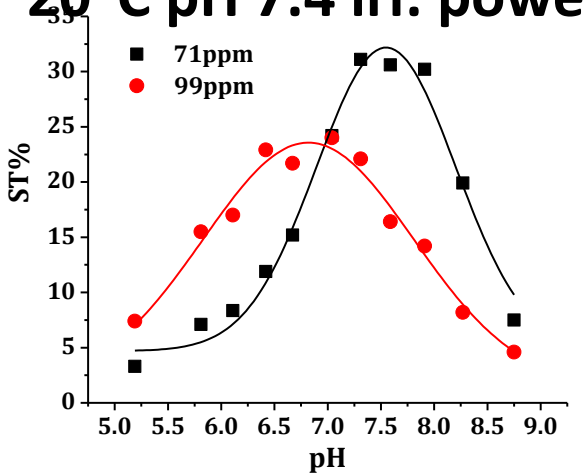

Yb-HPDO3A for measurement of pH and temperature

20°C pH 7.4 irr. power 24 μT

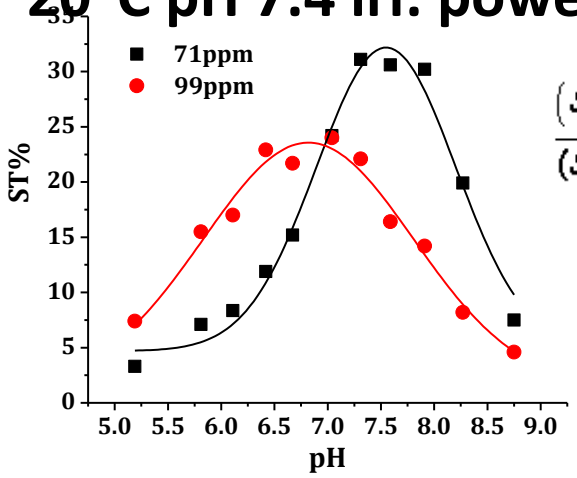

$$\frac{(ST)_{poolA}(1-(ST)_{poolB})}{(ST)_{poolB}(1-(ST)_{poolA})}$$

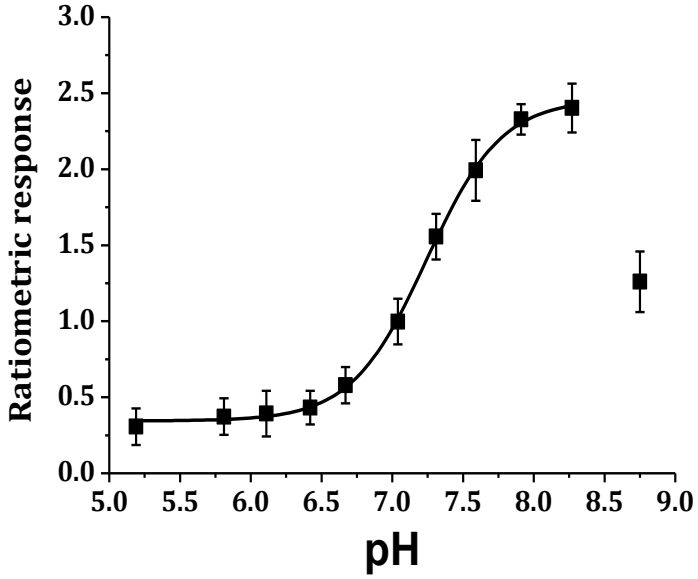

Yb-HPDO3A for measurement of pH and temperature

20°C pH 7.4 irr. power 24 µT

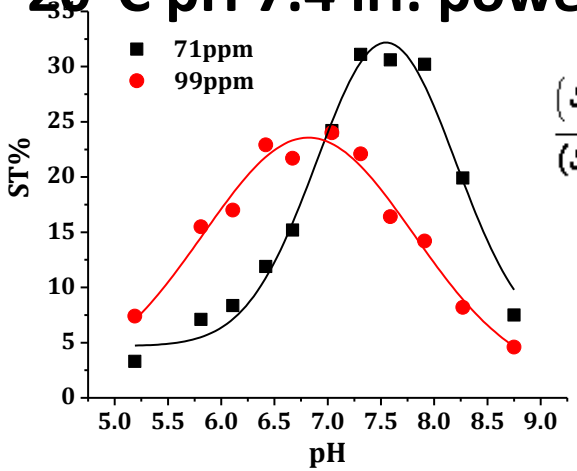

$$\frac{(ST)_{poolA}(1-(ST)_{poolB})}{(ST)_{poolB}(1-(ST)_{poolA})}$$

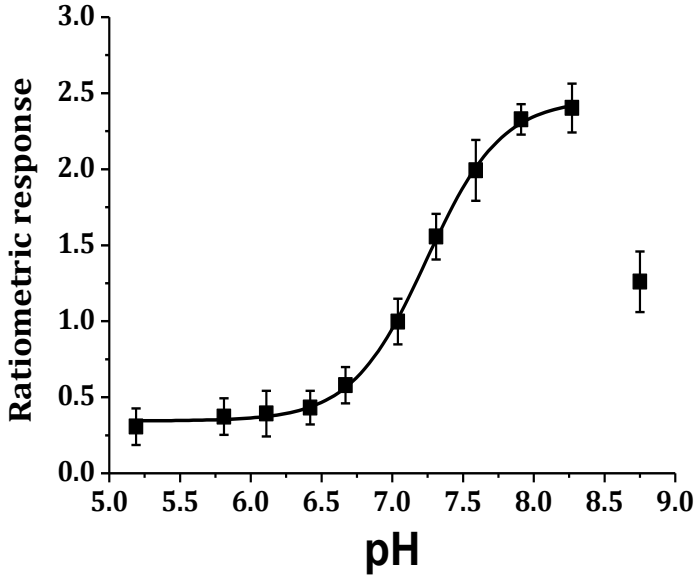

The role of temperature

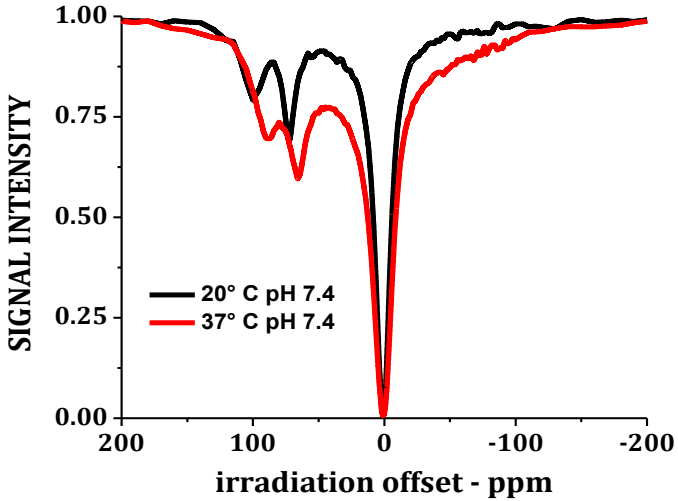

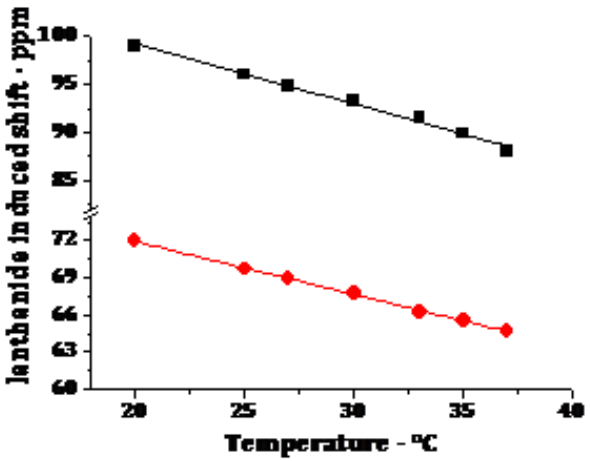

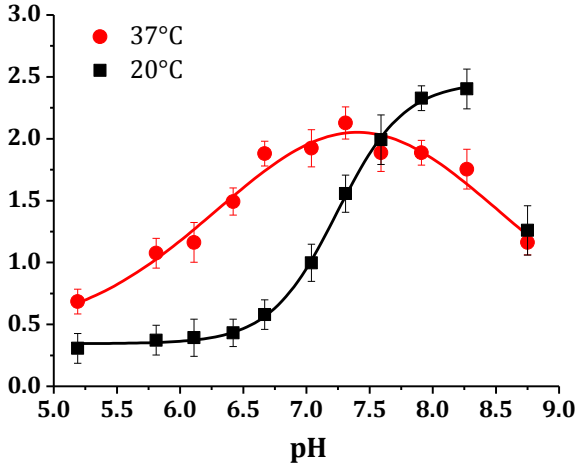

Saturation @ 71 and 99 ppm

Yb-HPDO3A as concentration-independent pH sensor

7 T - 20°C - Irr time 2 s - Irr. power 24 μT

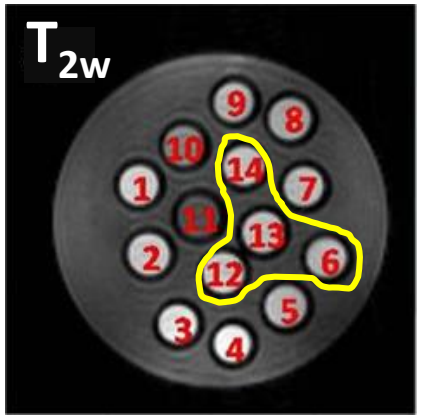

[YbHPDO3A] 24 mM

1. pH = 5.2
2. pH = 5.8
3. pH = 6.1
4. pH = 6.4
5. pH = 6.7
6. pH = 7.0
7. pH = 7.3
8. pH = 7.6
9. pH = 7.9
10. pH = 8.3
11. pH = 8.7

pH 7

6. 24 mM
12. 12 mM
13. 6 mM
14. 3 mM

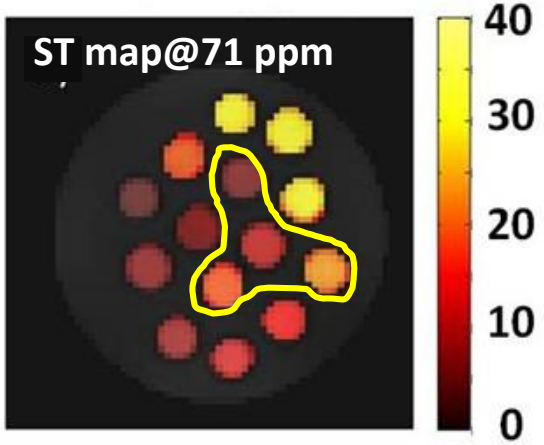

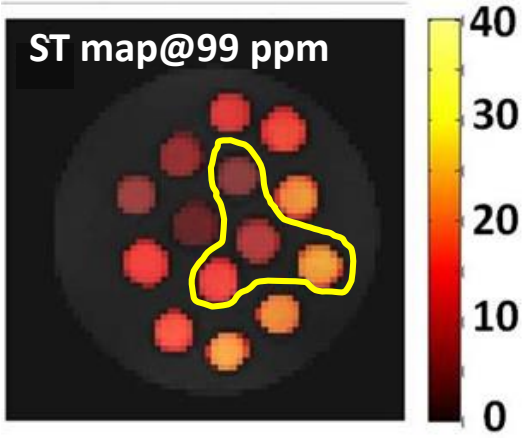

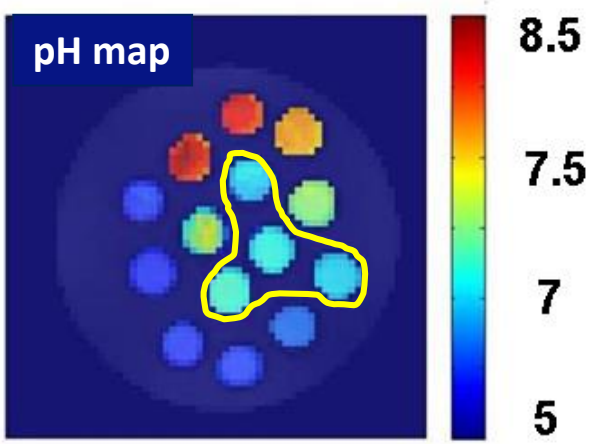

In vivo maps of extracellular pH in murine melanoma by CEST-MRI.

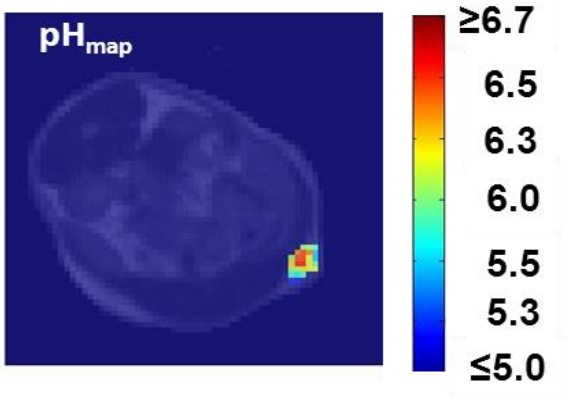

Early stage

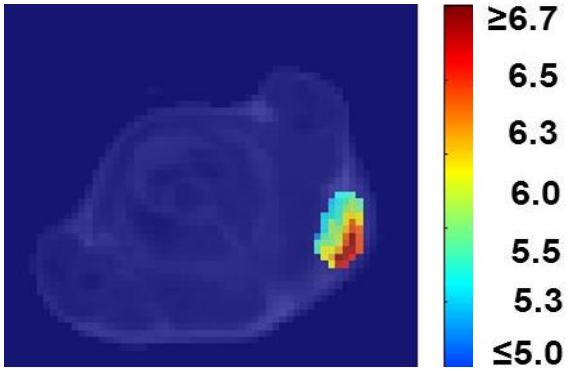

Middle stage

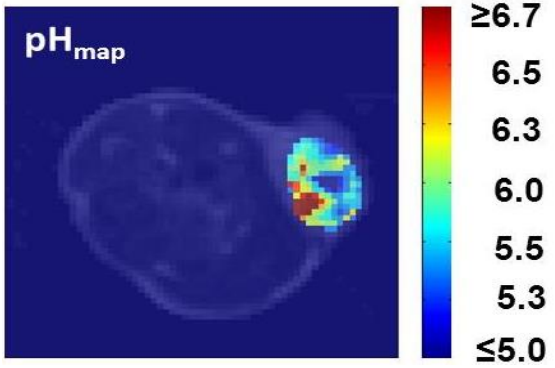

Late stage

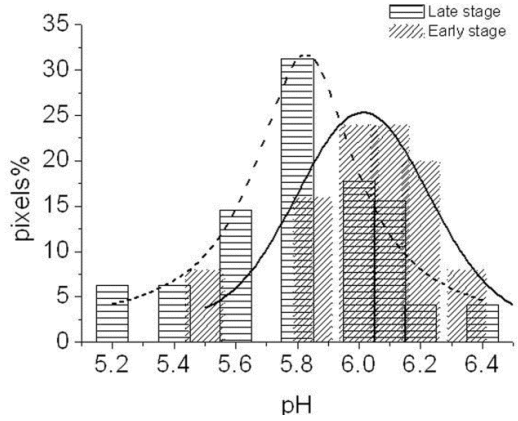

- The difference in the mean pH value is not relevant by changing the tumor stage.
- The heterogeneity of pH values is higher in late stage tumors.

Delli Castelli D*, Ferrauto G*, Cutrin JC, TerrenoE and Aime S. Magn Reson Med, 2013; . doi: 10.1002/mrm.24664

In vivo MRI visualization of different cell populations labeled with PARACEST agents

Ln-HPDO3A: a promising PARACEST platform

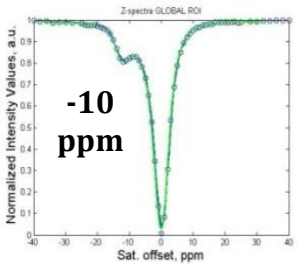

-10 ppm

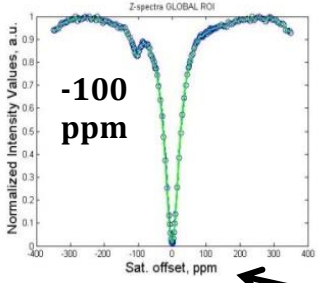

-100 ppm

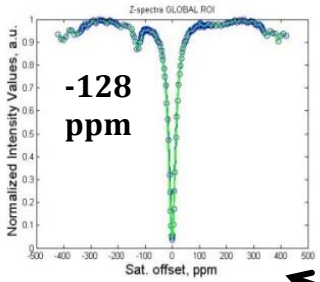

-128 ppm

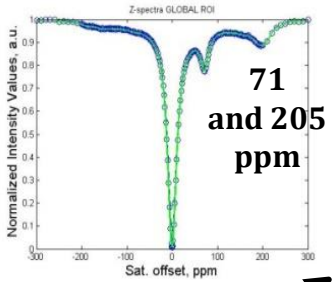

71 and 205 ppm

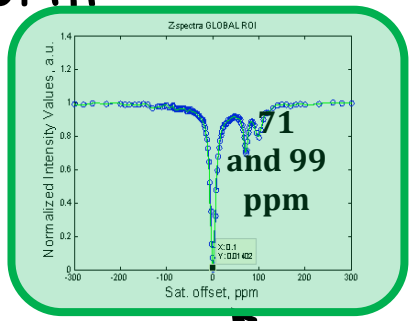

71 and 99 ppm

58	59	60	61	62	63	64	65	66	67	68	69	70
Ce	Pr	Nd	Pm	Sm	Eu	Gd	Tb	Dy	Ho	Er	Tm	Yb
- 6.3	- 11	- 4.2		- 0.7	+ 4.0	0	- 86	- 100	- 39	+ 33	+ 53	+ 22

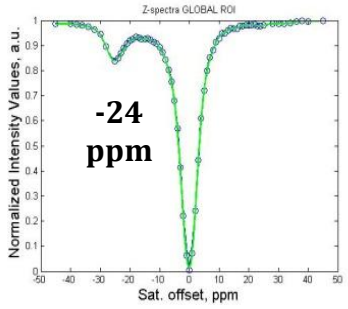

-24 ppm

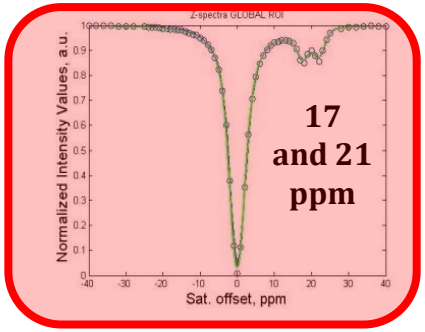

17 and 21 ppm

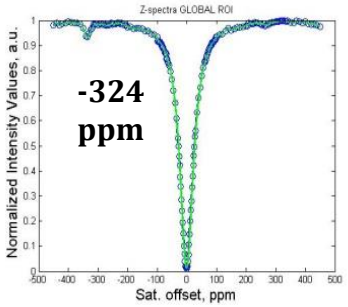

-324 ppm

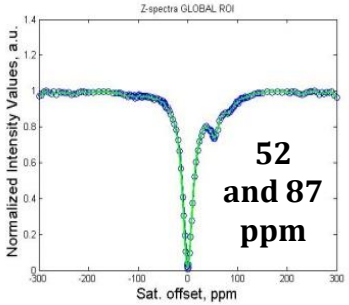

52 and 87 ppm

Multiplex detection of Ln-HPDO3A complexes

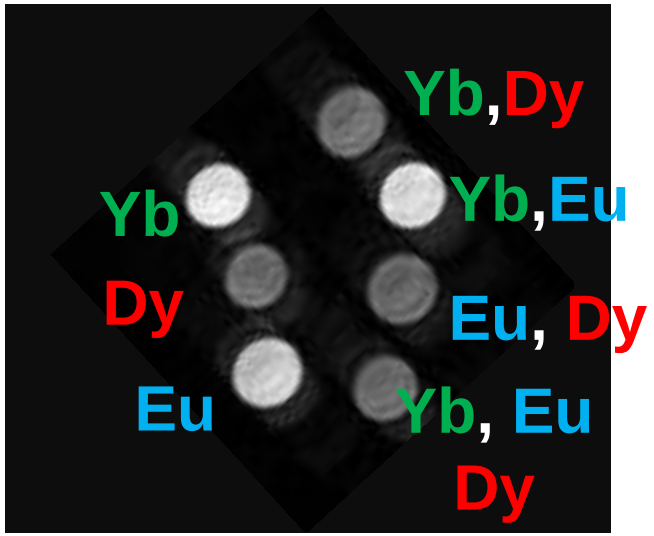

Yb
ST@71 ppm

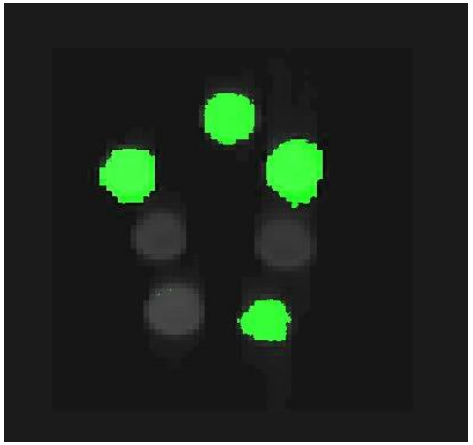

Eu
ST@17 ppm

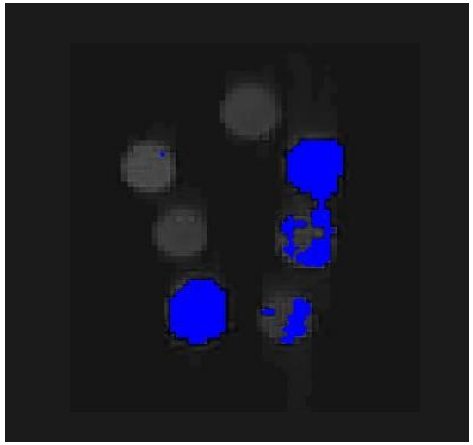

Dy
ST@-324 ppm

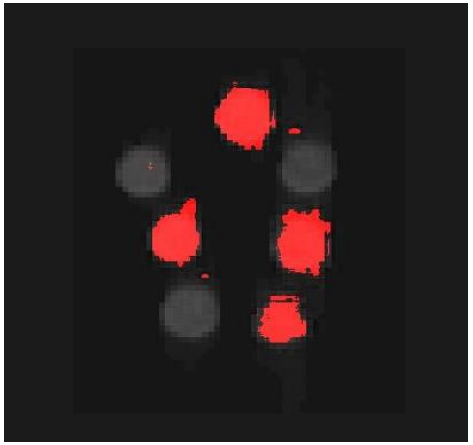

MERGE

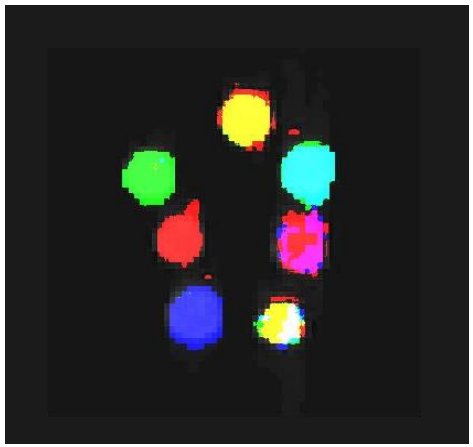

In vivo MRI visualization of different cell populations labeled with PARACEST agents.

Results

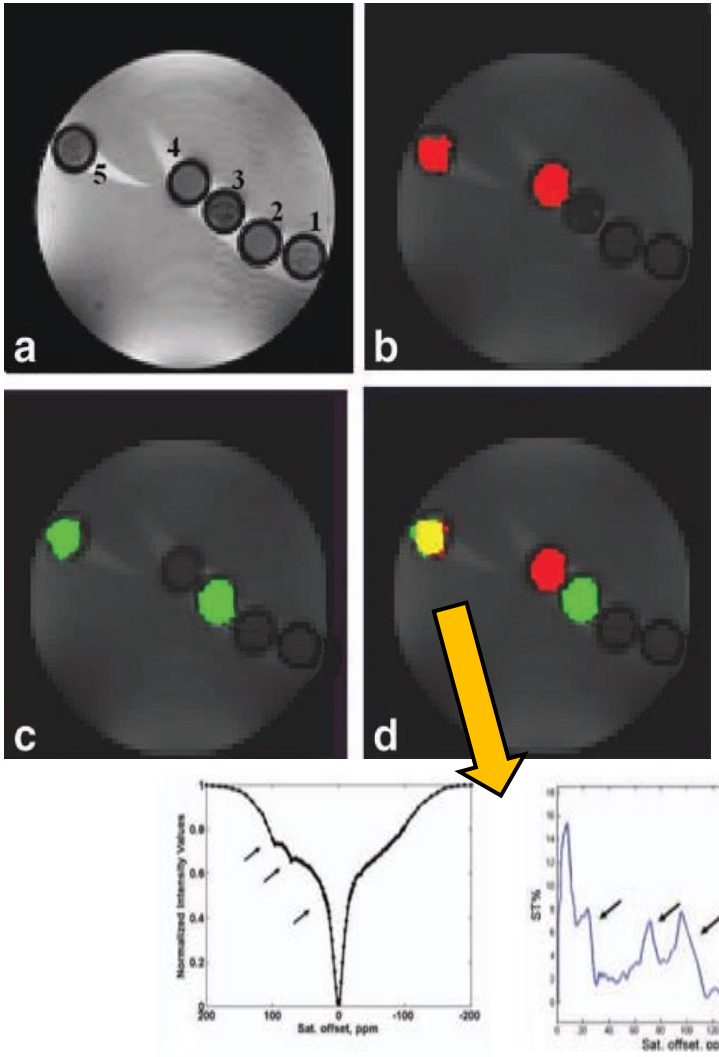

(1) Unlabeled J774A.1 cells;

(2) Unlabeled B16-F10;

(3) J774A.1 labeled with YbHPDO3A;

(4) B16-F10 cells labeled with EuHPDO3A;

(5) a mixture of cells labeled as in 3 and in 4 .

RED: CEST image at 20 ppm(Eu-HPDO3A);

GREEN: CEST map at 71 ppm (Yb-HPDO3A);

YELLOW: Merge of green & red

Ferrauto G., Delli Castelli D., TerrenoE. and Aime S. Magn Reson Med, 2011; 69: 1703–1711.

In vivo MRI visualization of different cell populations labeled with PARACEST agents.

Results

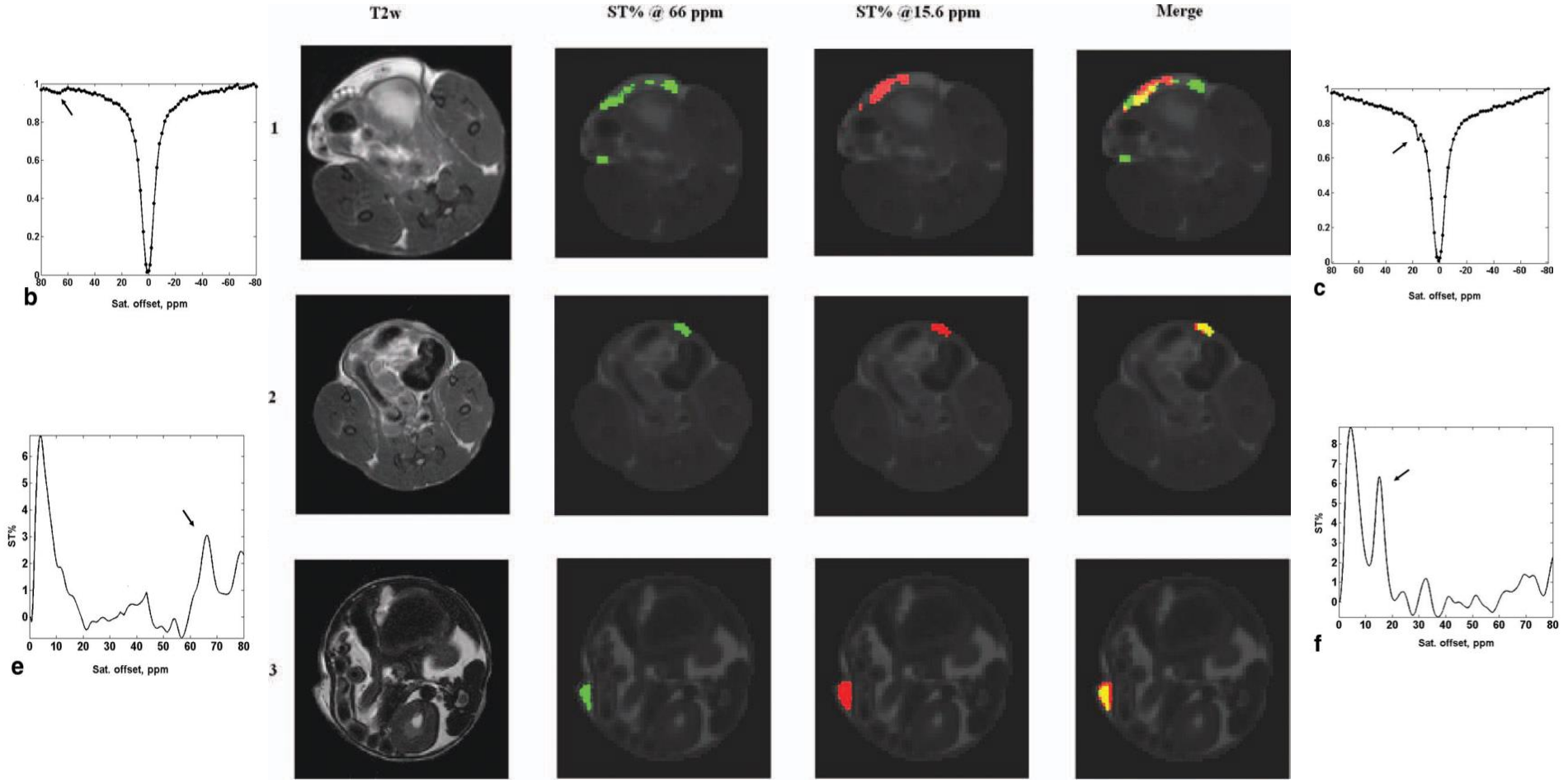

Ferrauto G., Delli Castelli D., TerrenoE. and Aime S. Magn Reson Med, 2011; 69: 1703–1711.

Classification of CEST agents

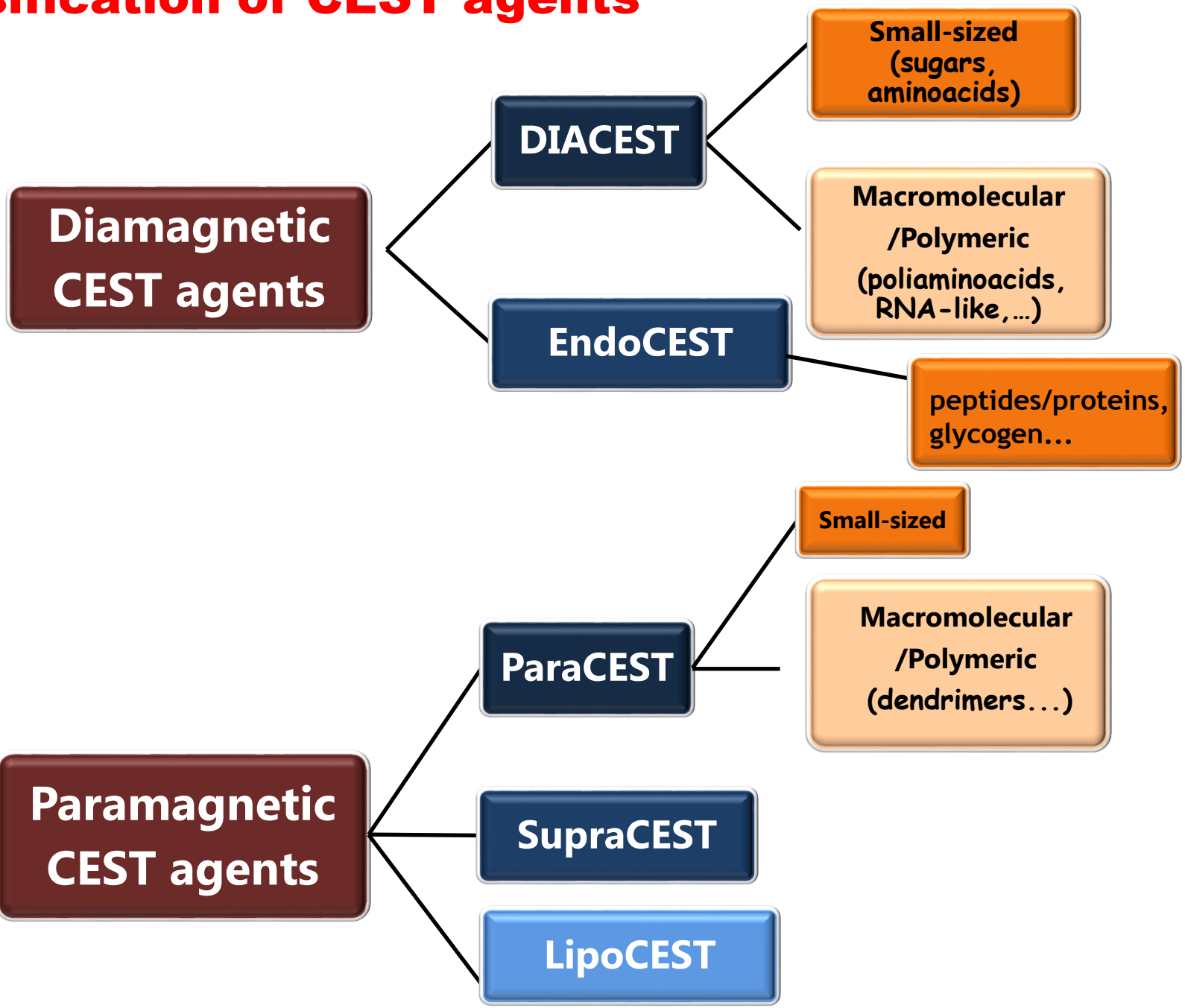

CEST agents for assessing tumor vascular permeability

Simultaneous injection of two agents with different size

Yb-G2

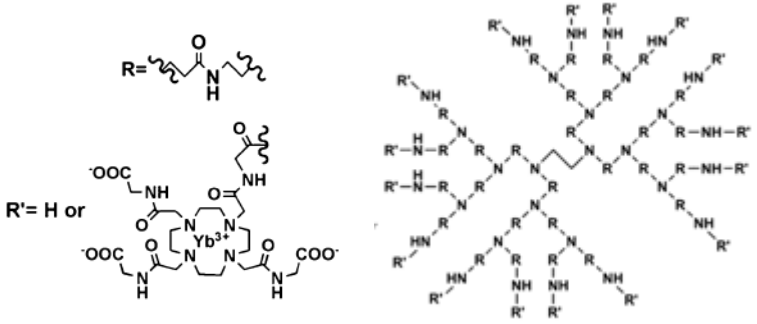

Eu-G5

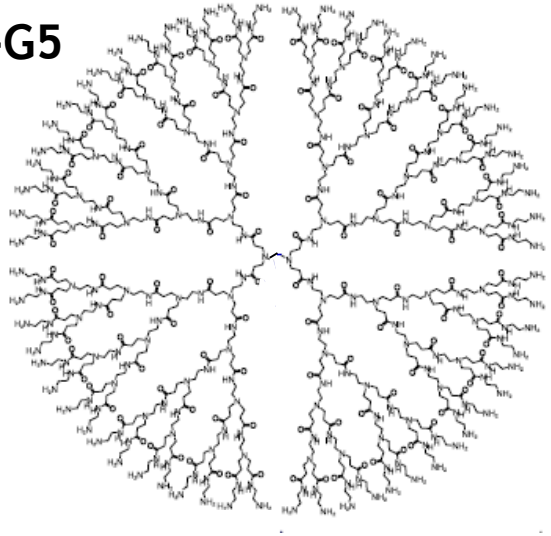

PARACEST agent	concentration to generate a 3.0% PARACEST effect: per lanthanide ion basis	per molecule basis
Eu-DOTA-Gly	1.62 mM	1.62 mM
Eu-G5	1.85 mM	0.045 mM
Yb-DOTA-Gly	1.43 mM	1.43 mM
Yb-G2	1.38 mM	0.242 mM

MCF-7 xenograft tumor on mice

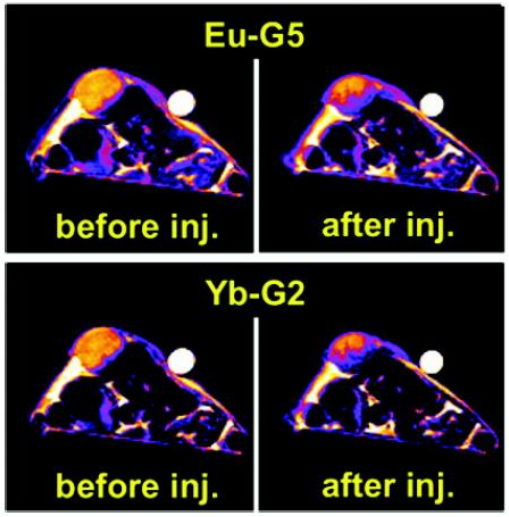

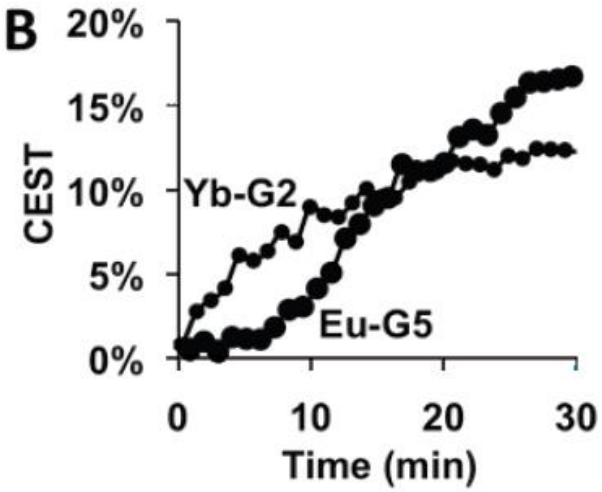

Meser Ali et al., Mol. Pharm. 2009, 6, 1409

Classification of CEST agents

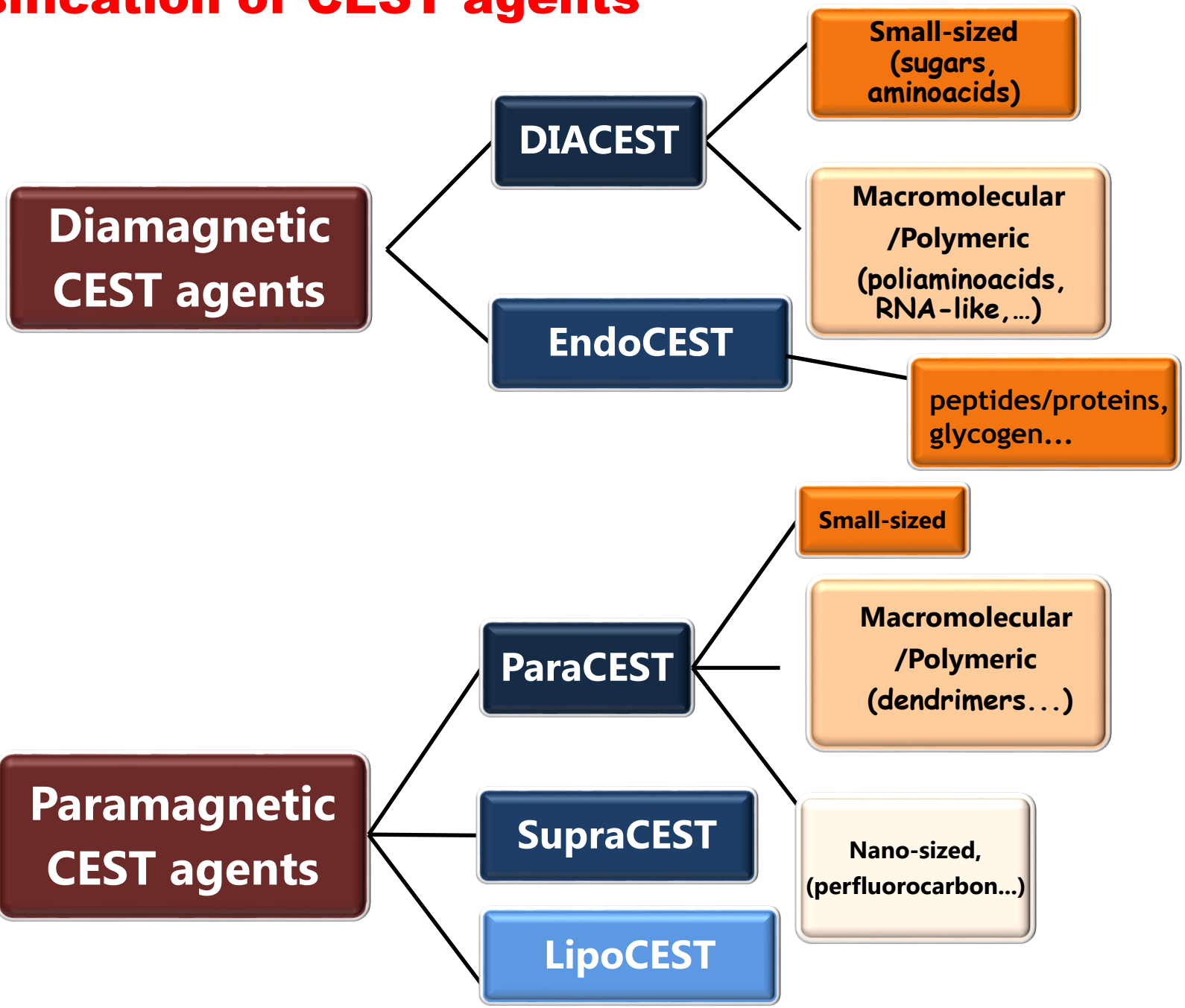

The route to high sensitivity: exploiting nanotechnology

Usually, the typical approach consists of loading a large number of CEST agents to the external surface of the nanosystem:

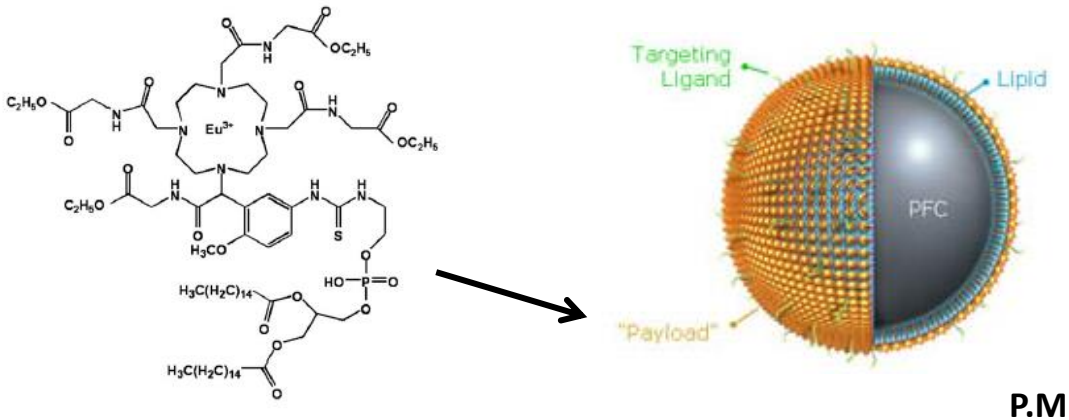

Perfluorocarbon nanoemulsions

P.M. Winter et al. *Mag. Reson. Med.*, 2006, 56, 1384

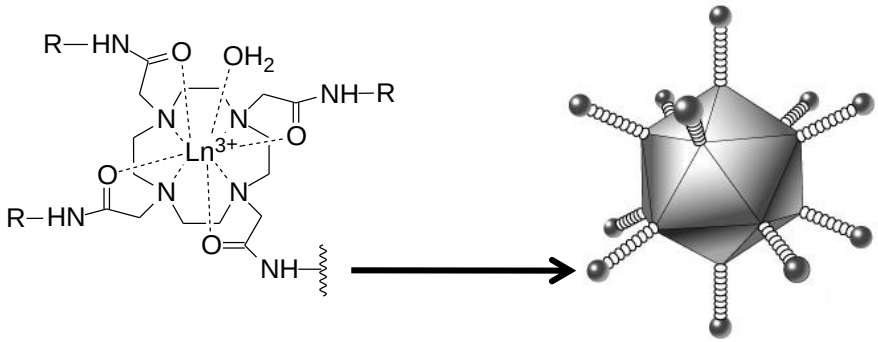

Adenovirus

O. Vasalatiy et al. *Bioconjugate Chem.*, 2008, 19, 598

The sensitivity of such nanoprobes is primarily dependent on the maximum payload that can be achieved (generally 10^3-10^5 PARACEST units per nanosystem)

The route to high sensitivity: exploiting nanotechnology

Ln^{III} chelates anchored on the surface of mesoporous silica NPs

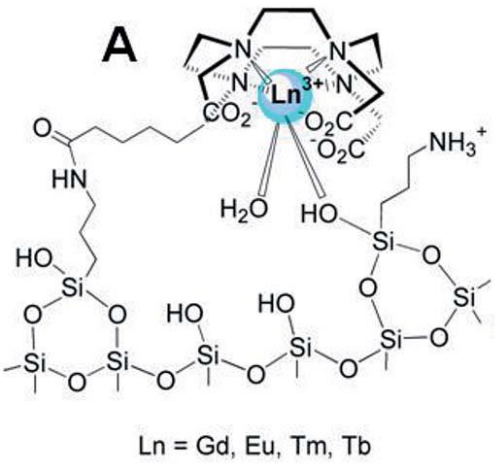

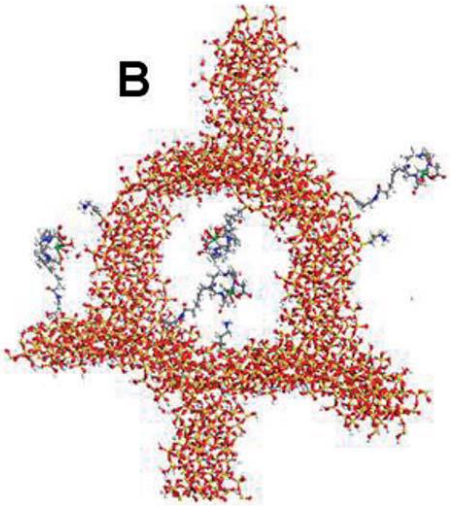

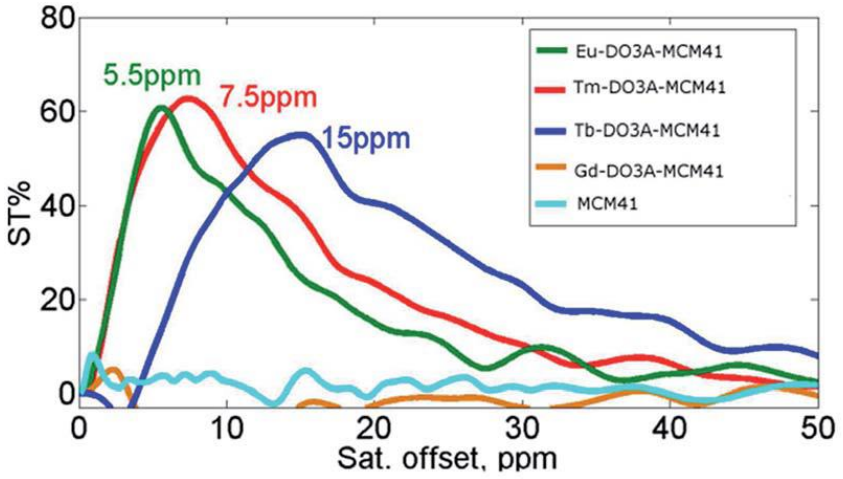

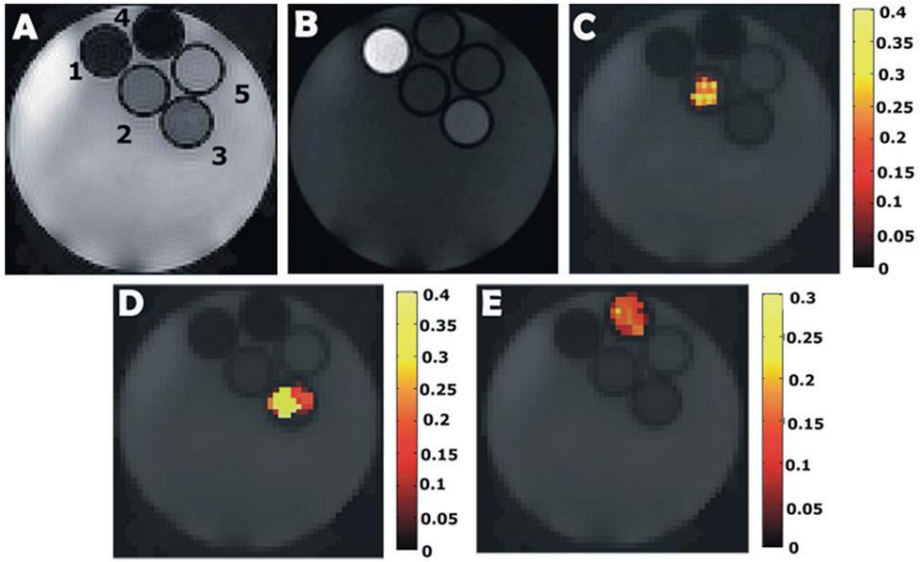

Ferrauto G. et al. Nanoscale 2014

Macromolecular Paramagnetic CEST agents

To exploit the reversible interaction between a paramagnetic Shift Reagent and a substrate rich of mobile protons

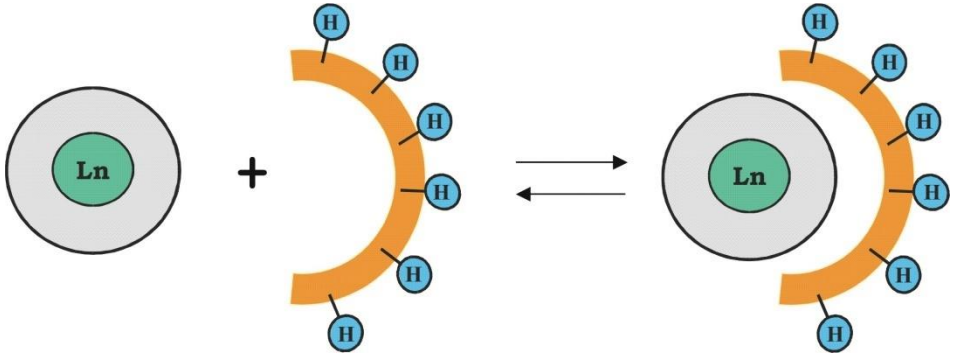

SUPRACEST

Example:

Interaction between

$[TmDOTP]^{5-}$

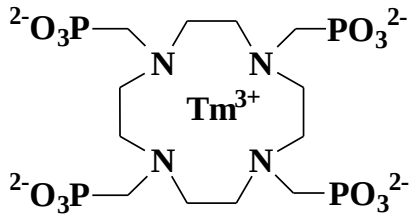

and polyArginine

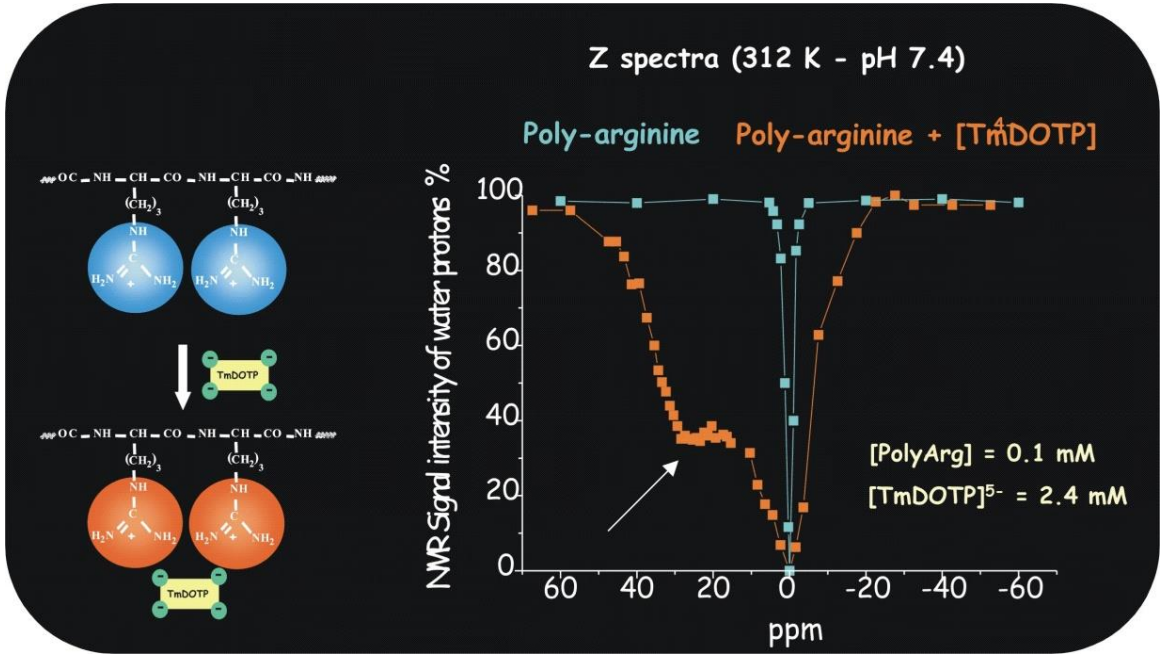

Sensitivity threshold (referred to the paramagnetic complex) of tens of μmolar

S. Aime et al., *Angew. Chemie Int. Ed.*, 2003, 42, 4527

Sensitivity

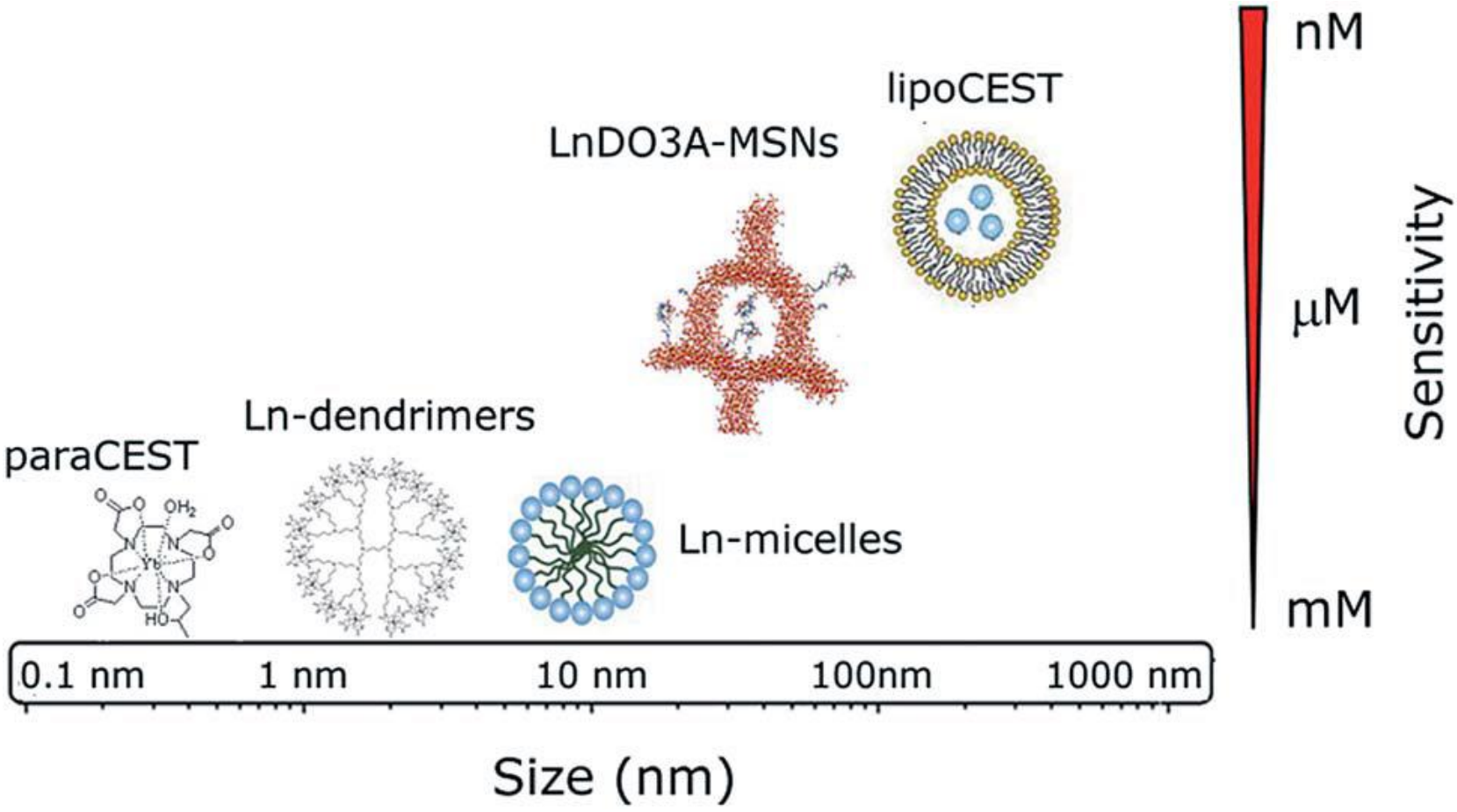

1) **Small-sized molecules** ⟶ small number of mobile protons (<10) per molecule

	Sensitivity	B_1 field intensity
a) Diamagnetic agents (sugars, aminoacids,…)	tens of mM	☺
b) Paramagnetic agents		
PARACEST → Amide, hydroxilic protons	few mM	☺
PARACEST → metal bound water protons	hundreds of μM	☹

2) **Macromolecular agents** ⟶ large number of mobile protons (~10^3) per molecule

a) Diamagnetic agents (poliaminoacids, RNA-like,…)	μM	☺
b) Paramagnetic agents		
SUPRACEST agents	few μM	☹

3) **Nanoparticles** ⟶ extremely high number of mobile protons (>10^6) per molecule

LIPOCEST agents	tens of pM	☺

Liposomes

Biocompatibles, extremely versatiles, successfully used in pharmaceutical field

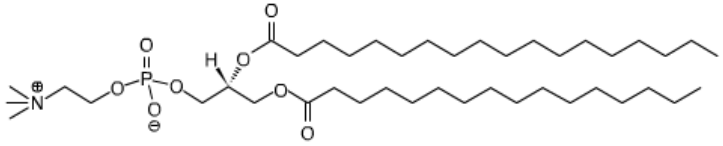

DPPC: DiPalmitoyl-PhosphatidylCholine

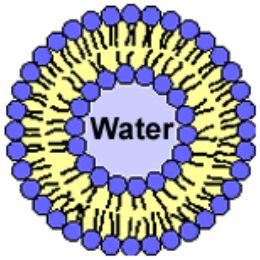

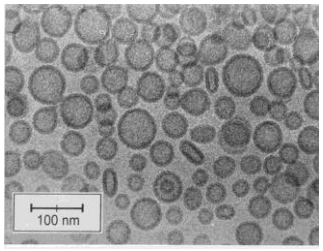

Cryo-TEM image

➢ **The external surface may be easily functionalized with a wide variety of chemicals including targeting vectors, or PEG chains for prolonging the blood half lifetime (Stealth® liposomes).**

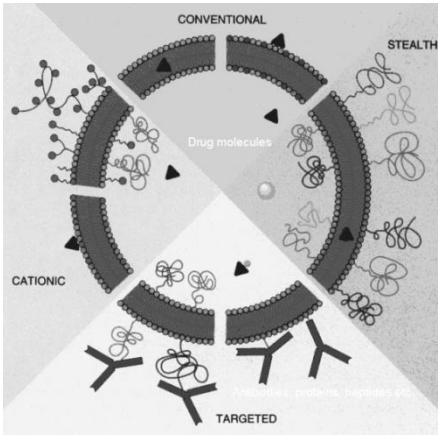

➢ **Liposomes can be passively accumulated in pathological body regions (tumors, atherosclerotic plaques,…)**

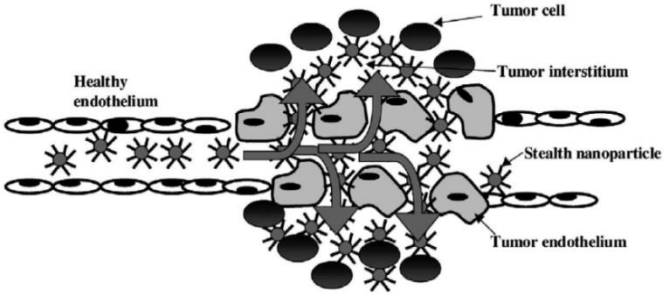

The ST efficiency ∝ to k_{ex} and number of mobile protons

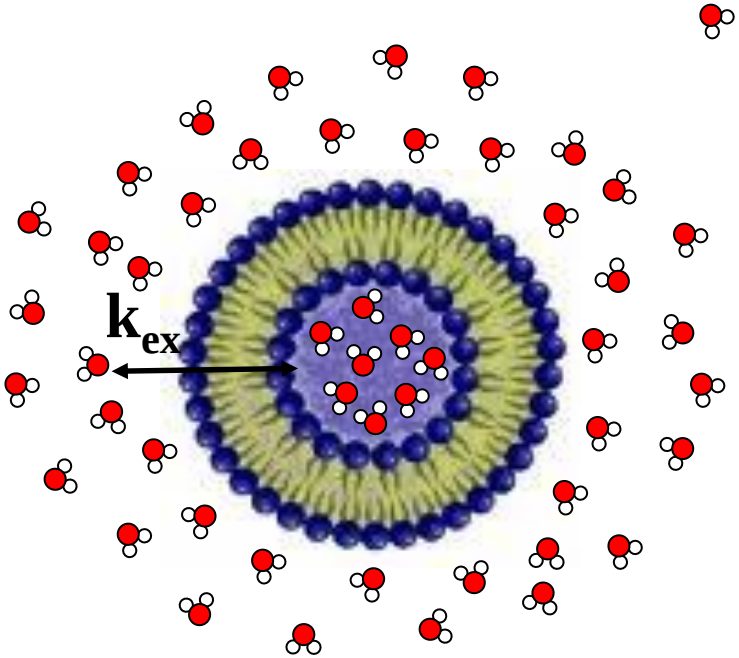

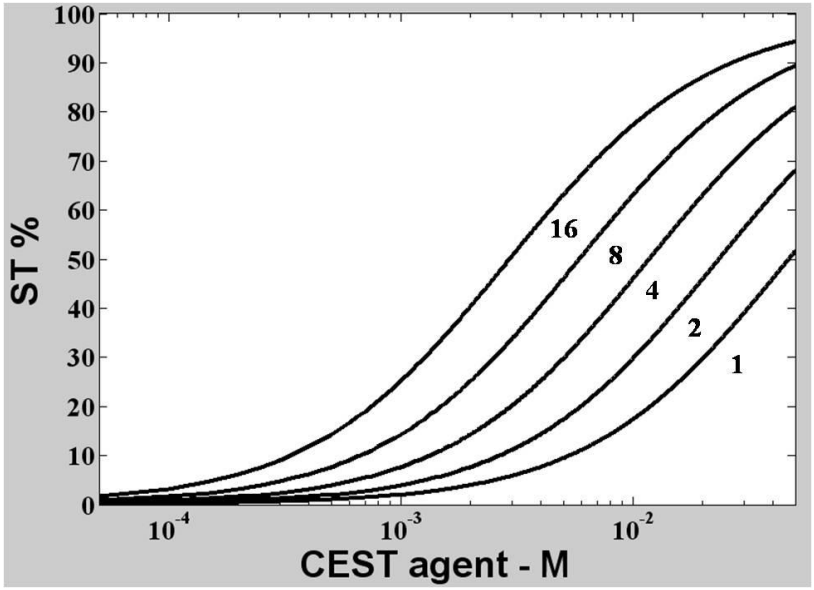

The number of mobile protons for Large Unilamellar Vescicles (LUV) range from $2{,}4 \times 10^6$ (50 nm) to $2{,}1 \times 10^9$ (500 nm)

⇓

Liposomes can be very efficient CEST Probes

How the resonance frequencies of inner and outer water protons can be separated ?

Encapsulating a paramagnetic shift reagent (SR) in the liposome

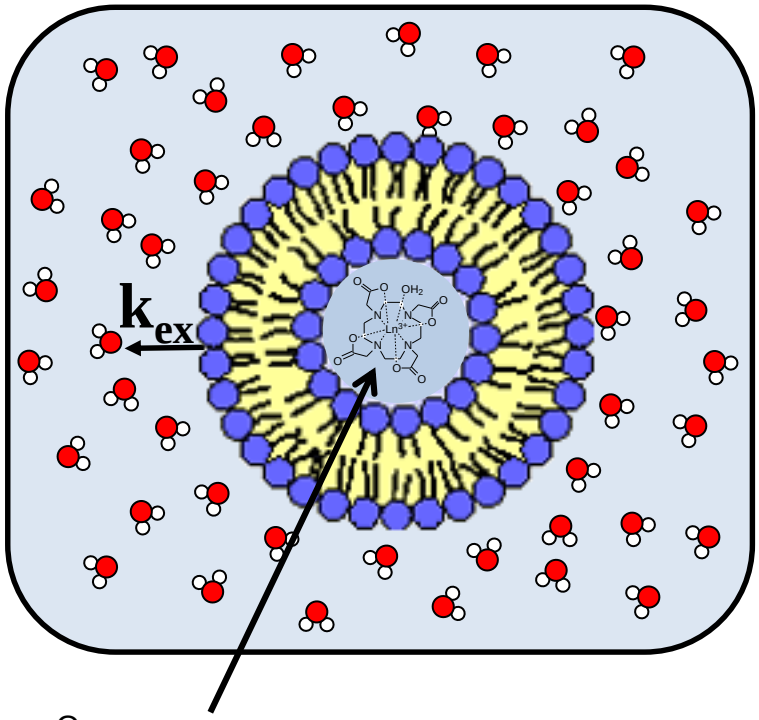

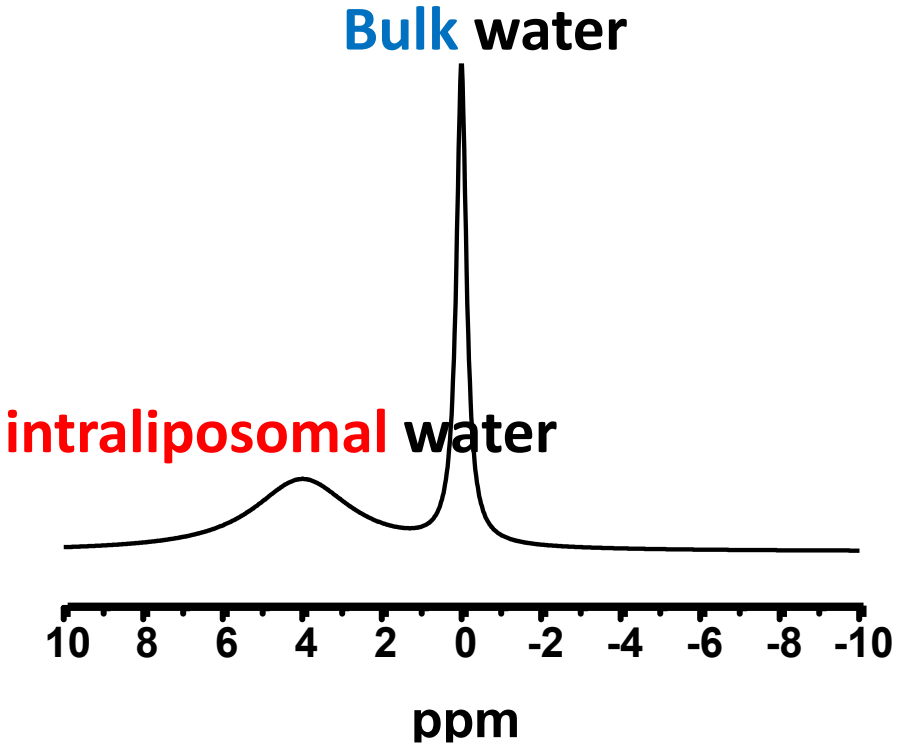

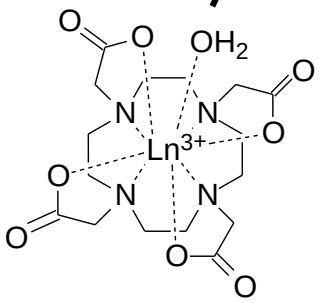

Lanthanide-based SR

Angew. Chem. Int. Ed., 2005, 44, 5513.

k_{ex} can be modulated by:

- varying the liposome membrane permeability (P)

(k_{ex}= P × S/V)

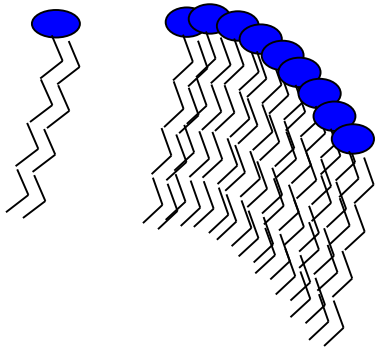

Saturated phospholipids
Membrane tightly packed
Slow exchange

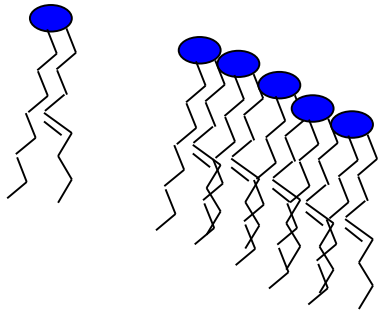

Unsaturated phospholipids
Less tightly packed
Fast exchange

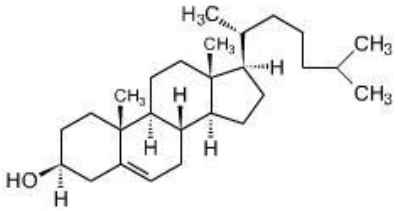

Cholesterol insert himself
in the hole
Reduce the exchange rate

- Varying the liposome size (k_{ex}= P × S/V=P x 3/radius)

k_{ex}

n° of mobile protons

LipoCEST agents: factors affecting sensitivity

- Water permeability of the liposome bilayer (P_w)

Can be modulated by changing the packaging properties of the phospholipids

Phospholipids with saturated aliphatic chains (e.g. di-palmitoyl) displays lower P_w than unsaturated ones (e.g. di-oleyl)

Cholesterol intercalates in the bilayer and reduces P_w

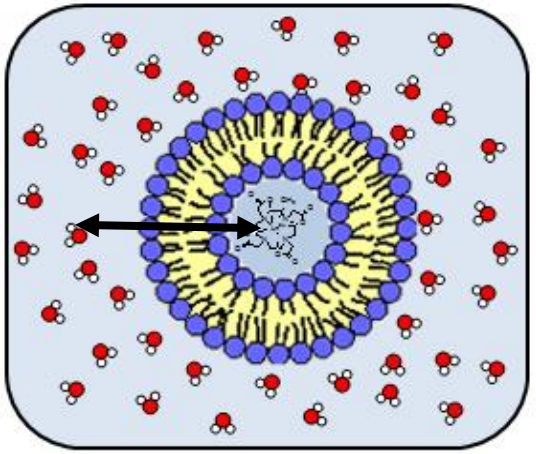

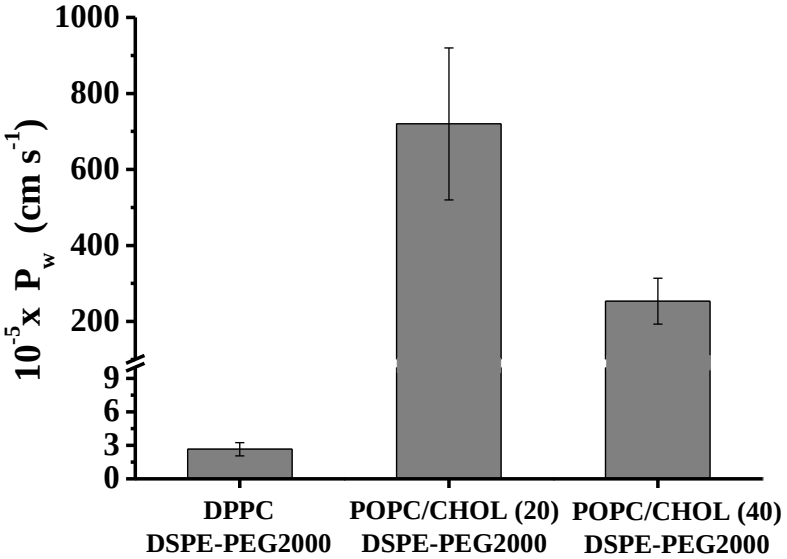

J. Inorg. Biochem., 2008, 102, 1112.

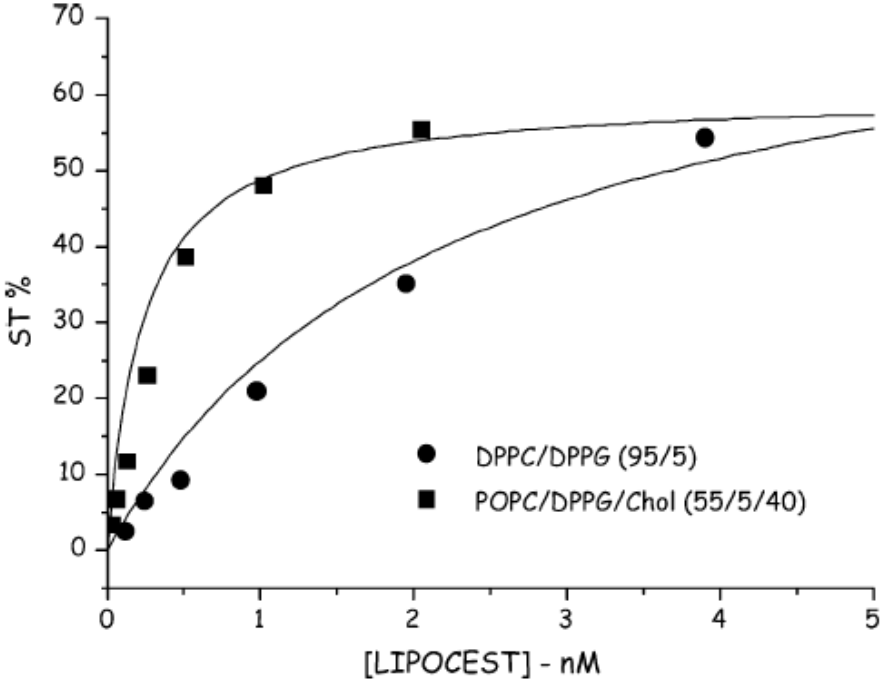

The chemical shift of the water protons (δ) in the presence of a paramagnetic SR is the sum of three contributions:

$$\delta = \delta_{DIA} + \delta_{HYP} + \delta_{BMS}$$

δ_{DIA} often negligible

δ_{HYP} requires a "chemical" interaction between the paramagnetic center (the Ln(III) ion) and the water molecule

(through bond: contact shift; through space: pseudocontact shift)

δ_{BMS} does not require a "chemical" interaction and it is dependent on the bulk magnetic susceptibility of the compartment containing the SR

In the case of spherical compartment δ_{BMS}=0 →

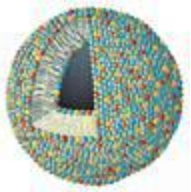

Conventional liposomes

Shift Reagent for intraliposomal water protons

When $k_{ex} >> \Delta\omega$ then:

$$\delta_{\substack{intralipo \\ water}} = \frac{[H_2O]_{bound\ to\ SR}}{[H_2O]_{total}} \times \delta_{\substack{bound \\ water}}$$

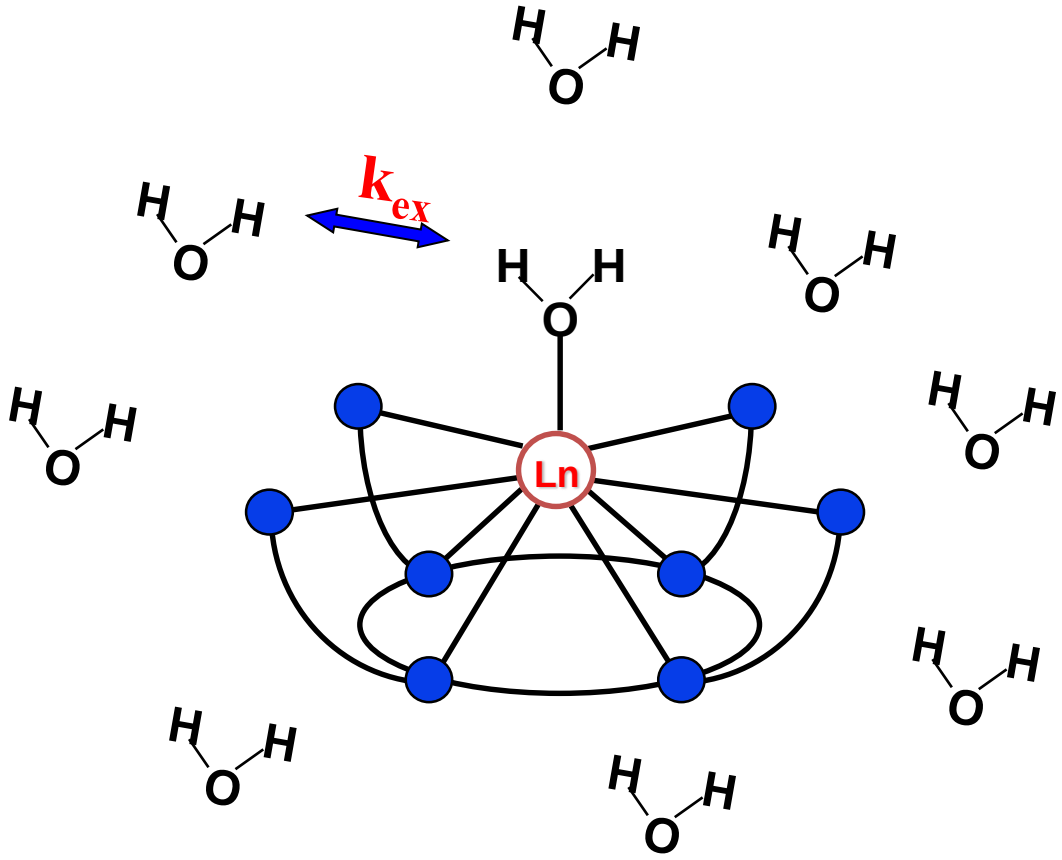

$$\delta_{\substack{bound\\water}} = \delta_{HYP} = \delta_{\substack{pseudo\\contact}} \propto \Delta\chi \times G$$

- $\Delta\chi$ is the magnetic anisotropy of the lanthanide complex Ln

$$\Delta\chi = C_J \times A_0^2 \langle r^2 \rangle$$

- C_J is a constant of the metal

$C_J > 0$ for Eu, Er, Tm e Yb

$C_J < 0$ for Ce, Pr, Nd, Sm, Tb, Dy and Ho

$C_J = 0$ for Gd

- $(A_0^2 \langle r^2 \rangle)$ depends on the crystal field

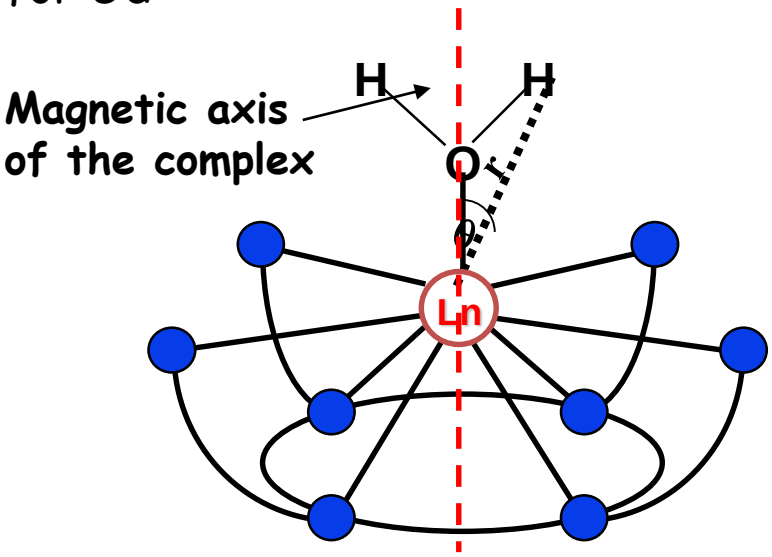

- $G \propto \frac{3\cos^2\theta - 1}{r^3}$

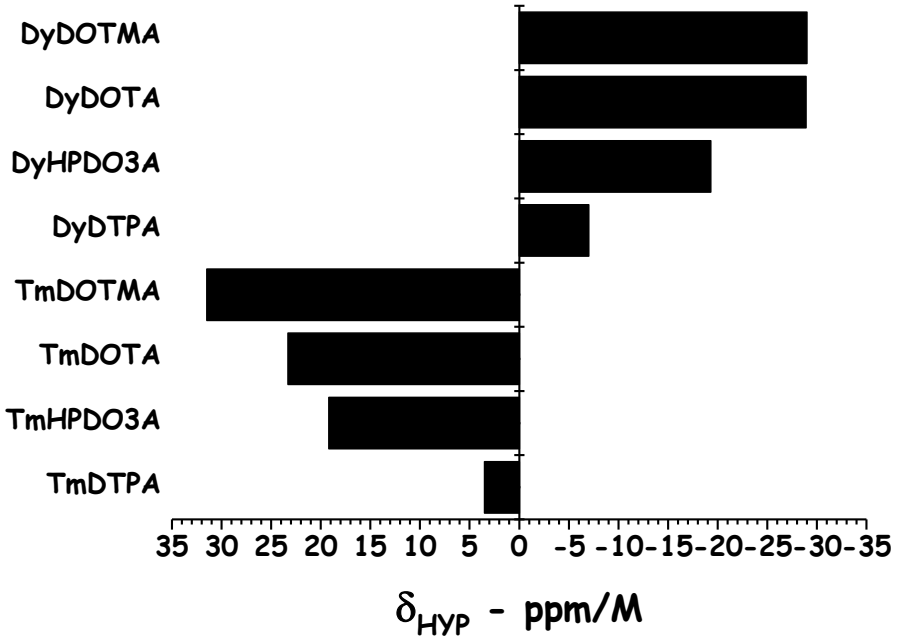

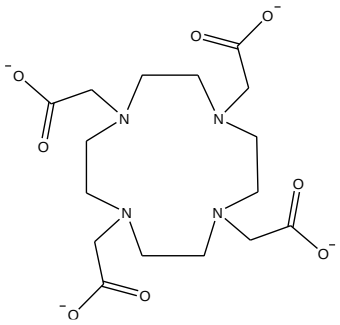

DOTA

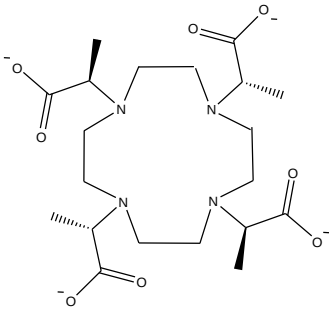

DOTMA

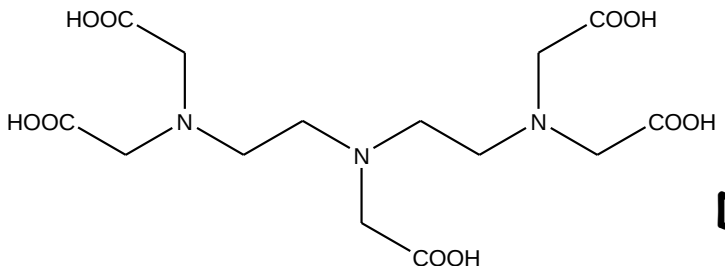

DTPA

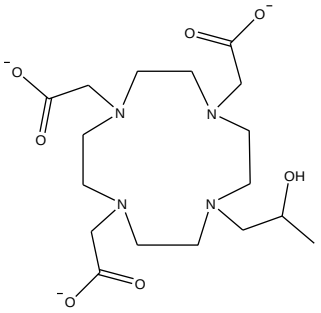

HPDO3A

-Shift differences are due to the geometric differences among the complexes (parameter G)

LipoCEST agents: sensitivity

LipoCEST formulation: POPC/DPPG/Chol (55/5/40 in moles) size:250 nm

Experimental condition: 7 T – 37°C – pH 7.4 - B_2 field 6 μT

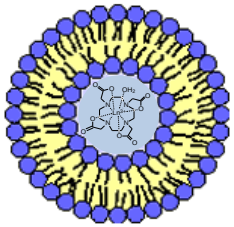

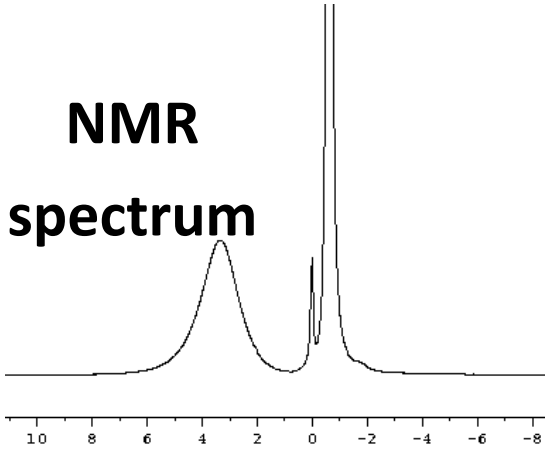

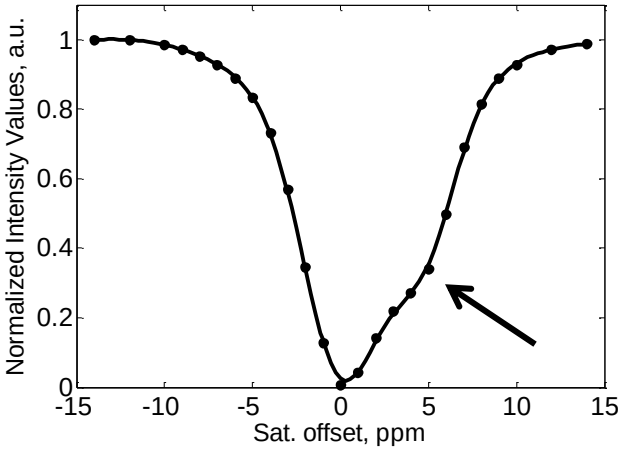

Z-spectrum sample 1

LipoCEST conc.

1. **1.5 nM**
2. **750 pM**
3. **320 pM**
4. **160 pM**
5. **80 pM**
6. **40 pM**

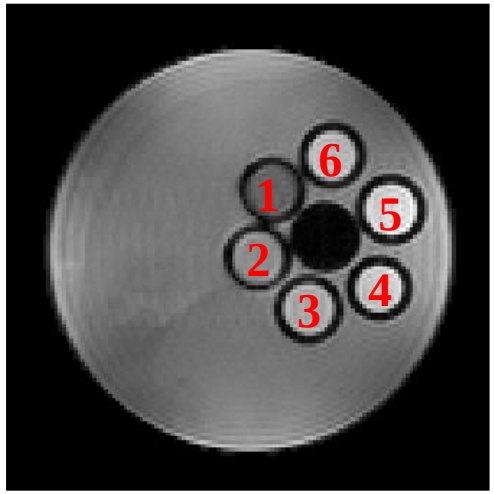

T_{2W} Image

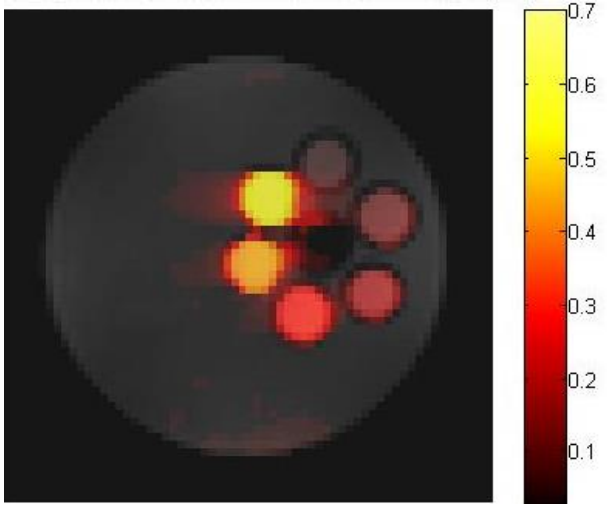

CEST map @ 3.8 ppm

First generation LIPOCEST: spherical liposomes

Pro: Highly sensitive (pM range)

Con: Little frequency range

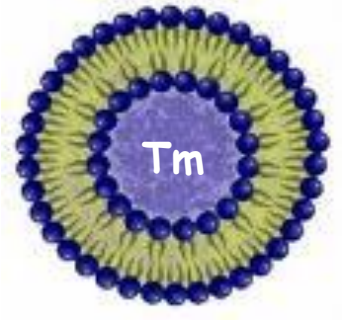

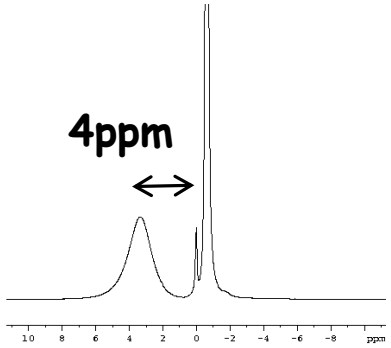

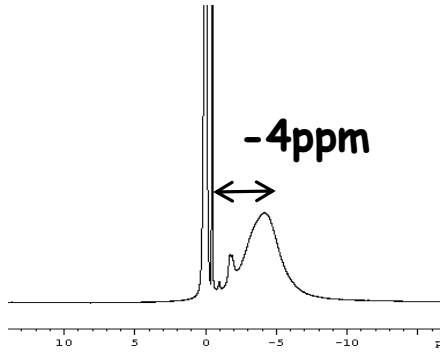

How to increase the shift? ⟶ Exploiting the BMS shift

$$LIS_{\substack{Bulk \\ water}} = BMS + Dip$$

BMS depends on the concentration of the shift reagent and its sign depends on the shape and orientation (wrt B_0) of the compartment in which the shift reagent is confined

Second generation of LIPOCEST: non-spherical liposomes

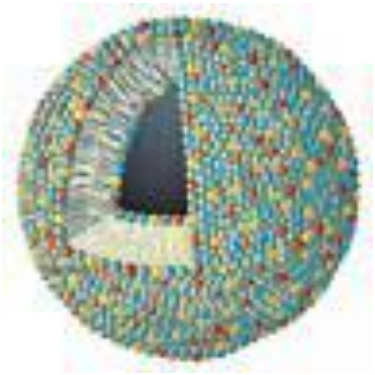

Osmotic shrinkage

$-H_2O$

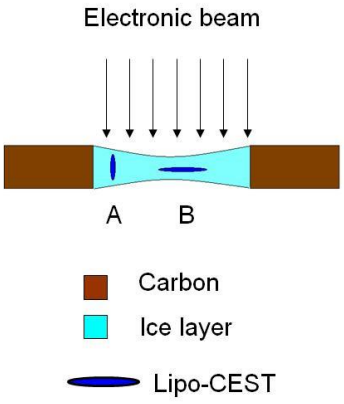

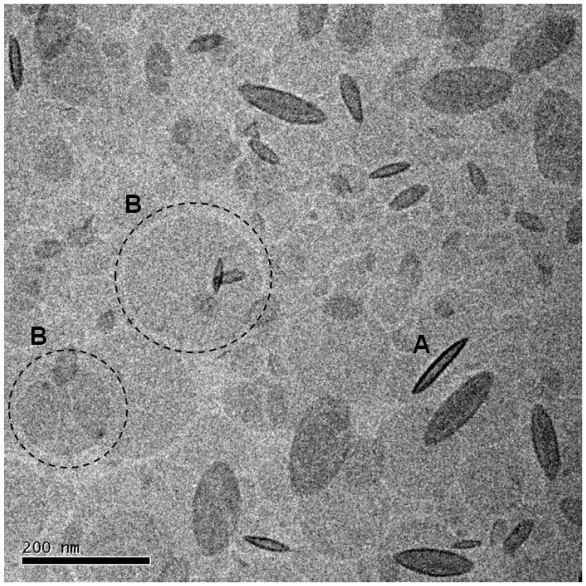

Cryo-TEM images of osmotically shrunken LIPOCEST agents

in collaboration with E. Sanders and N. Sommerdijk from University of Eindhoven (NL)

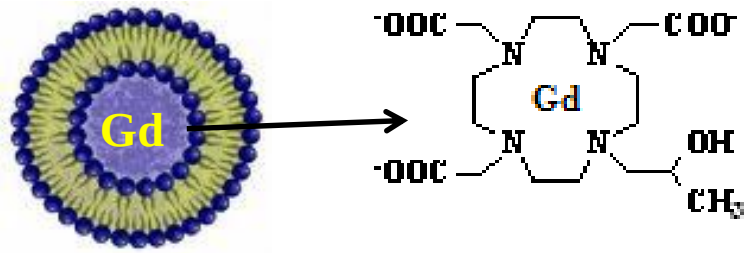

Before dialysis

[GdHPDO3A]

$$C_j\,\mathrm{Gd}=0 \Rightarrow \Delta\chi = 0 \Rightarrow \delta_{\substack{bound\\water}} = \delta_{dia}$$

Gd(III)-complexes has Dip = 0

$$BMS \propto [SR] \times \left(\mu_{eff}\right)^2$$

μ_{eff} Gd = 7.94

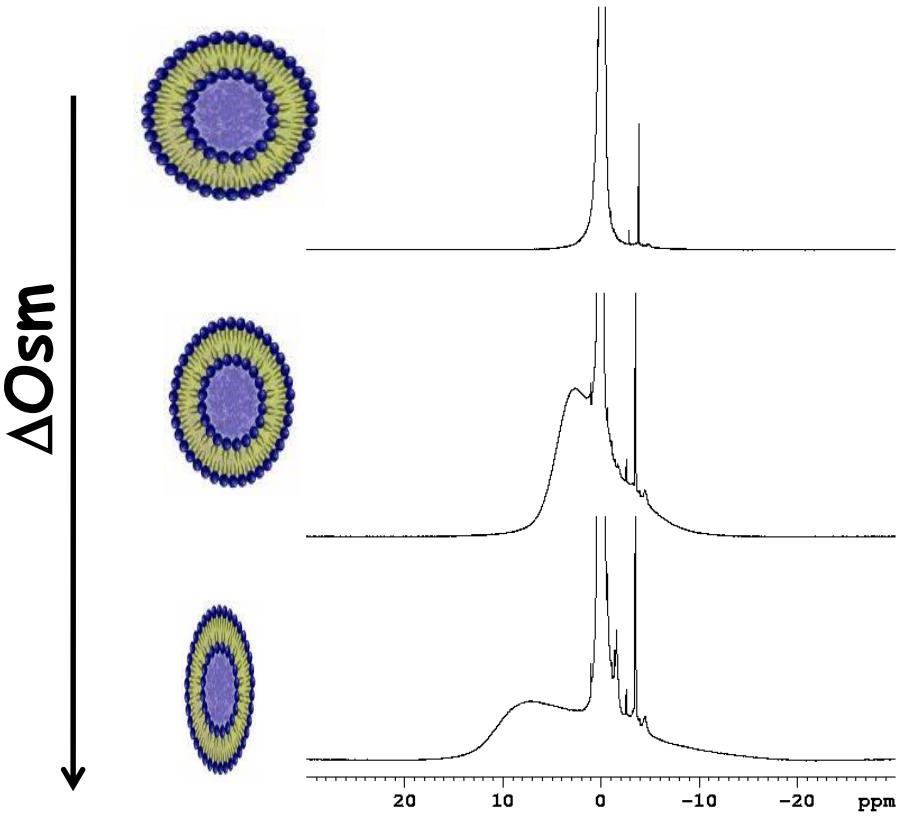

Lanthanides showing the **higher** values for μ_{eff}:

Gd, Tb, Dy, Ho, Er and Tm

Aime S. et al., J. Am. Chem. Soc., 2007, 129, 2430

Hydrophilic SR

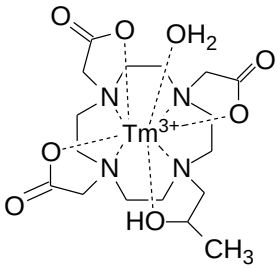

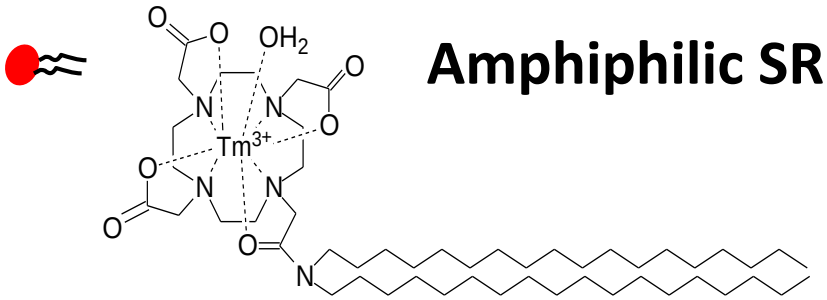

Amphiphilic SR

2nd generation

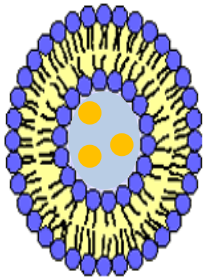

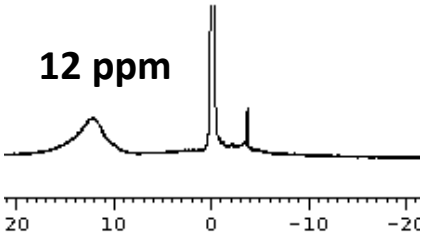

$$LIS_{\substack{int\,ralipo \\ water}} = Dip + BMS$$

3rd generation

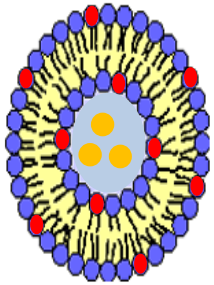

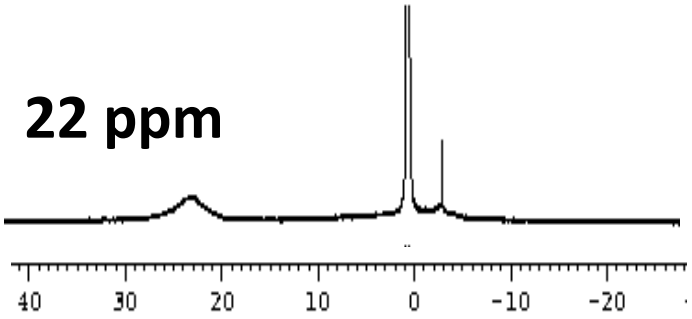

Terreno E. *et al., Angew. Chemie Int. Ed., 2007, 46, 966.*

A further Δ^{LIPO} increase can be achieved by encapsulating neutral multimeric SRs

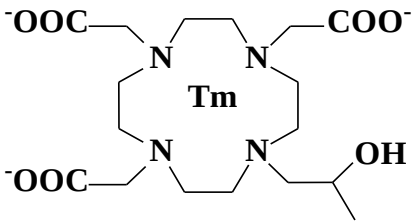

[Tm-HPDO3A]

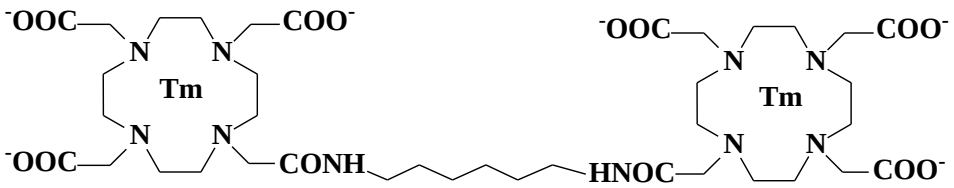

[Tm-dimer]

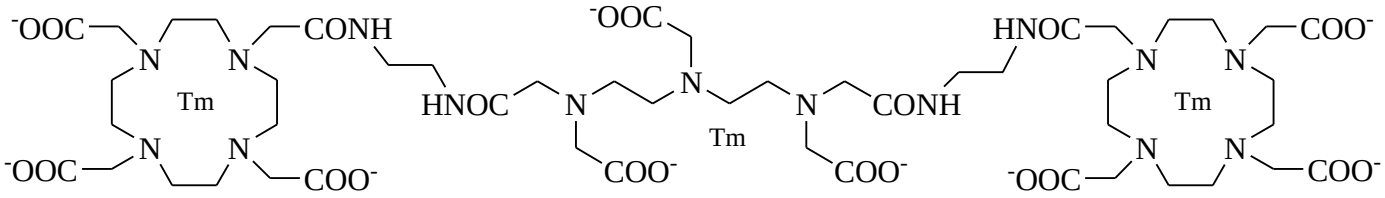

[Tm-trimer]

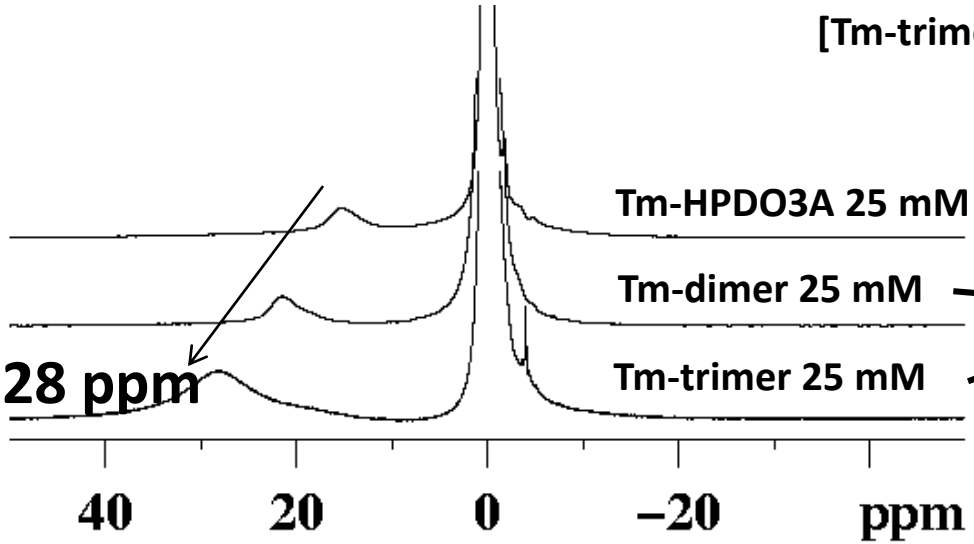

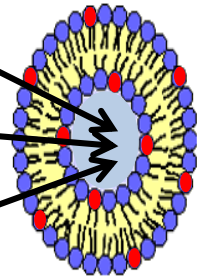

DPPC/Tm-1/DSPE-PEG2000
(75/20/5 mol %)

Terreno E. *et al., Chem. Commun.,* 2008, 600

In addition to increase the magnitude of $\Delta^{LIPO,}$ the incorporation of amphiphilic SRs may also affect he sign of the shift through the modulation of the magnetic alignment of the vesicles.

The sign of the BMS contribution depends on the orientation of the compartment with respect to the external B_0 field

For a cylinder

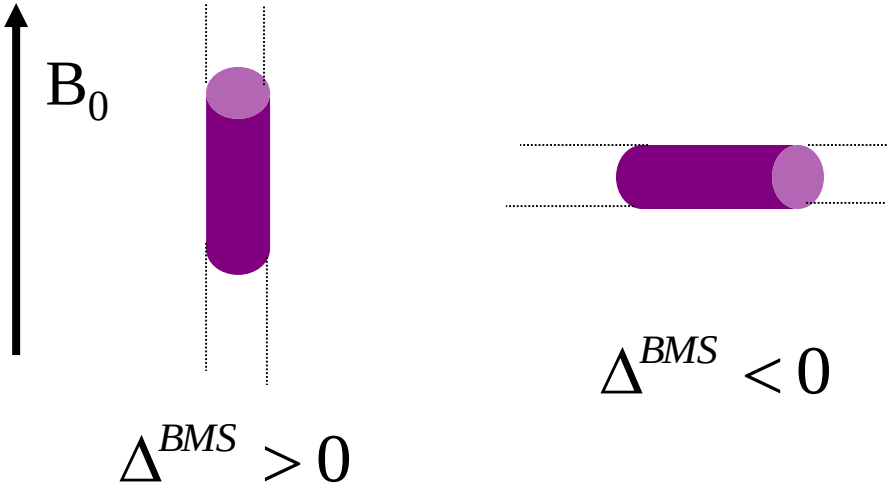

As non-spherical vesicles, also the osmotically shrunken LIPOCEST could orient themselves in the field, thus changing the Δ^{LIPO} sign

Phospholipid-based systems, e.g bicelles, are oriented in the field with their principal symmetry axis perpendicular to B_0

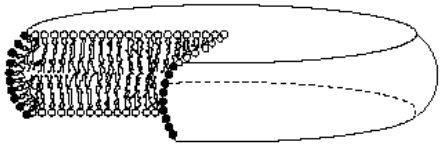

bicelle

The driving force of the orientation is the interaction between B_0 and the magnetic susceptibility anisotropy ($\Delta\chi$) of the phospholipidic membrane.

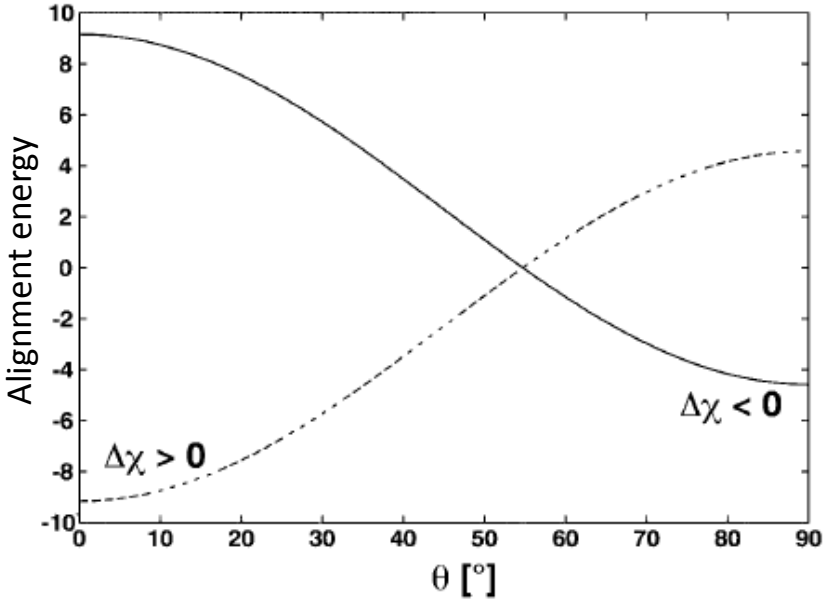

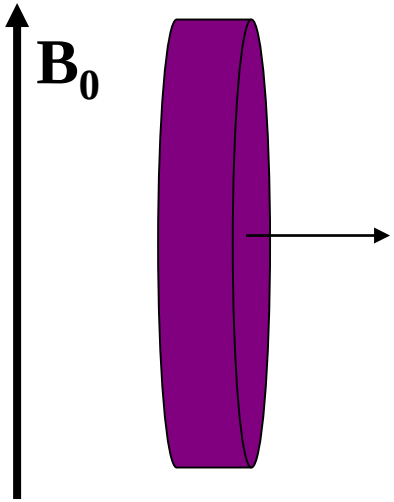

$\Delta\chi < 0$

Incorporation in the membrane of a lanthanide complex with

$\Delta\chi > 0$

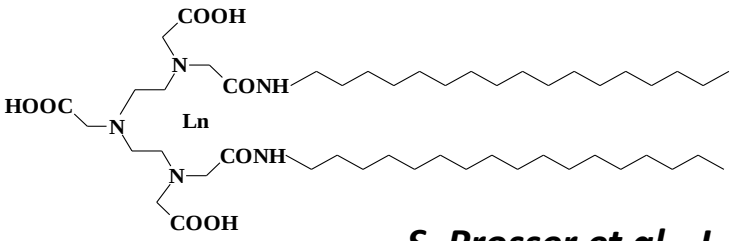

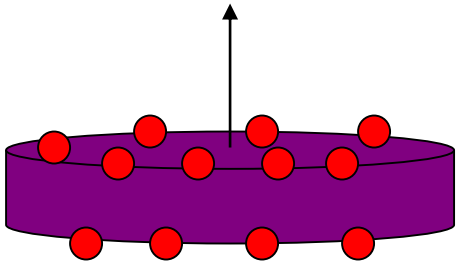

$\Delta\chi > 0$

S. Prosser et al., J. Magn. Res., 1999, 141, 256.

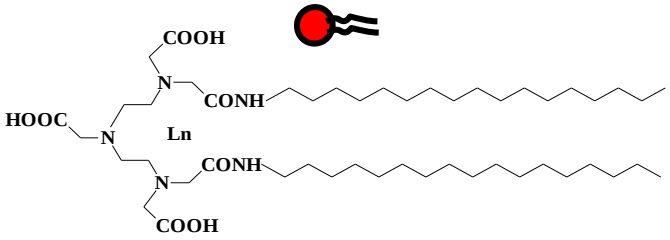

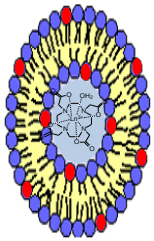

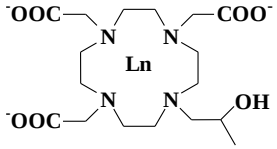

[LnHPDO3A]

$$(\Delta\chi)^{SR} = C_j^{Ln} \times A_0^2 \left\langle r^2 \right\rangle$$

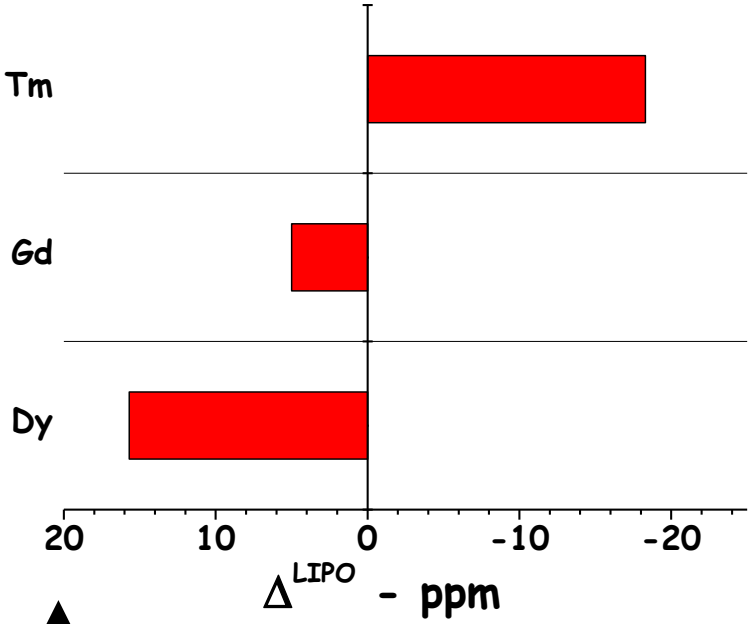

Tm $C_J > 0$ $(\Delta\chi)^{SR} > 0$ $(\Delta\chi)^{LIPO} > 0$

Gd $C_J = 0$ $(\Delta\chi)^{SR} = 0$ $(\Delta\chi)^{LIPO} < 0$

Dy $C_J < 0$ $(\Delta\chi)^{SR} < 0$ $(\Delta\chi)^{LIPO} < 0$

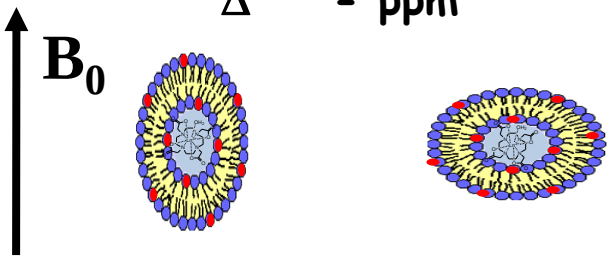

$(\Delta\chi)^{LIPO} < 0$ $(\Delta\chi)^{LIPO} > 0$

with the same amphiphilic ligand it is possible to change the liposome orientation by changing the Ln(III) ion

[Tm-HPDO3A]

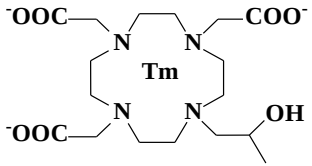

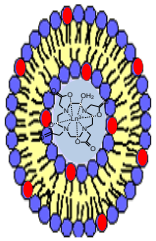

$$(\Delta\chi)^{SR} = C_j^{Ln} \times A_0^2 \left\langle r^2 \right\rangle$$

Tm $C_J > 0$

Tm(III) complexes

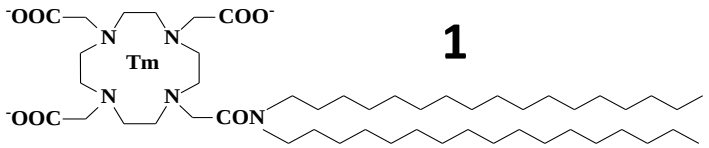

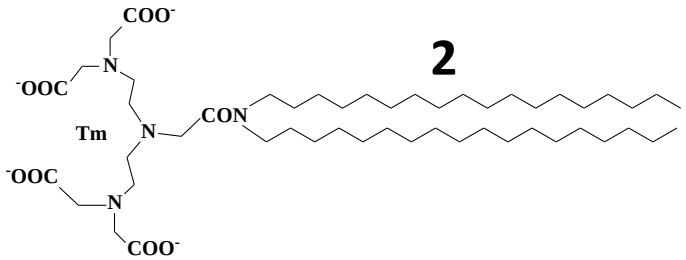

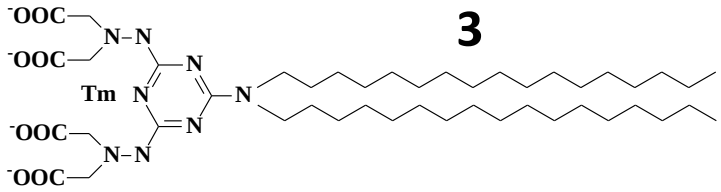

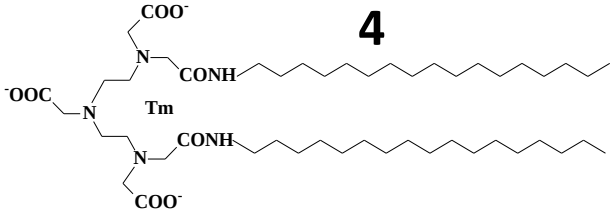

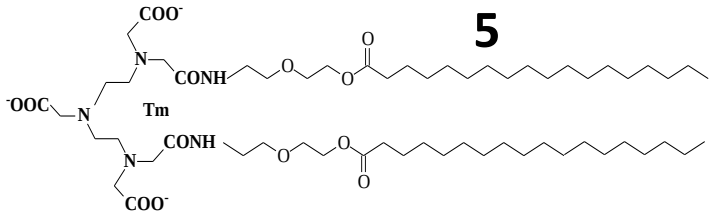

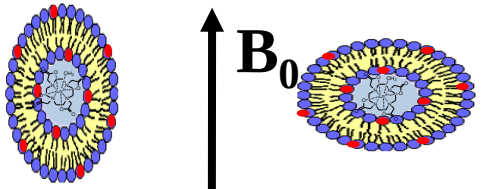

$(\Delta\chi)^{LIPO} < 0$ $(\Delta\chi)^{LIPO} > 0$

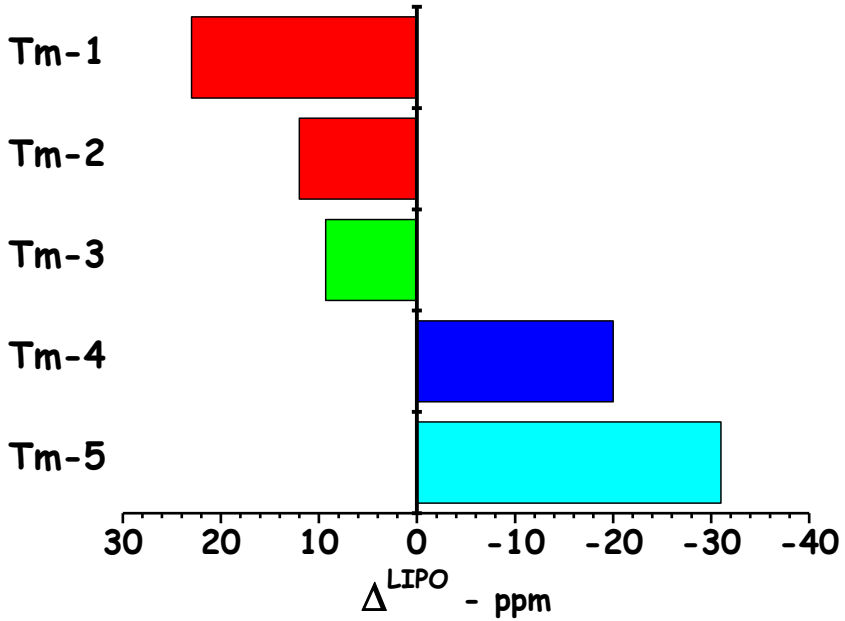

Delli Castelli D. *et al., Inorg. Chem., 2008, 47, 2928.*

Extending the range of Δ^{LIPO} values

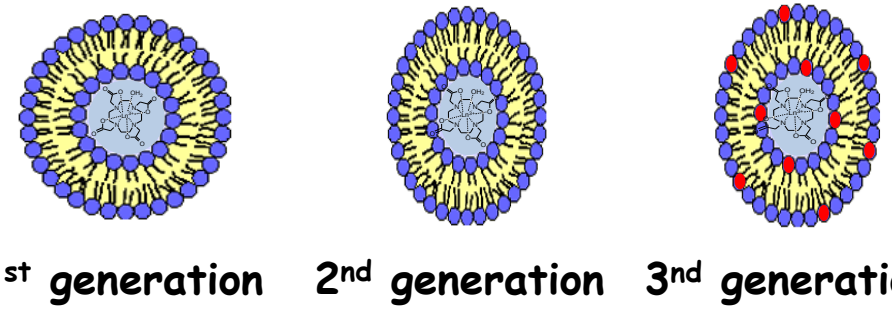

1st generation 2nd generation 3nd generation

Δ^{LIPO}

Entrapping monomeric or multimeric neutral hydrophilic shift reagents

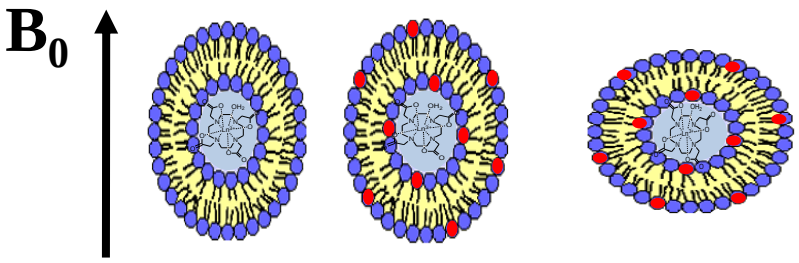

$\Delta^{LIPO} > 0$ $\Delta^{LIPO} < 0$

The Δ^{LIPO} sign for not spherical LipoCEST agents depends on their orientation in the B_0 field

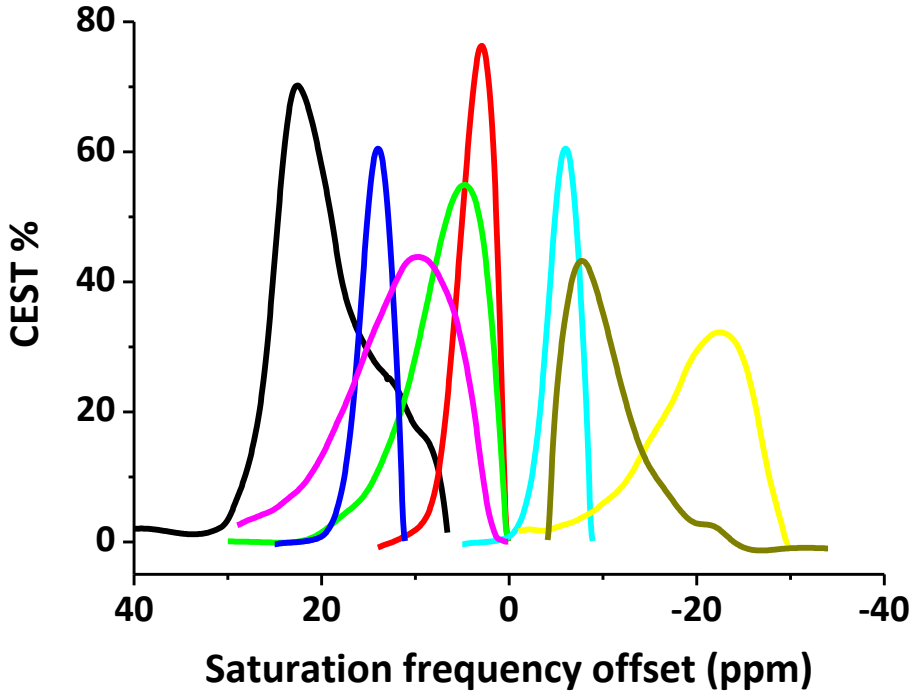

Terreno E. *et al., Methods Enzymol. , 2009, 464, 193.*

In vivo Multiple detection of LipoCEST agents

Subcutaneous injection

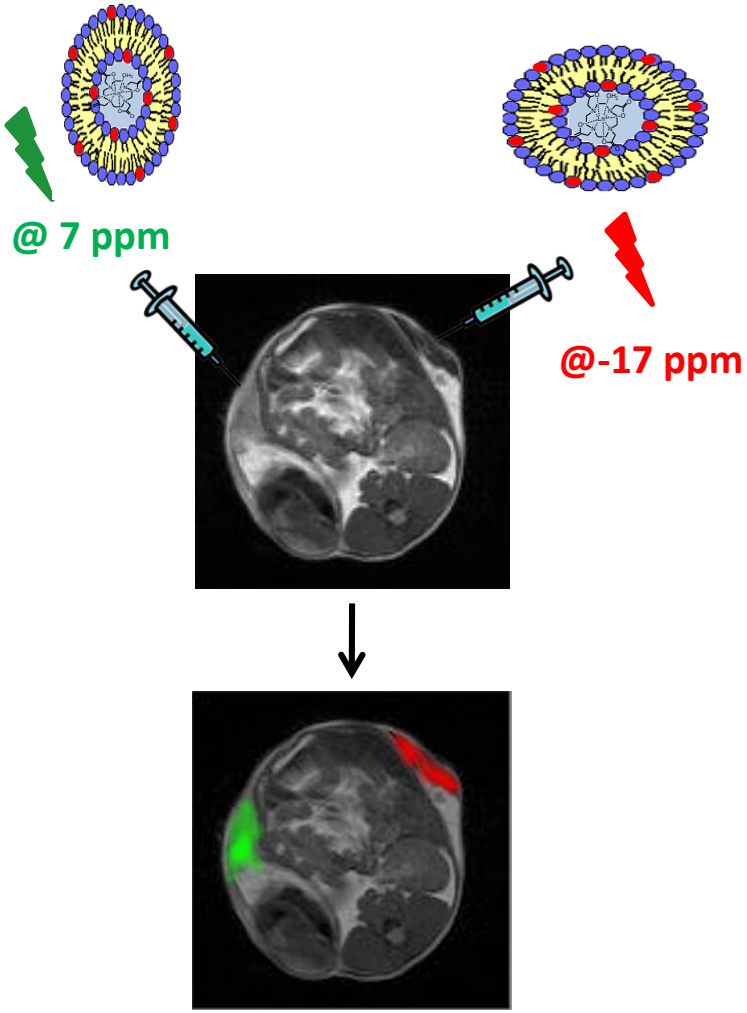

Intramuscolar injection

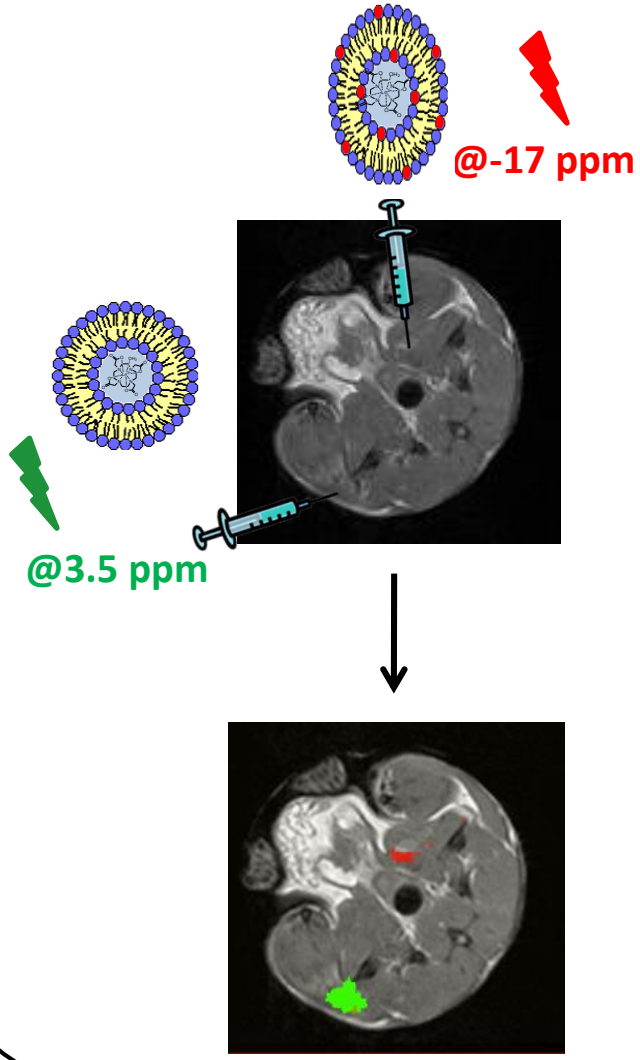

Cells as CEST agents

Aim : To use cells loaded with Ln-based Shift Reagents as CEST agents

In analogy with lipoCEST, cells can be loaded with Ln-complexes acting as Shift Reagents.

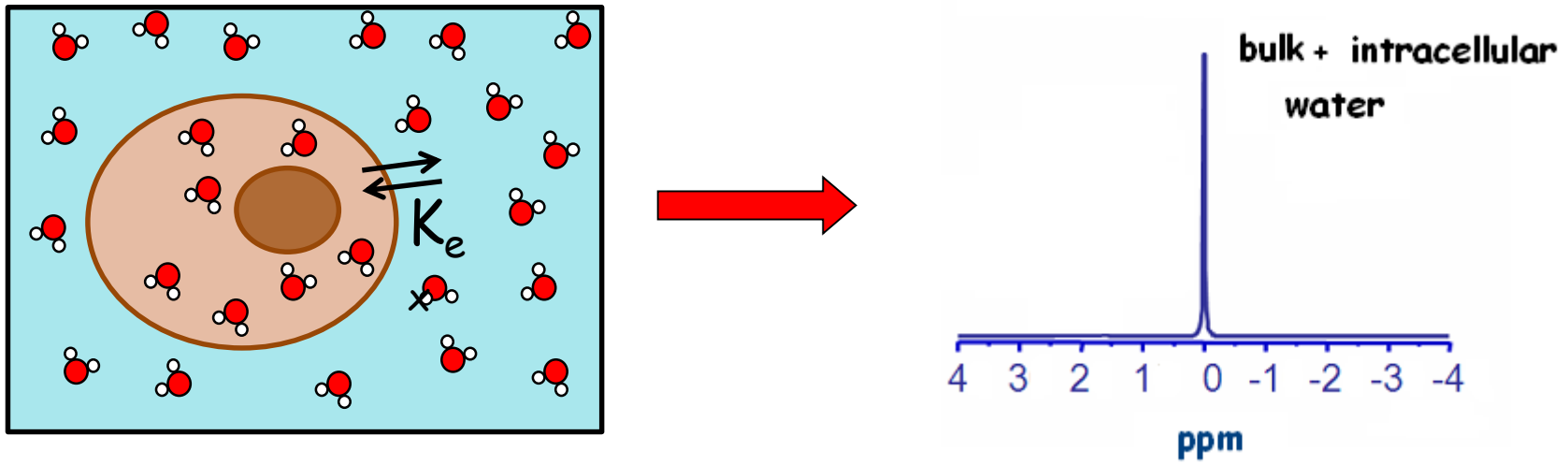

Cells as CEST agents

Aim : To use cells loaded with Ln-based Shift Reagents as CEST agents

In analogy with lipoCEST, cells can be loaded with Ln-complexes acting as Shift Reagents.

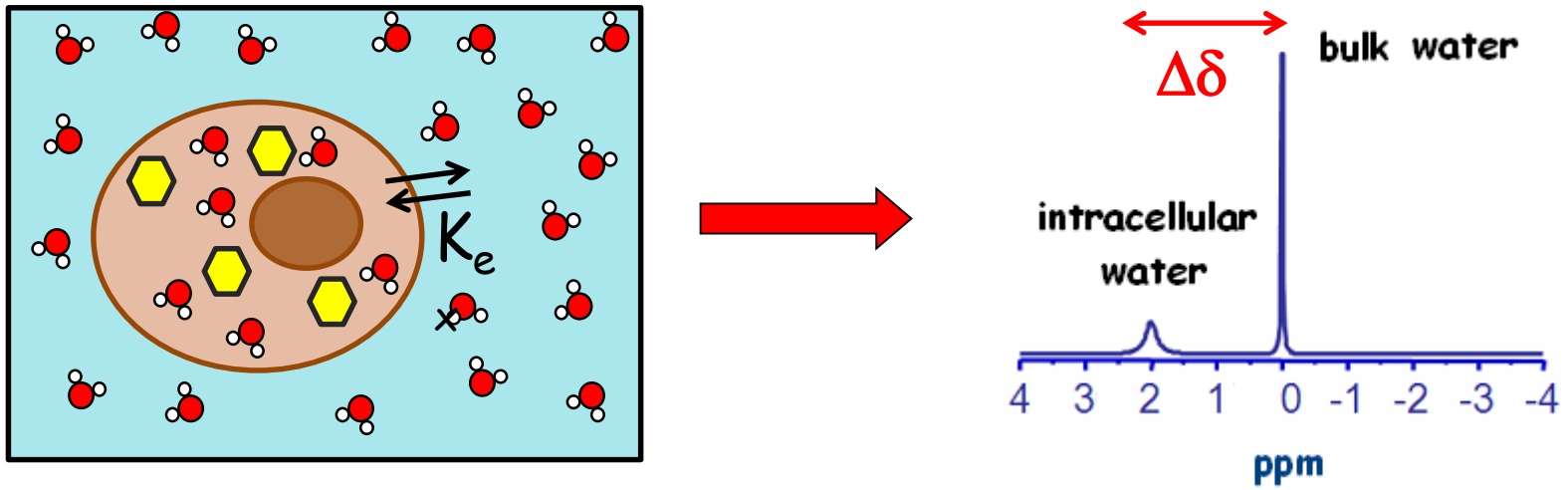

= paramagnetic shift reagent

Lanthanide induced shift

$$LIS_{\substack{Bulk \\ water}} = BMS + Dip$$

Lanthanide induced shift

$$LIS_{\substack{Bulk \\ water}} = BMS + Dip$$

Spherical compartment

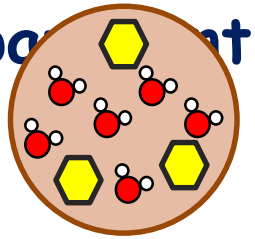

$$LIS_{\substack{Bulk \\ water}} = BMS + Dip$$

Lanthanide induced shift

$$LIS_{\substack{Bulk\\water}} = BMS + Dip$$

Spherical compartment

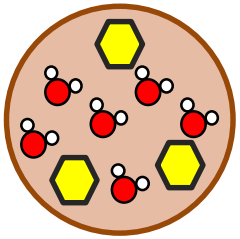

$$LIS_{\substack{Bulk\\water}} = BMS + Dip$$ X

$$Dip = \frac{[H_2O]_{bound\ to\ SR}}{[H_2O]_{total}} \times \delta_{\substack{bound\\water}}$$

$$\delta_{\substack{bound\\water}} \propto \Delta\chi \times G$$

$$\Delta\chi = C_J \times A_2^0 \langle r^2 \rangle$$

$$G \propto \frac{3\cos^2\theta - 1}{r^3}$$

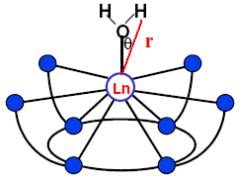

Lanthanide induced shift

$$LIS_{\substack{Bulk\\water}} = BMS + Dip$$

Spherical compartment

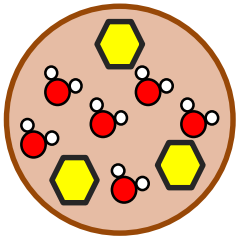

$$LIS_{\substack{Bulk\\water}} = BMS + Dip$$ X

$$Dip = \frac{[H_2O]_{bound\ to\ SR}}{[H_2O]_{total}} \times \delta_{\substack{bound\\water}}$$

$$\delta_{\substack{bound\\water}} \propto \Delta\chi \times G$$

$$\Delta\chi = C_J \times A_2^0 \langle r^2 \rangle$$

$$G \propto \frac{3\cos^2\theta - 1}{r^3}$$

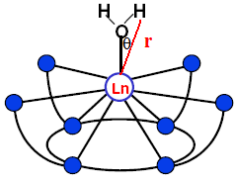

$C_J > 0$ for Eu, Er, Tm e Yb

$C_J < 0$ for Ce, Pr, Nd, Sm, Tb, Dy and Ho

$C_J = 0$ for Gd

Cells as CEST agents

Lanthanide induced shift

$$LIS_{\substack{Bulk\\water}} = BMS + Dip$$

Spherical compartment

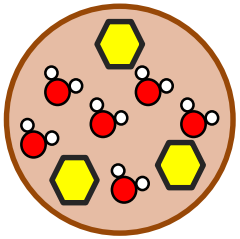

$$LIS_{\substack{Bulk\\water}} = BMS + Dip$$ X

Not-Spherical compartment

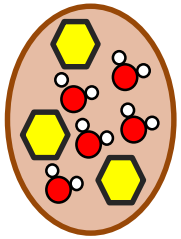

$$LIS_{\substack{Bulk\\water}} = BMS + Dip$$

$$Dip = \frac{[H_2O]_{bound\ to\ SR}}{[H_2O]_{total}} \times \delta_{\substack{bound\\water}}$$

$$\delta_{\substack{bound\\water}} \propto \Delta\chi \times G$$

$$\Delta\chi = C_J \times A_2^0 \langle r^2 \rangle$$

$$G \propto \frac{3\cos^2\theta - 1}{r^3}$$

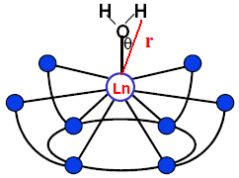

Cells as CEST agents

Lanthanide induced shift

$$LIS_{\substack{Bulk\\water}} = BMS + Dip$$

Spherical compartment

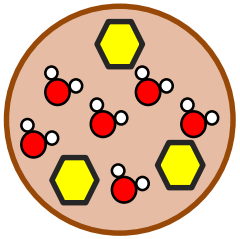

$$LIS_{\substack{Bulk\\water}} = BMS + Dip$$ X

$$Dip = \frac{[H_2O]_{bound\ to\ SR}}{[H_2O]_{total}} \times \delta_{\substack{bound\\water}}$$

Not-Spherical compartment

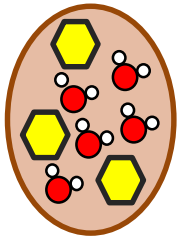

$$LIS_{\substack{Bulk\\water}} = BMS + Dip$$

$$BMS \propto [SR] \times (\mu_{eff})^2$$

BMS contribution is much higher than the Dipolar one

$$\delta_{\substack{bound\\water}} \propto \Delta\chi \times G$$

$$\Delta\chi = C_J \times A_2^0 \langle r^2 \rangle$$

$$G \propto \frac{3\cos^2\theta - 1}{r^3}$$

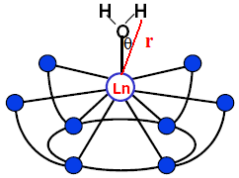

Separation of red blood cells

Blood was taken from donors

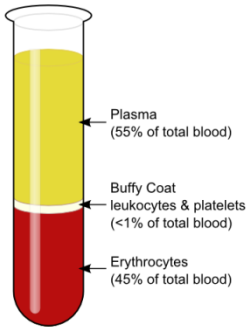

RBC separation by using Ficoll Histopaque

RBCs were washed with PBS

Ferrauto G. et al. J.Am. Chem. Soc. 2014

Cells as CEST agents

Separation of red blood cells

Blood was taken from donors

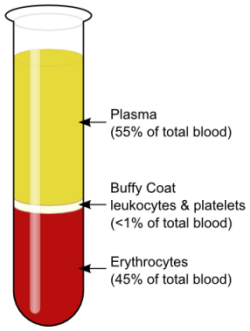

RBC separation by using Ficoll Histopaque

RBCs were washed with PBS

Labeling of RBCs by hypotonic swelling procedure

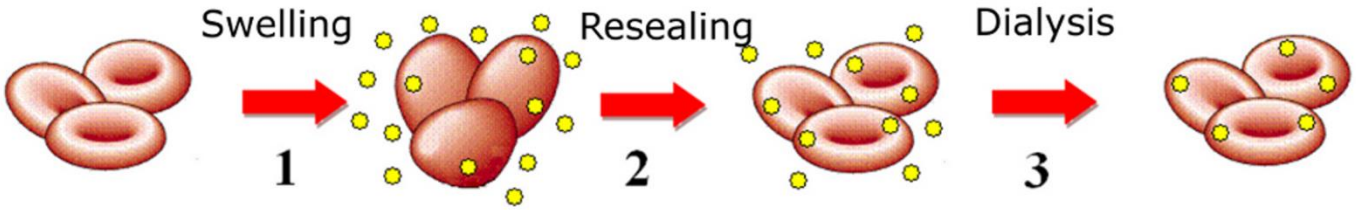

- Shift Reagents

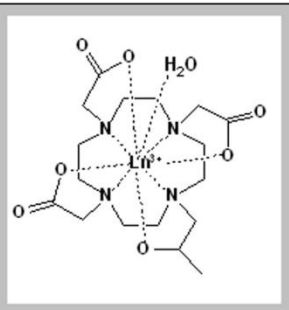

Ln= Eu, Gd, Dy, Tm, Yb

Ferrauto G. et al. J.Am. Chem. Soc. 2014

Cells as CEST agents

Z-spectrum and ST profile of Dy-HPDO3A- loaded RBCs (*black*) and control RBCs (*red*)

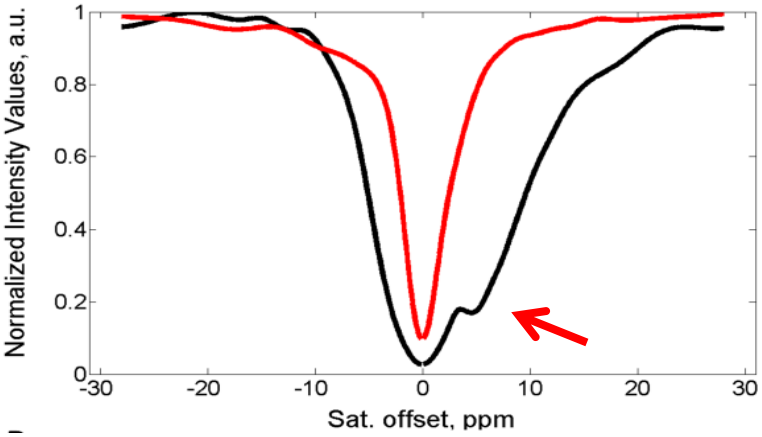

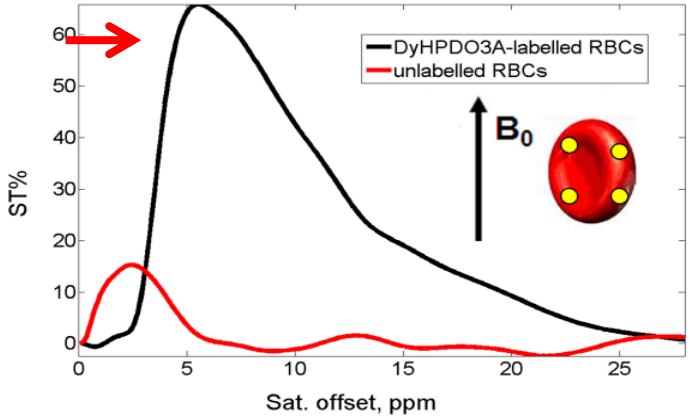

- A large ST effect (65%) is visible at *ca.*5 ppm from water signal

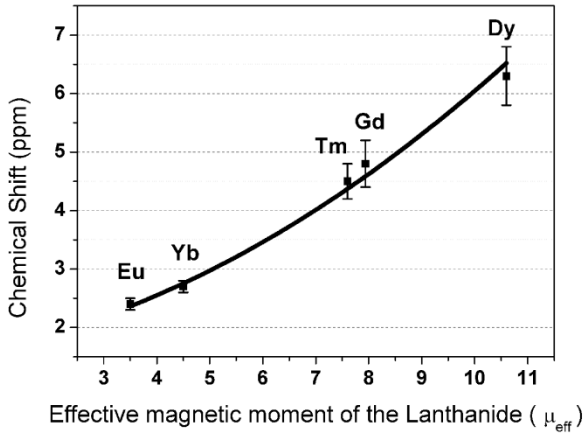

Cells as CEST agents

Changing the sign of BMS term

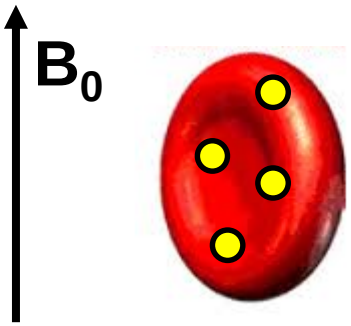

Shift Reagent (DyHPDO3A)

$(\Delta\chi)^{Phospholipids} < 0$

$BMS > 0$

$$\Delta\chi = C_J \times A_0^p \left\langle r^p \right\rangle$$

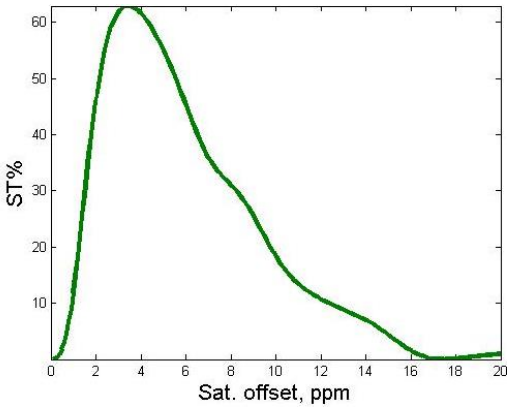

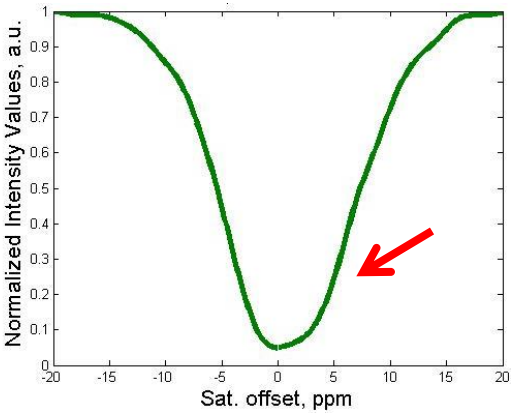

Cells as CEST agents

Changing the sign of BMS term: Incorporation of a Ln-complex with different BMS contribution

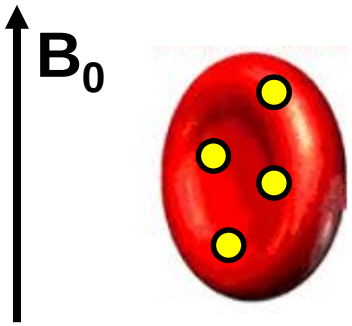

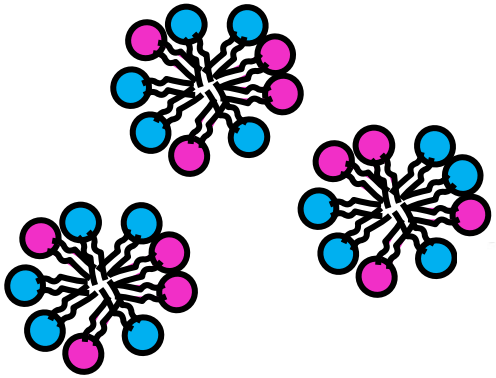

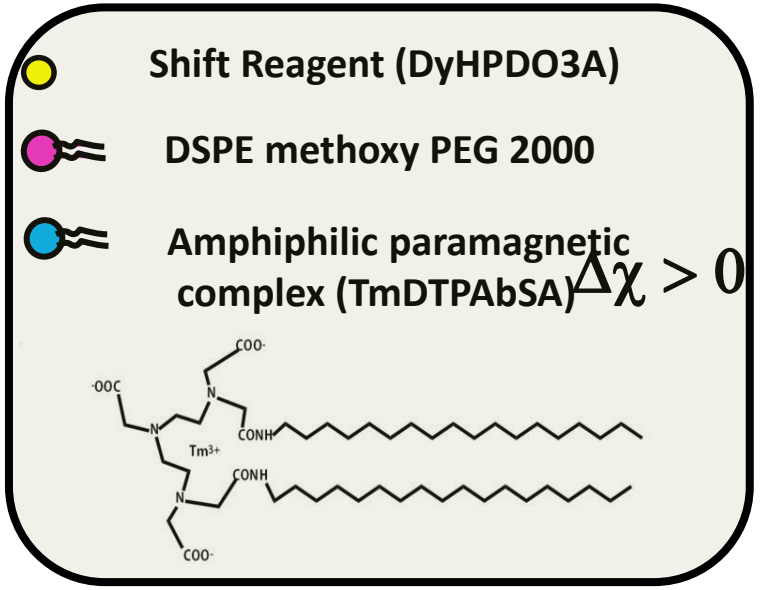

$(\Delta\chi)^{Phospholipids} < 0$

$\mathbf{BMS} > 0$

Amphiphilic paramagnetic complexes were incorporated in cellular membrane by incubating cells with micelles

$$\Delta\chi = C_J \times A_0^p \left\langle r^p \right\rangle$$

Cells as CEST agents

Changing the sign of BMS term: Incorporation of a Ln-complex with different BMS contribution

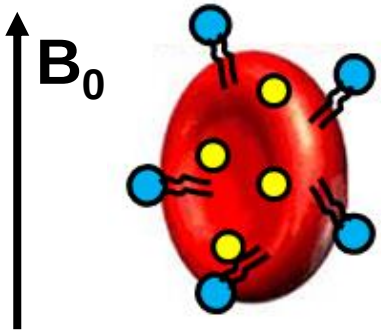

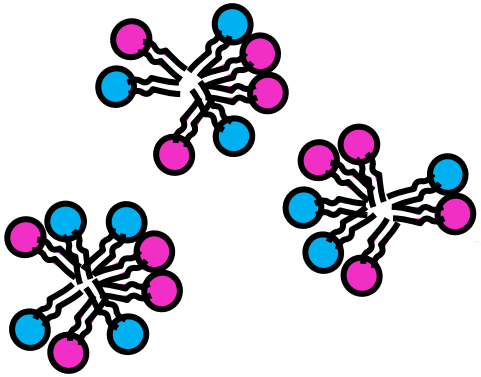

Shift Reagent (DyHPDO3A)

DSPE methoxy PEG 2000

Amphiphilic paramagnetic complex (TmDTPAbSA) $\Delta\gamma > 0$

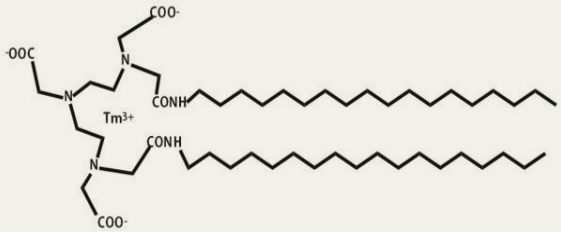

$(\Delta\chi)^{LIPO} > 0$

BMS < 0

$$\Delta\chi = C_J \times A_0^p \left\langle r^p \right\rangle$$

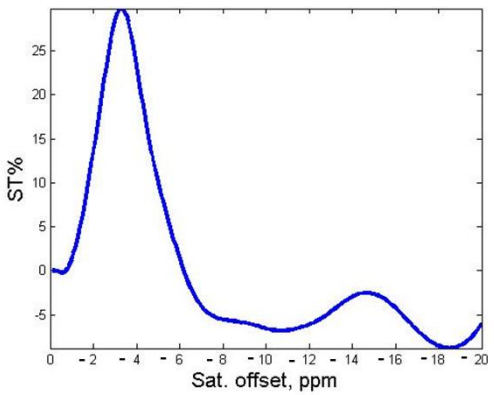

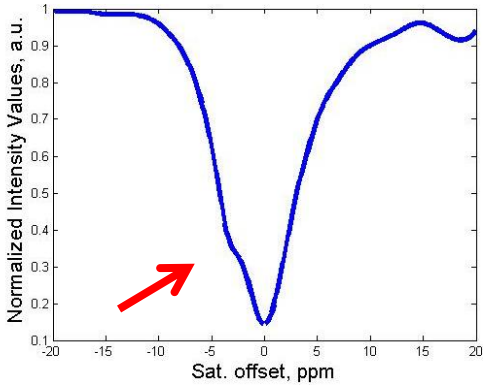

Cells as CEST agents

Changing the sign of BMS term: Incorporation of a Ln-complex with different BMS contribution

$(\Delta\chi)_{RBC} < 0$

$\mathbf{BMS} > 0$

Chemical Shift at 3.6 ppm

$(\Delta\chi)_{Ln\text{-}RBC} > 0$

$\mathbf{BMS} < 0$

Chemical Shift at -3.4 ppm

The incorporation of a paramagnetic complex with $(\Delta\chi) > 0$ in the cellular membrane changes the orientation of the RBC into the magnetic field

Generation of multiparametric maps by using Dy-RBCs

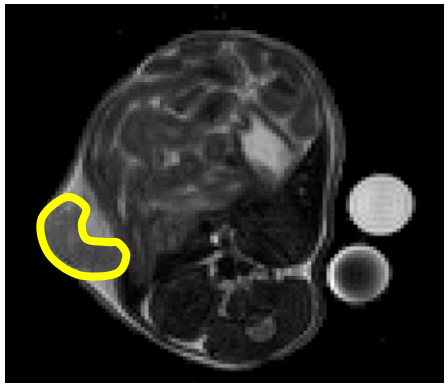

T_{2w} image of a mouse with xenograft TSA tumor

1° step: Injection of Dy-RBCs

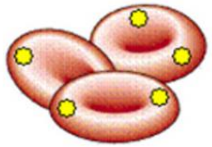

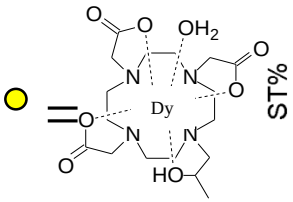

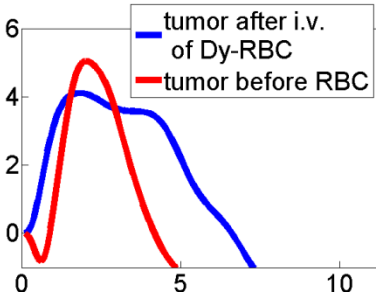

Map at 4ppm

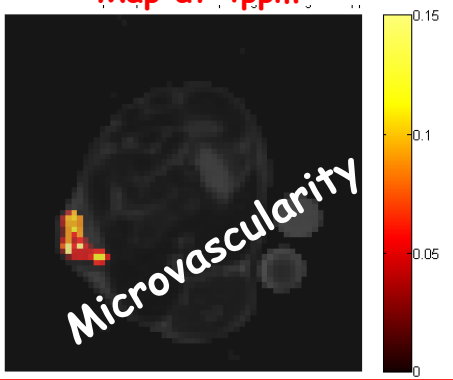

2°Step: Injection of Yb-HPDO3A

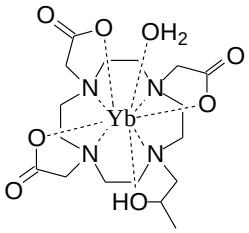

Map at 67ppm

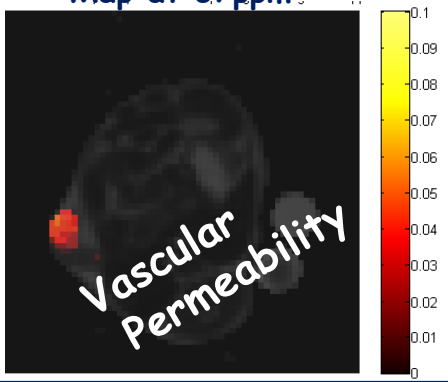

+

Ratio 91ppm/ 67 ppm

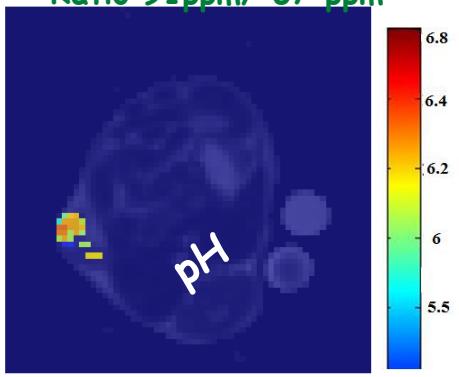

Some readings…

S. Zhang et al., *Acc. Chem. Res., 36, 783, 2003*

- M. Woods et al., *Chem. Soc. Rev., 35, 500, 2006*

- J. Zhou et al., *Progr. NMR Spectr., 48, 109, 2006*

- S. Viswanathan et al., Chem. Rev., 110, 2960, 2010

- E. Terreno et al., *Contrast Media Mol. I., 5, 78, 2010*

- Hancu I. et al., *Acta Radiol., 51, 910, 2010*

Field homogeneity

The pixel-by-pixel evaluation of the spatial distribution of the frequency offset of the bulk water is necessary to avoid CEST artifacts…

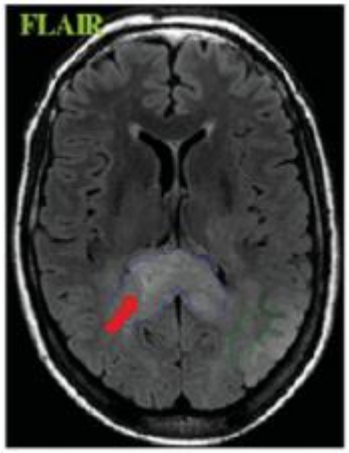

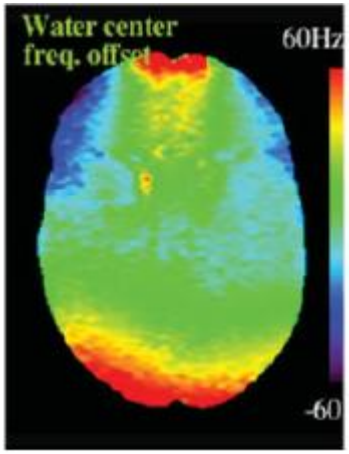

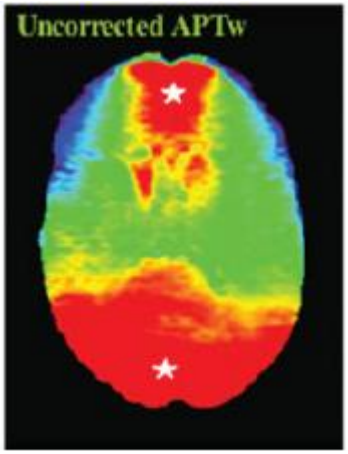

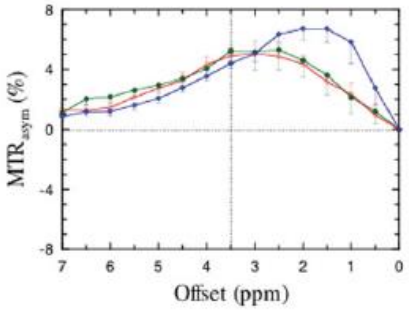

Human astrocytoma

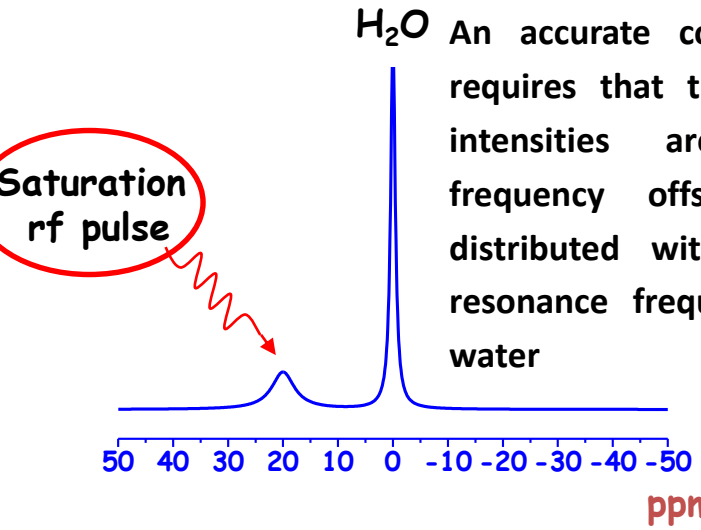

An accurate contrast assessment requires that the two MR signal intensities are measured at frequency offsets <u>symmetrically</u> distributed with respect to the resonance frequency of the bulk water

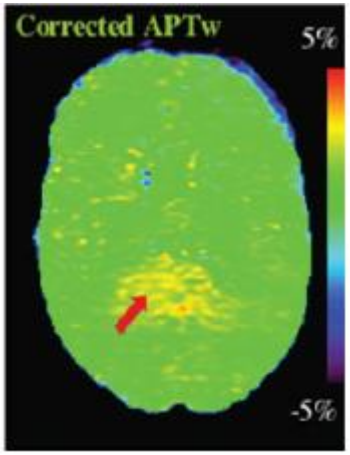

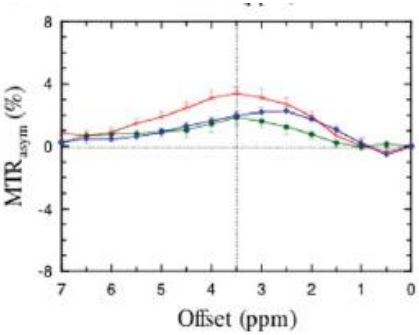

Zhou *et al.*, MRM 2008, 60, 842

Field homogeneity

…but, of course, acquiring B_0 maps takes time

Several methods have been proposed so far:

- B_0 (and also B_2) compensation algorithm (Sun *et al.*, MRM 2007)

☺ relatively fast (in addition to the couple of CEST scans, it requires few images for generating the B_0/B_1 maps)

☹ Not suitable for large inhomogeneities

- WAter Saturation Shift Referencing (WASSR) (Kim *et al.*, MRM 2009)

☺ excellent accuracy; optimal for detecting CEST contrast from very little shifted agents

☹ Time consuming (an additional Z spectrum is required)

- Z-spectrum interpolation (Zhou *et al.*, Nat. Med. 2003 – Stancanello *et al.*, CMMI 2008)

☺ broad applicability, good accuracy

☹ Relatively time consuming (depending on the frequency sampling)

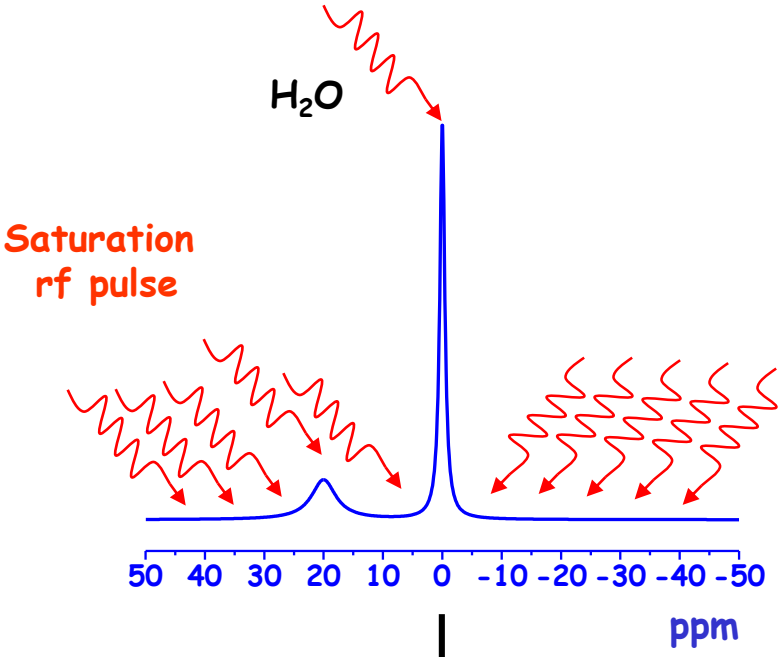
H2O
Saturation
rf pulse
50 40 30 20 10 0 -10 -20 -30 -40 -50
ppm

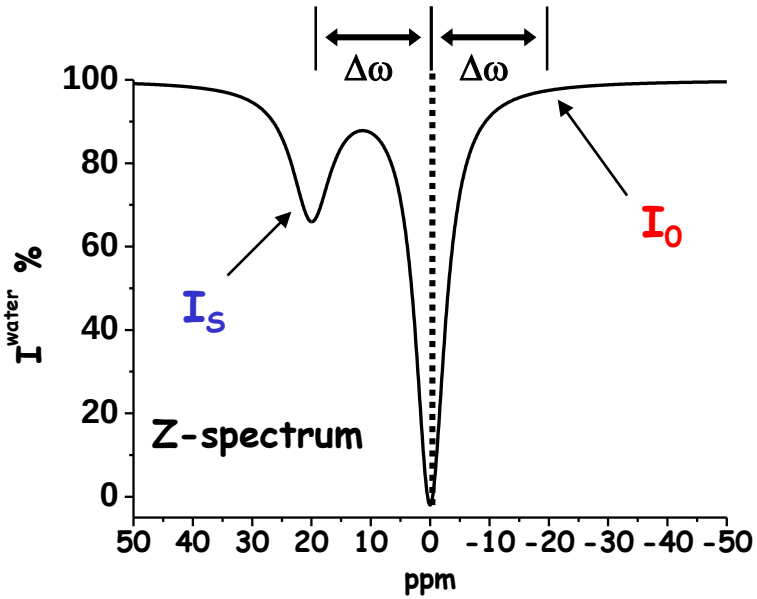
Δω
Δω
100
80
60
40
20
0
I water %
Is
I0
Z-spectrum
50 40 30 20 10 0 -10 -20 -30 -40 -50
ppm

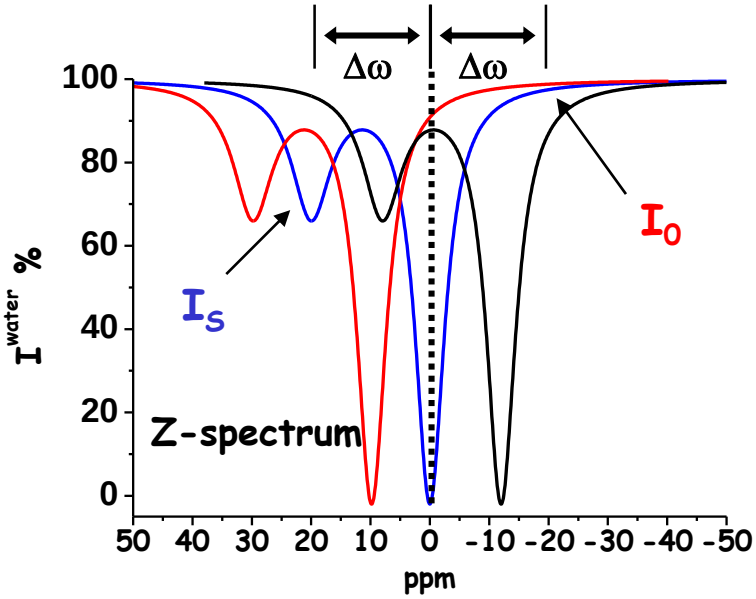
Δω
Δω
100
80
60
40
20
0
I water %
Is
I0
Z-spectrum
50 40 30 20 10 0 -10 -20 -30 -40 -50
ppm

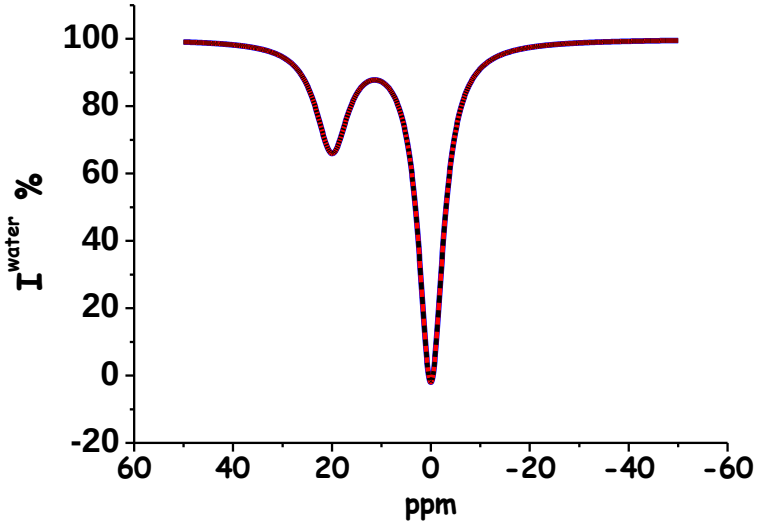
100
80
60
40
20
0
-20
I water %
60 40 20 0 -20 -40 -60
ppm

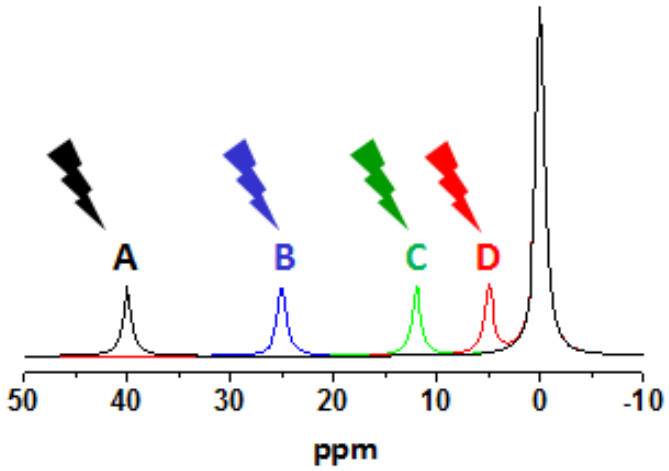

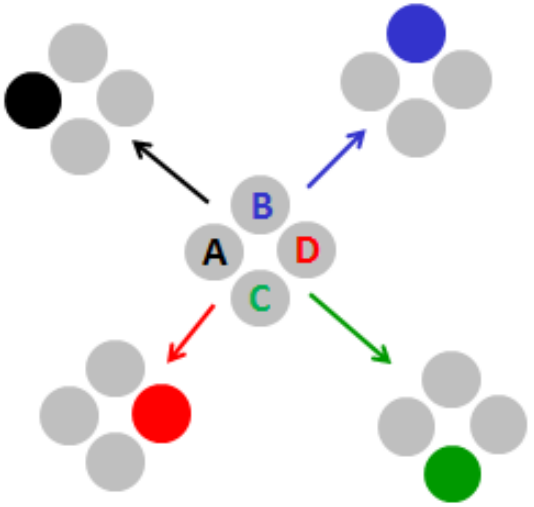

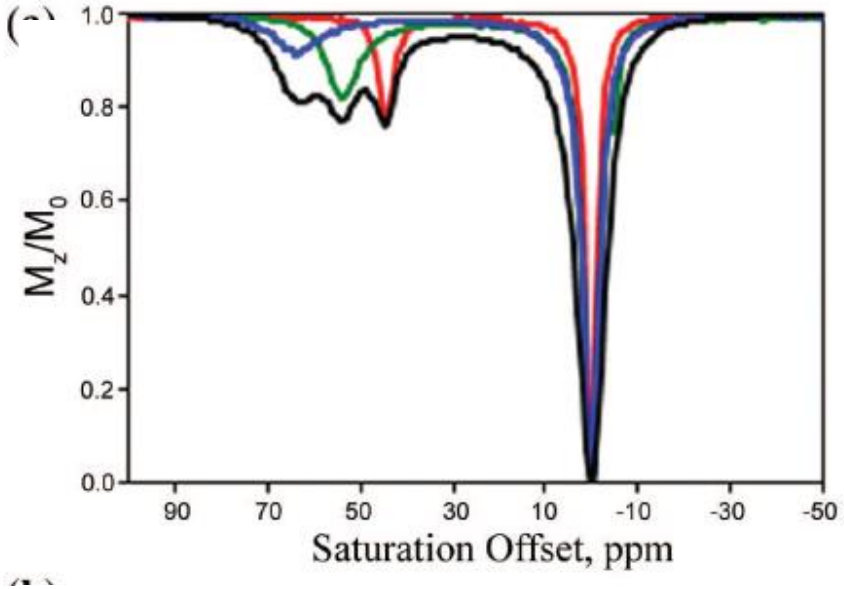

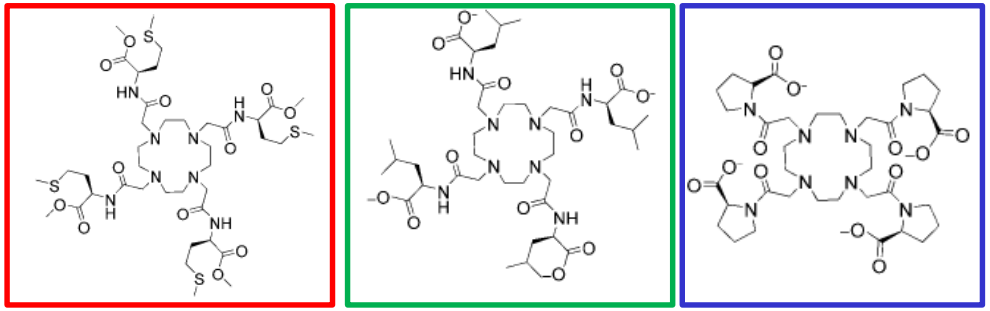

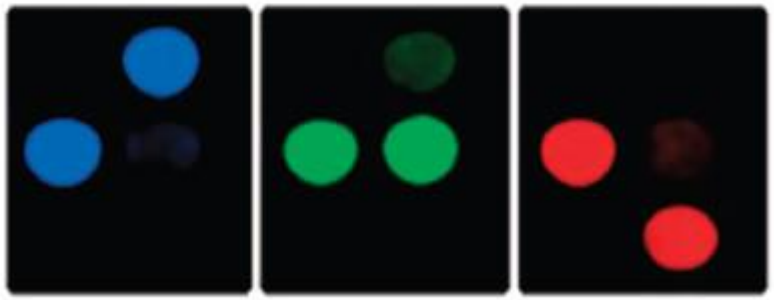

*Subha Viswanathan, S. James Ratnakar, Kayla N. Green, Zoltan Kovacs, Luis M. De León-Rodríguez, and A. Dean Sherry**

Angew. Chem. Int. Ed. **2009**, *48*, 9330–9333

Multiple detection of LipoCEST agents: buffer vs. agar

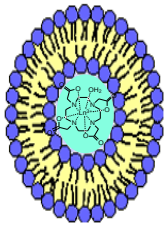

Δ^{LIPO} 6.7 ppm

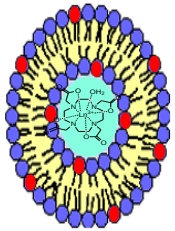

Δ^{LIPO} 18 ppm

7 T – 312 K – sat. intensity 6 μT

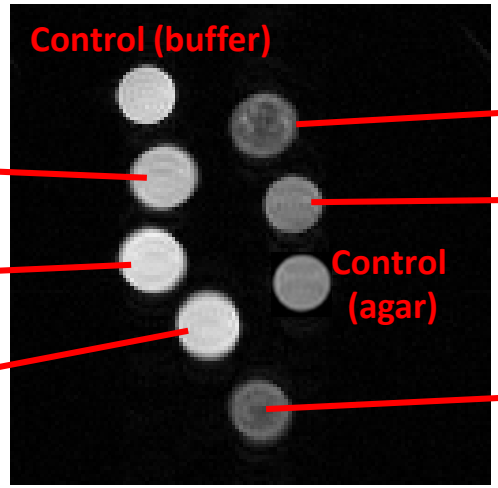

In buffer

A + B

A

B

A

B

A + B

In agarose gel

6.7 ppm

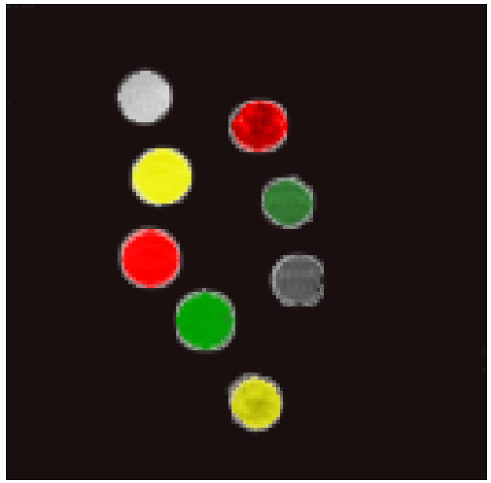

@18 ppm

Cells as CEST agents

Results:

RBCs labelled by using different LnHPDO3A complexes

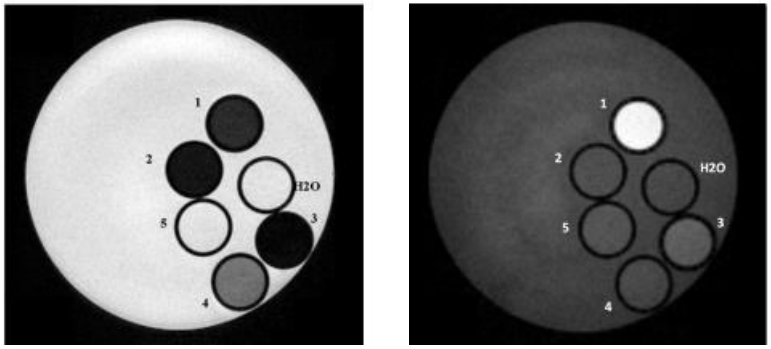

(A) T_{2w} and (B) T_{1w} map of a phantom consisting of glass capillaries containing:

1. GdHPDO3A-loaded RCBs,
2. EuHPDO3A-loaded RCBs,
3. DyHPDO3A-loaded RCBs,
4. YbHPDO3A-loaded RCBs,
5. unloaded RBCs;

Cells as CEST agents

Results:

RBCs labelled by using different LnHPDO3A complexes

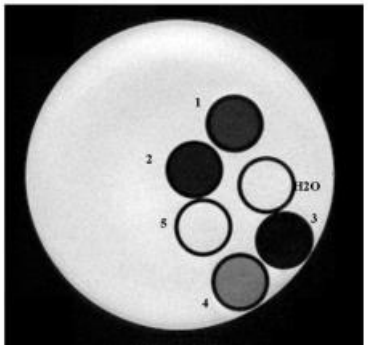

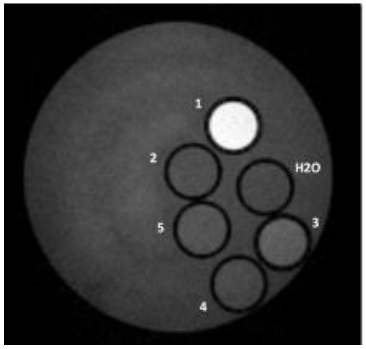

(A) T_{2w} and (B) T_{1w} map of a phantom consisting of glass capillaries containing:

1. GdHPDO3A-loaded RCBs,
2. EuHPDO3A-loaded RCBs,
3. DyHPDO3A-loaded RCBs,
4. YbHPDO3A-loaded RCBs,
5. unloaded RBCs;

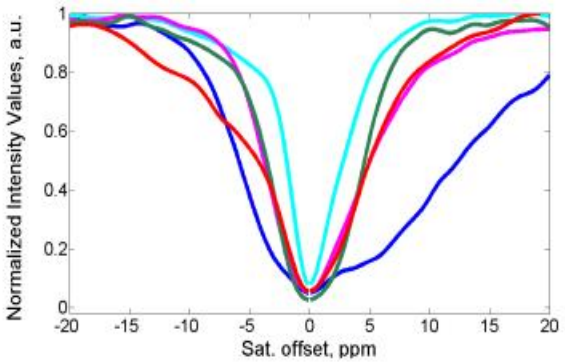

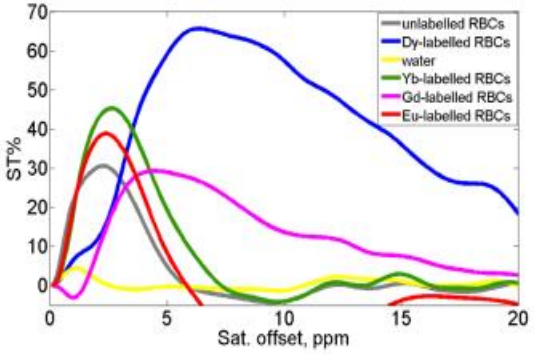

Z- and ST-spectra showing different chemical shifts by changing the metal ion

Cells as CEST agents

Results:

RBCs labelled by using different LnHPDO3A complexes

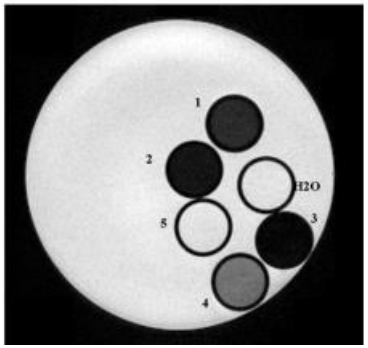

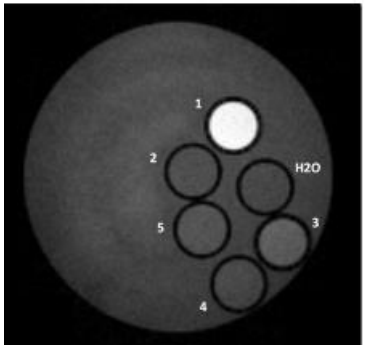

(A) T_{2w} and (B) T_{1w} map of a phantom consisting of glass capillaries containing:

1. GdHPDO3A-loaded RCBs,
2. EuHPDO3A-loaded RCBs,
3. DyHPDO3A-loaded RCBs,
4. YbHPDO3A-loaded RCBs,
5. unloaded RBCs;

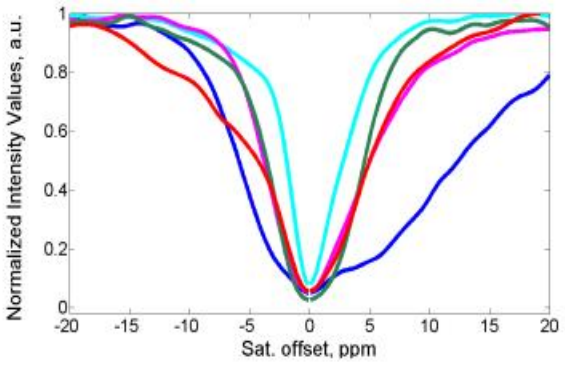

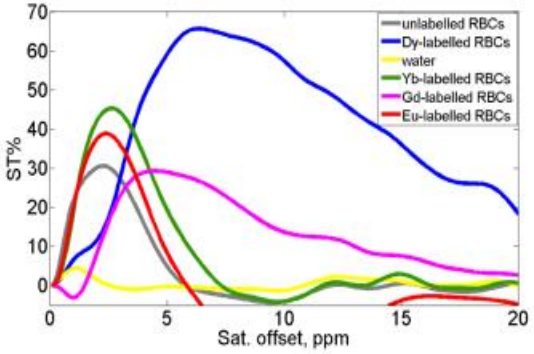

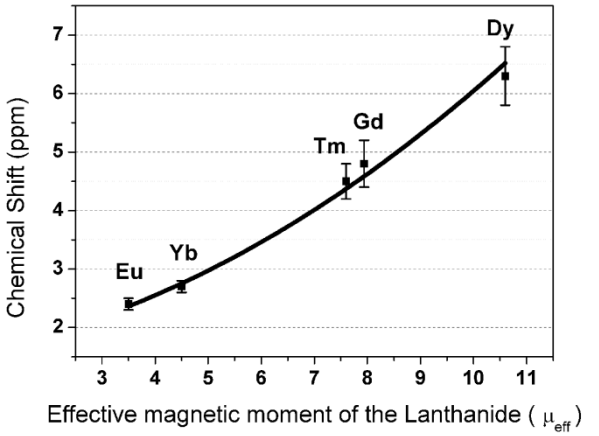

Z- and ST-spectra showing different chemical shifts by changing the metal ion

$\Delta\delta$ is proportional to μ_{eff} of the Ln

(Dy=10.6, Gd=7.94, Tm=7.6, Yb=4.5, Eu=3.5)

$$\delta_{BMS} \propto [c] \times \mu_{eff}^2$$

Cells as CEST agents

Results:

Detection of the threshold for the visualization of Dy-labelled RBCs

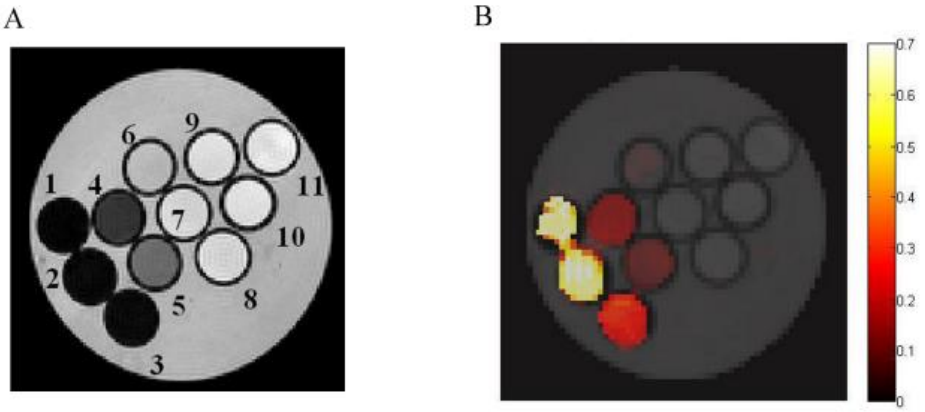

(A) T_{2w} and (B) STmap@5.6 ppm of a phantom containing Dy-labelled (1-5) or unlabelled (6-10) RBCs in a concentration range of $1x10^6$ to 4×10^6 /mm^3

(C) Correlation between number of RBCs/mm^3 and ST% for labelled (*black*) and unlabelled (*red*) cells

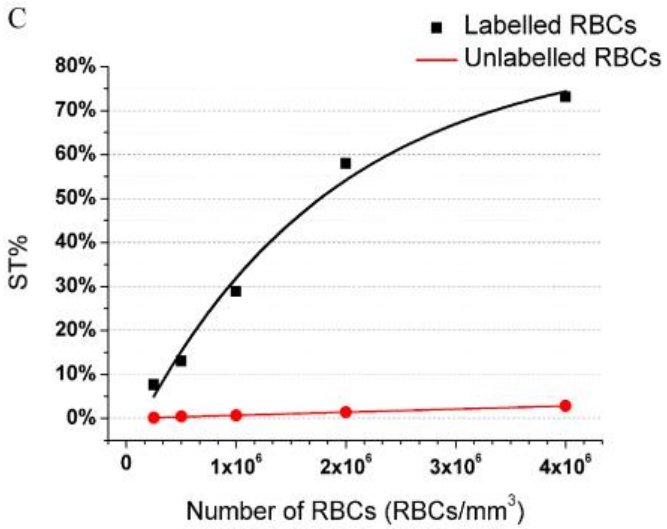

CEST ST% it is still detectable up to *ca.* $2.5x10^5$ Dy-loaded RBCs/mm^3 (corresponding to ***ca.*** **5%** of naturally occurring RBCs)

LIPOCEST agents

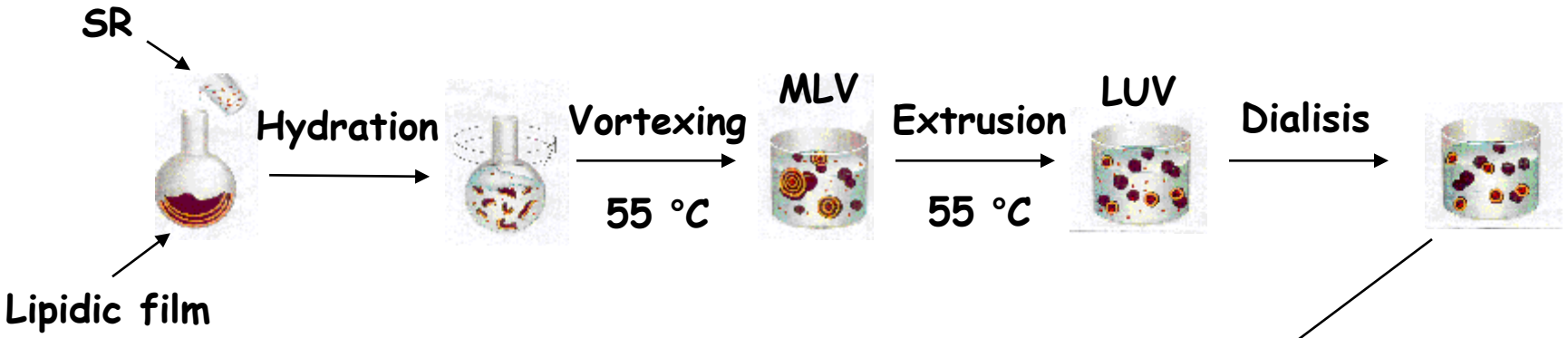

SR unit

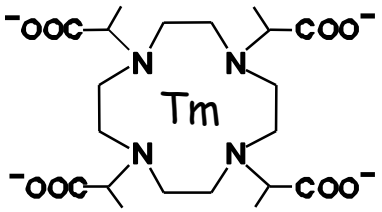

[TmDOTMA]$^-$

0.12 M inside liposomes

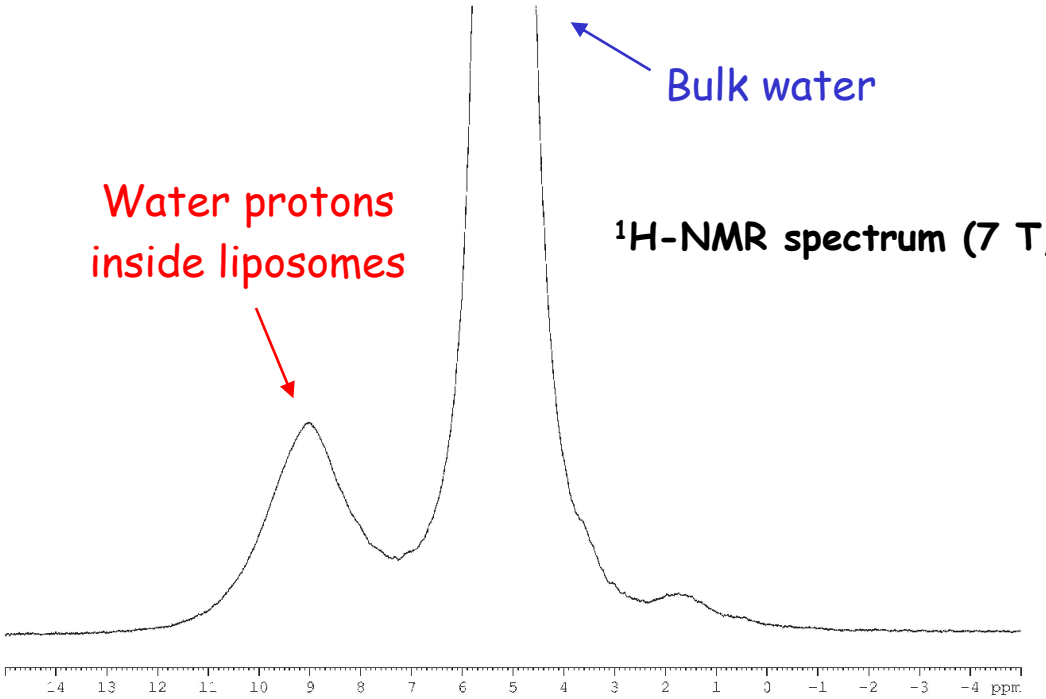

DPPC/DPPG 95/5 (w/w) liposomes